5-1993

Hydrogeology and Hydrochemistry of The Delta Wadi El-Arish Area Sinai Peninsula, Egypt

Medhat A. El-Bihery

HYDROGEOLOGY AND HYDROCHEMISTRY OF THE DELTA WADI EL-ARISH AREA SINAI PENINSULA, EGYPT

by

Medhat A. El-Bihery

A thesis submitted in partial fulfillment
of the requirements for the degree

of

MASTER OF SCIENCE

in

Geology

Approved:

UTAH STATE UNIVERSITY
Logan, Utah

1993

ACKNOWLEDGMENTS

I would like to thank the Water Research Center in Egypt for the scholarship that supported my graduate studies. I am grateful to Professor Hassan Ibrahim for giving me the opportunity to study in the United States.

A special thanks goes to Dr. Thomas E. Lachmar for his guidance, support, and advice during my graduate program.

Dr. Fiesinger is greatly appreciated for his help and for being my graduate committee member. Dr. Kolesar is also appreciated for his help and for being my committee member. Also I would like to thank Eng. Saleh Nour for his help during my thesis research.

Finally, I deeply thank my parents, my sister, and my brothers for their great encouragement.

Medhat A. El-Bihery

CONTENTS

Page

Page

LIST OF TABLES

LIST OF FIGURES

ABSTRACT

Hydrogeology and Hydrochemistry of
The Delta Wadi El-Arish Area
Sinai Peninsula, Egypt

by

Medhat A. El-Bihery, Master of Science
Utah State University, 1993

Major professor: Dr. Thomas E. Lachmar
Department: Geology

Delta Wadi El-Arish, Sinai Peninsula, Egypt, forms one of the most important parts of Egypt for industrial and agricultural expansion projects. This study focuses on the hydrogeology and the hydrochemistry of the Quaternary aquifer in the delta Wadi El-Arish area. Accurate information about the groundwater characteristics of the Quaternary aquifer will allow implementation of a sound water management policy for the Wadi El-Arish area.

The objectives of this study include: 1) determining the relationships between groundwater extraction and water levels and water quality using water-level measurements, total extraction of the wells, and chemical analyses of water samples; 2) determining the direction of groundwater flow using water-level measurements; 3) calculating the hydraulic parameters of the Quaternary aquifer using pumping test data;

and 4) determining the hydrochemical characteristics of groundwater in the Quaternary aquifer.

The results of this study indicate that:

1. Potentiometric surface elevations have decreased by an average of about 0.5 m.

2. Potentiometric surface elevations have decreased in response to an increase in extraction rates.

3. The transmissivity of the lower Pleistocene calcareous sandstone (kurkar) unit is higher than the transmissivity of the upper Pleistocene sand and gravel alluvial deposits.

4. Groundwater in the upper Pleistocene sand and gravel aquifer is augmented with groundwater leaking from the overlying Holocene sand deposits through the intervening sandy clay aquitard.

5. Total dissolved solids (TDS) concentrations have been increased by an average of about 1,500 ppm.

6. An increase in sea water intrusion in the northern part of the study area has occurred.

7. Groundwater in the calcareous sandstone kurkar is of lower quality than groundwater in the alluvium sand and gravel.

Management of the groundwater resources should include the following recommendations:

1. No new pumping wells should be drilled in the area.

2. Accurate estimates for the total recharge should be

determined using a more detailed water budget for the delta Wadi El-Arish area.

3. Change from flood irrigation systems to drip or sprinkler systems should be used to reduce the water loss.

4. The operation of wells should be managed by an automatic control system.

(161 pages)

CHAPTER I

INTRODUCTION

Background

The delta Wadi El-Arish area, north Sinai Peninsula, forms one of the most important parts of Egypt. During World War I, troops stayed in the area to obtain their water needs from shallow wells drilled in alluvium and sand dunes. During World War II, the water resources received a great deal of attention; but, unfortunately, not one of the investigations was completed. During the 1960s, 30 shallow irrigation wells (60 $\pm$ m deep) and eight deep wells (100 $\pm$ m deep) were drilled between the El-Arish and Rafaa areas. After the second Israeli withdrawal from Sinai in 1979, the government replaced the 30 wells mentioned above with 30 new wells. In addition, another 10 wells were drilled for more land irrigation. From 1982 until 1989, the number of wells in the El-Arish area has increased to 145, three times that of 1982 (RIWR, 1989), due to increasing water requirements associated with the increase in irrigated lands.

Location and Extent of the Study Area

Wadi El-Arish extends from the Mediterranean Sea in the north to the mid-Sinai Peninsula in the south. Wadi El-Arish covers an area of about 19,500 km^2, which is about one-third of the Sinai Peninsula in Egypt, as shown in Figure 1. The study has been conducted in the delta Wadi

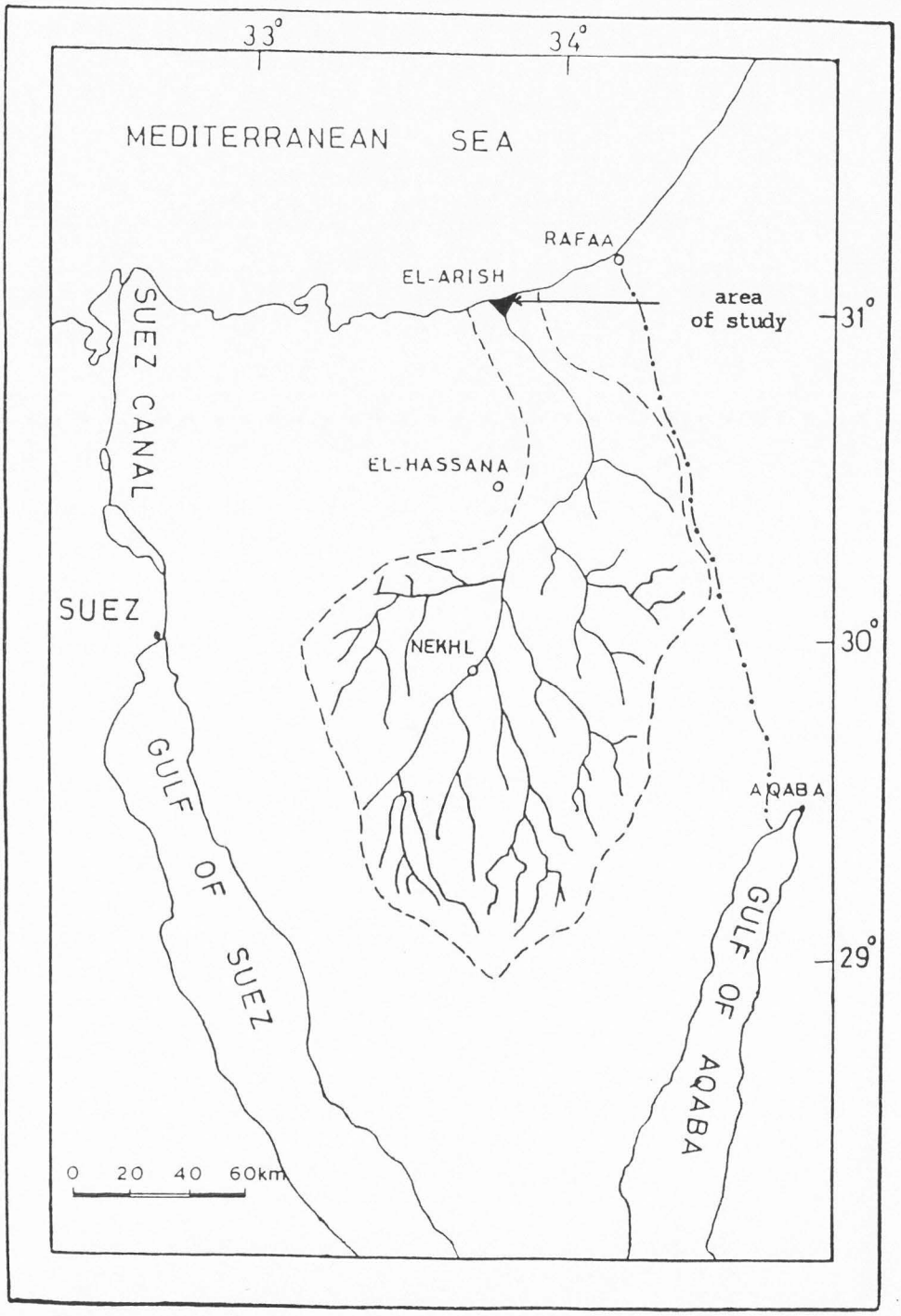

Fig. 1. Location map of the study area.

El-Arish area. The delta Wadi-El-Arish area represents the northern part of Wadi El-Arish. This area, as shown in Figure 1, is bounded by the Mediterranean Sea to the north and latitude 31° 00′ in the south, and between longitude 33° 45′ and 33° 52′ east.

Objectives and Scope of The Study

In recent years, a great amount of attention has been directed towards the construction of agricultural and industrial projects in the Wadi El-Arish area. Accordingly, the increasing development has created greater demand for water that could cause a deterioration of water quality in the groundwater reserves.

The main objectives of the study are:

1. To analyze the hydrogeological data collected on the Quaternary aquifer in the El-Arish area in order to get more information about its hydrogeologic characteristics.

2. To determine the relationship between groundwater extraction and water levels and water quality.

The study includes the determination of the aquifer hydraulic parameters using pumping test data, specifically the drawdown data from a long-duration constant-discharge test, the determination of the direction of groundwater flow, and the determination of the hydrochemistry of the aquifer. In addition, groundwater genesis has been

evaluated using techniques devised by Sulin (1948) to determine the origin of groundwater and the suitability of groundwater for irrigation.

CHAPTER II

LITERATURE REVIEW

Geological Studies

Both surface and subsurface geological studies have been conducted in the study area. These studies are included in the reports by Hume (1929), Moon and Sadek (1921), Farag (1947), Shata (1955), Paver and Jordan (1956), Said and Barakat (1958), Said (1962), Salem (1963), Geofizika (1963), Taha (1968), and El-Shazly et al. (1980).

The surface geological map was constructed from information obtained by Moon and Sadek (1921), Shata (1955), Paver and Jordan (1956), Pavlov and Ayuty (1961), and El-Shazly et al. (1980), as shown in Figure 2. The surface of the study area (Figure 2) is covered by Quaternary sedimentary deposits, except in a small area in the southwest where the Tertiary and Cretaceous rocks are exposed.

During the 1960s, after the 30 shallow wells and 8 deep wells were drilled, subsurface geological studies of the study area were carried out by Salem (1963), Taha (1968), and Dames and Moore (1984). The geology of the area can be summarized from these studies as follows, from the youngest units to the oldest.

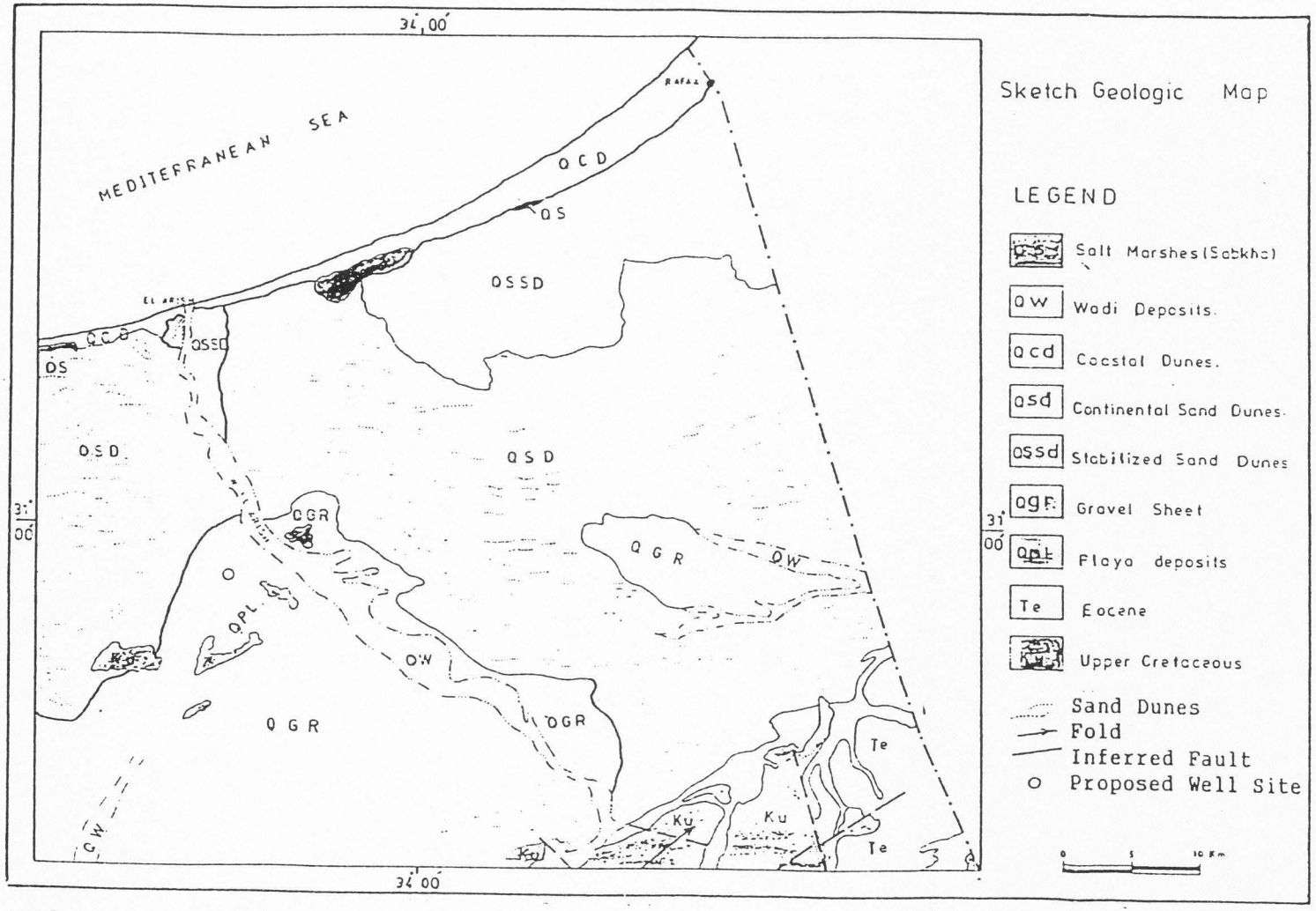

Fig. 2. Sketch geologic map (modified after El-Shazly et al. 1980).

Holocene Deposits

These deposits are distributed in the study area and also to the east, particularly in the coastal area. These deposits have variable thicknesses, and include sand dune accumulations and alluvial deposits.

Sand dune accumulations. These accumulations exist as elongated dune ridges dominating the coastal belt, continental sand dunes, and stabilized sand dunes.

Alluvial deposits. The alluvial deposits include beach deposits and wadi deposits. Beach deposits contain loose sand and poorly consolidated sandstone with shell fragments. The sandstone is mainly quartz grains with calcareous cement. The wadi deposits are distributed along the Wadi El-Arish channel and its tributaries. The deposits range in thickness from 5 to 25 m and they are mainly composed of mixtures of sand, clay, silt, and calcareous materials.

Pleistocene Deposits

These deposits are up to 80 m thick and, according to Shata (1959), Salem (1963), and Taha (1968), are classed as follows.

Alluvial deposits of Wadi El-Arish. The alluvial deposits of Wadi El-Arish occupy the greater part of the area. Three series have been reported, the upper, middle, and lower. The upper series (13 m thick) is light brown, cross-bedded, medium to coarse sands intercalated with yellow silt. The middle series (10 m thick) consists of

alternating sands and yellow calcareous clays. The lower series (43 m thick) consists of alternating gravel and coarse sands interbedded with yellow calcareous clay.

Taha (1968) reported that there are other gravel beds (23 m thick) intercalated with calcareous silt below this lower series, and he reported also that these gravel beds are completely missing south of Lahfan. Taha (1968) described the gravel beds as gray and brown gravel interbedded with calcareous silt. These gravel beds fine upward and are explained as deltaic deposits.

Old beach deposits. These deposits are mainly composed of fine to coarse, well-sorted sand and sandstone intercalated with clay beds. These deposits are found on the coastal zone between the El-Arish and Rafaa areas.

Calcareous sandstone (kurkar). Taha (1968) divided the kurkar into two series: 1) the upper continental kurkar, which is 20 m thick; and 2) the lower series, which is 40 m thick and contains many shell fragments and is described as a sequence of marine deposits.

The kurkar deposits rarely extend more than 10 km to the south of the Mediterranean Sea. Calcareous sandstone (kurkar) is overlain by alluvial deposits and is underlain by a Pliocene conglomerate layer.

Pliocene Formation

According to Shata (1960) and Salem (1963), the Pliocene formation is divided into two distinct series: 1)

the upper series is composed of conglomerate and is found at the base of the Pleistocene deposits; and 2) the lower series is composed of yellow marl beds.

Miocene Formation

This formation is composed of dark green sticky clay that is overlain by the Pliocene yellow marl.

Eocene Formation

The Eocene formation is not penetrated by any well drilled in the delta Wadi El-Arish area. Shata (1960) divided it into three series: 1) the upper series, which is composed of gypsum, clay, and chalk (50 m thick); 2) the middle series, which is composed of siliceous and chalky limestone (60-100 m thick); and 3) the lower series, which is composed of limestone and chalk with flint (60 m thick).

Shata (1955) studied the geological structure of the northern Sinai Peninsula. He stated that the study area is situated along the southern flank of the great South Mediterranean Synclinal Basin. This basin is bounded to the south by the NE-SW trending anticlinal structures El-Halal, Yelleg, El-Maghara, and Risan Eniza. The following structures were studied by Shata (1955): 1) Risan Eniza--El-Kharruba anticline; 2) El-Arish--El-Massaeid syncline; 3) El-Gora--El-Magdaba syncline; 4) Rafaa anticline; and 5) NE-SW fault systems at Lahfan, Risan Eniza, El-Khabra, and El-Gora.

Based upon geophysical and oil exploration drilling interpretation, a recent structural map of the study area and surrounding areas was produced (RIWR, 1989), as shown in Figure 3.

Hydrogeological Studies

Hydrogeological and hydrochemical studies of the delta Wadi El-Arish area have been conducted by many workers and agencies. These studies include those by Paver and Jordan (1956), Saad (1962), Geofizika (1963), Taha (1968), Dames and Moore (1984), and the General Authority for Rehabilitation Projects and Agricultural Development (GARPAD) (1984).

The hydrogeological studies demonstrated that the greatest potential for development of groundwater exists in the Quaternary formations, which include several distinct aquifer systems with different hydrochemical characteristics. These previous studies can be summarized as follows.

Paver and Jordan (1956) studied the 28 wells that existed in delta Wadi El-Arish at that time. They used water-level measurements from these wells to draw a potentiometric map of the El-Arish area in 1954, as shown in Figure 4. They stated that the main recharge to the Quaternary aquifer of delta Wadi El-Arish is by direct

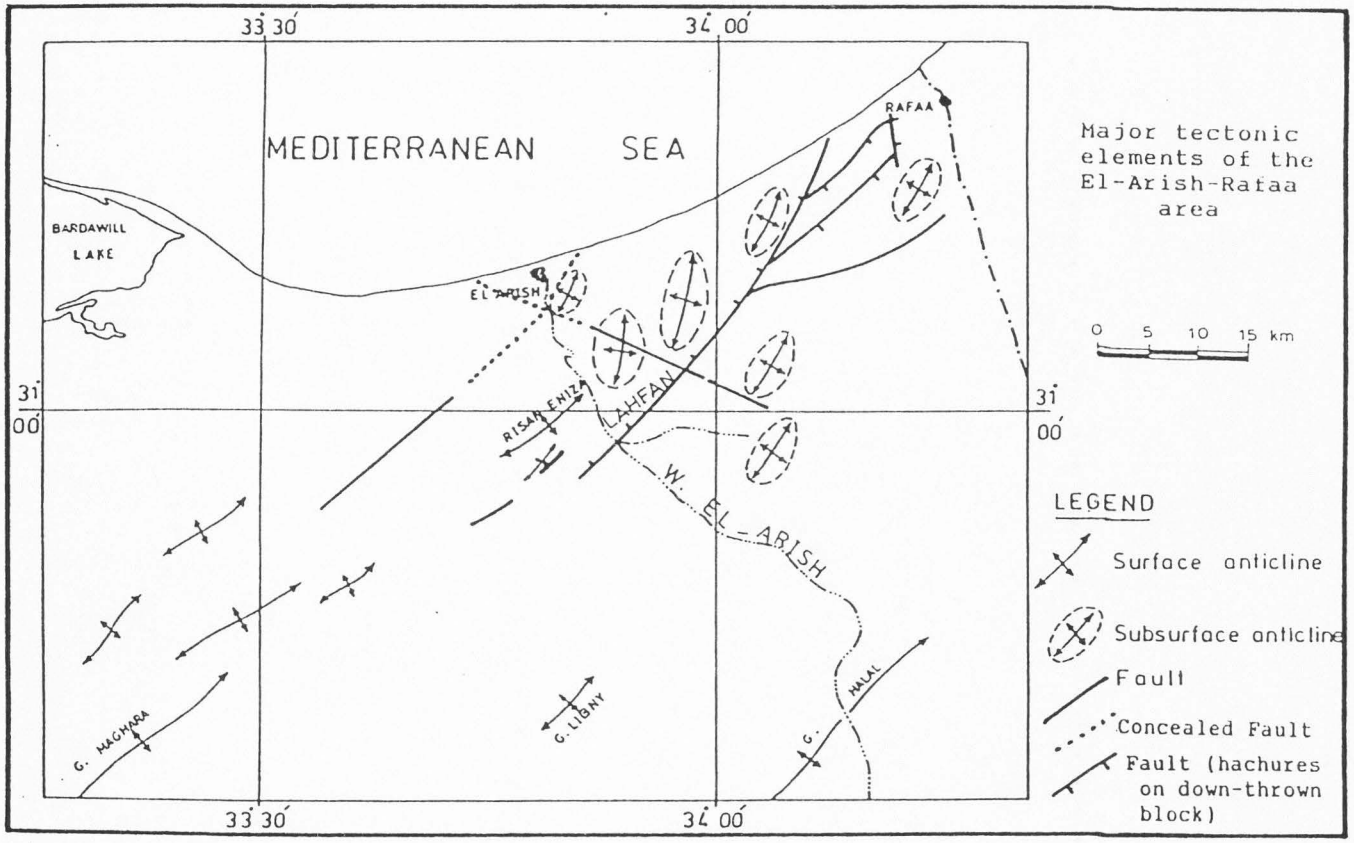

Fig. 3. Structural map (after RIWR, 1989).

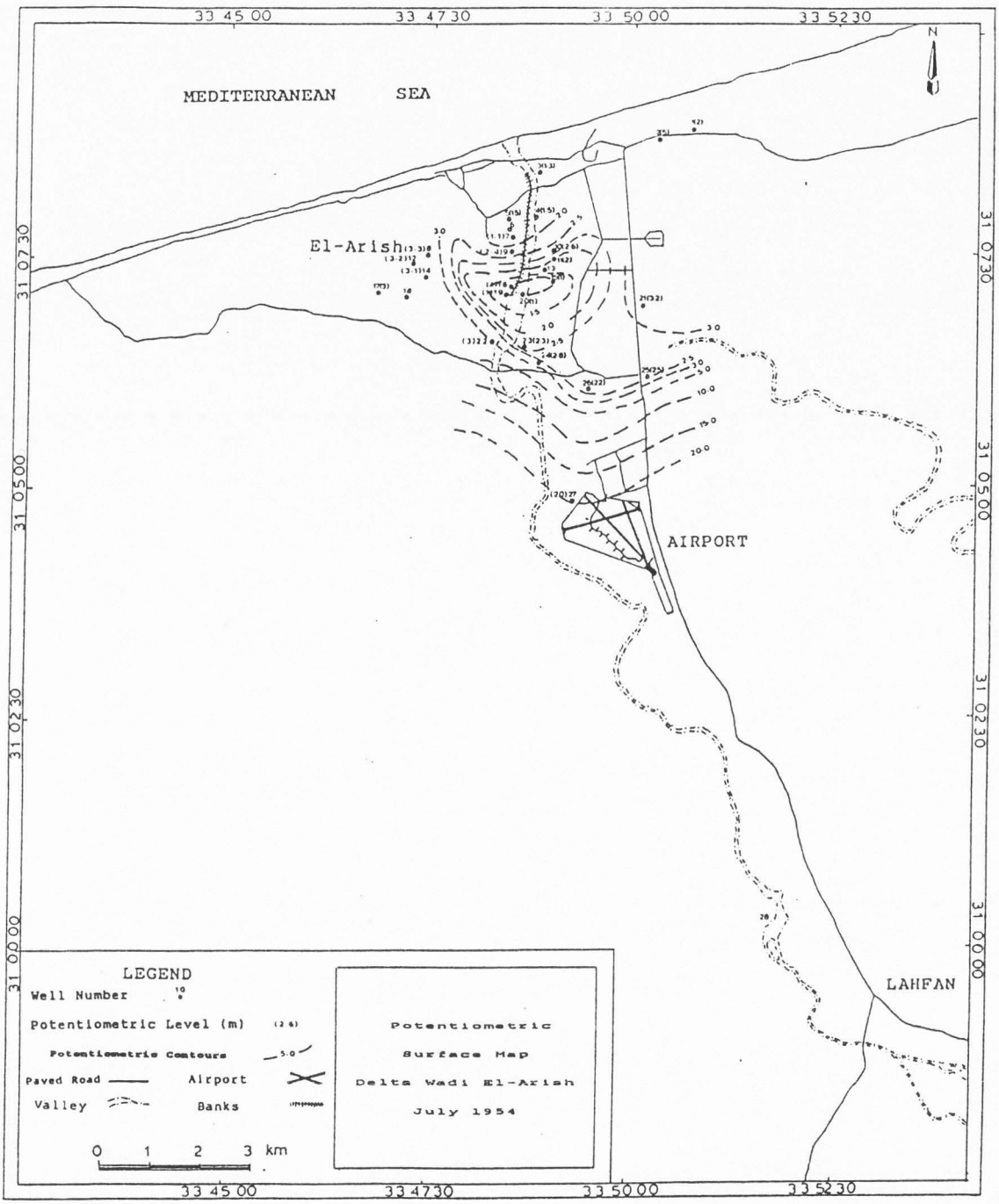

Fig. 4. Potentiometric surface map, July 1954 (from Paver and Jordan, 1956).

rainfall, infiltration from surface runoff, and subsurface flow from the south and southeast. They estimated the recharge at about 25,000 m^3/day. They also reported that extraction of groundwater was 5,600 m^3/day in 1954.

Saad (1962) reported that recharge to the Quaternary aquifer is by infiltration from local rainfall (10,000 m^3/day) in addition to upward leakage of groundwater from the deep Cretaceous formation through the fault at Lahfan (20,000 m^3/day). Saad calculated the horizontal hydraulic gradient in 1962 to be 0.0032, and measured water-level fluctuations of about 0.5 m from April 1961 to September 1962. He carried out pumping tests on two wells (No. 22 and No. 29) tapping the Quaternary aquifer, and estimated the transmissivity to be 1,000-2,000 m^2/day and the storativity to be 0.003-0.087.

Geofizika (1963) conducted a field survey of the wells in the El-Arish area and reported that the major recharge to the Quaternary aquifer is by upward leakage from the older Cretaceous aquifer through the Lahfan fault instead of direct infiltration from rainfall or from the surrounding sand dunes. It was also reported that the hydraulic gradient was 0.006, and that 21,400 m^3/day was extracted from 34 wells in 1962. The hydraulic conductivity was determined from three pumping tests conducted by Geofizika, and ranged from 10 to 80 m/day. The potentiometric map in 1962, as shown in Figure 5, showed declines in the

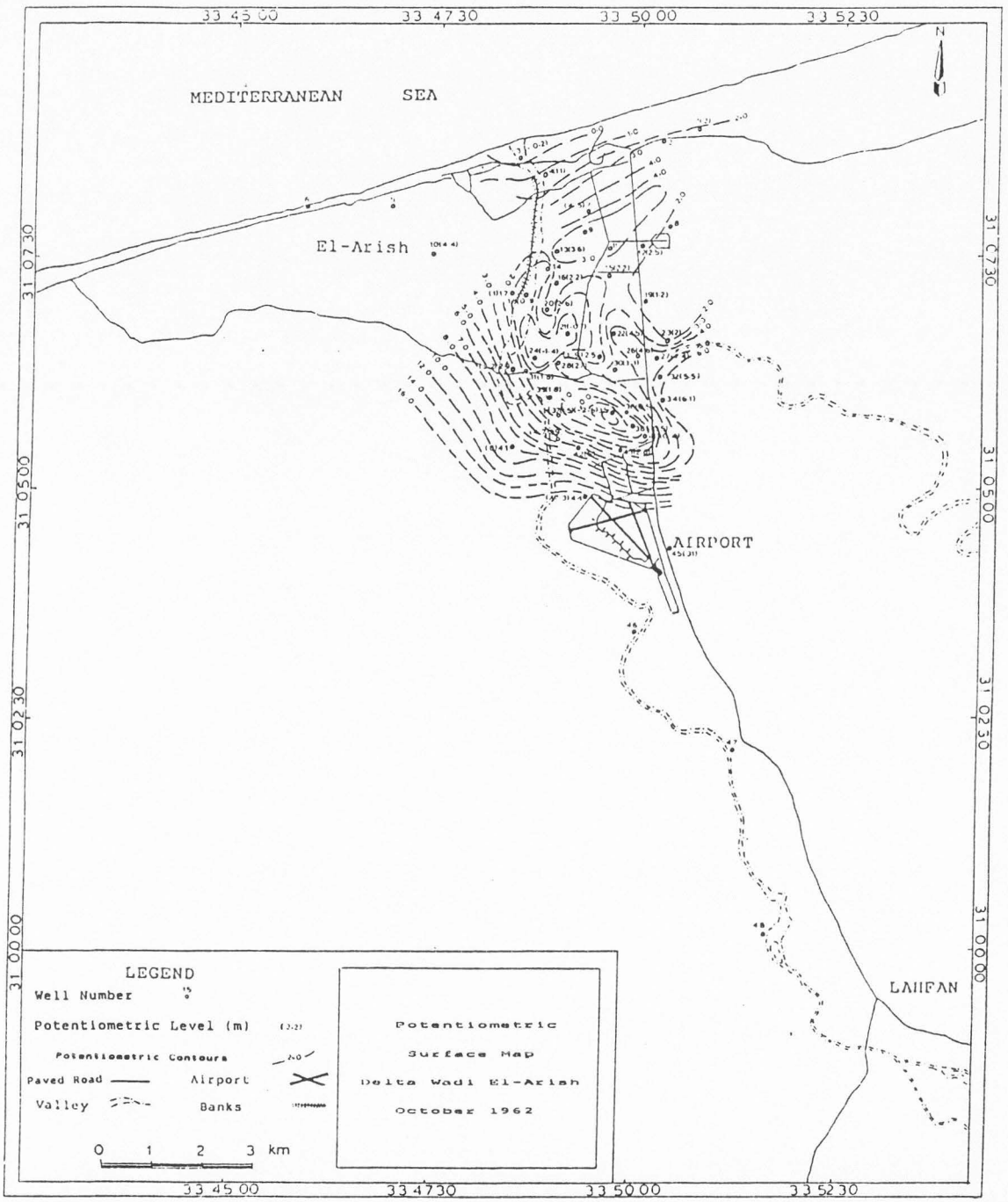

Fig. 5. Potentiometric surface map, October 1962 (Geofizika, 1963).

potentiometric surface near the El-Arish airport and to the east of El-Arish town of 0.7 to 2.6 m as a result of overpumping.

Taha (1968) studied the hydrogeology of the Quaternary aquifer in the El-Arish area. He interpreted the geological, hydrogeological, and hydrochemical data, and subdivided the aquifer system into the following units: 1) Sand dunes; 2) upper Pleistocene alluvial deposits (sand and gravel intercalated with silt); 3) old beach deposits (sand, sandstone, and clayey sand) in the area between El-Arish and Rafaa; and 4) lower Pleistocene calcareous sandstone (kurkar) in the area between El-Arish and Rafaa containing water slightly more saline than in the Wadi El-Arish area.

Dames and Moore (1984) conducted a field survey of water levels and water salinity in 1981 and drew a potentiometric map in the El-Arish area, as shown in Figure 6. They said that about one-third of the total recharge to the Quaternary aquifer is from the deep Cretaceous aquifer through the fault at Lahfan, which was estimated to be 27,000 m^3/day, and the rest of the recharge is from infiltration from direct rainfall and subsurface flow. They estimated that groundwater extraction rate from 50 wells was 25,000 m^3/day.

Based upon water-level measurements obtained by REGWA in 1982, GARPAD (1984) reported that the total recharge to the El-Arish aquifer is about 46,700 m^3/day from

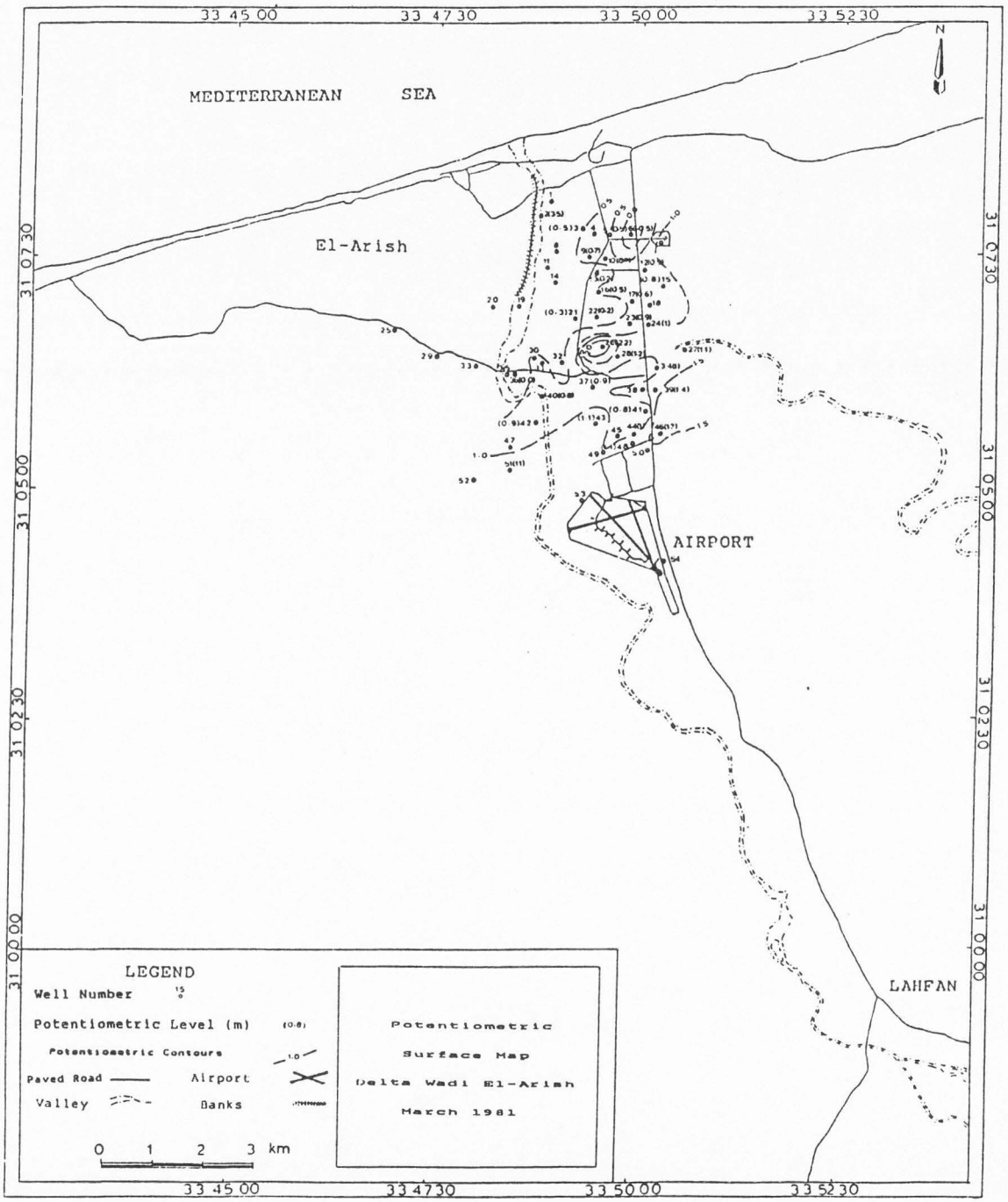

Fig. 6. Potentiometric surface map, March 1981 (Dames and Moore, 1984).

infiltration from direct rainfall and subsurface flow from the south. It was also reported that the total groundwater extraction from 116 wells was about 51,000 m^3/day in 1982. The groundwater extraction rate in 1982 was about twice the rate in 1981 because 116 wells were included in the 1982 study (GARPAD, 1984), while only 50 wells were included in the 1981 study (Dames and Moore, 1984). GARPAD concluded that in order for the system to be balanced, 4,300 m^3/day has to be derived by vertical leakage from the underlying calcareous sandstone (kurkar), which has caused the deterioration in water quality in the area.

Hydrochemical Studies

Paver and Jordan (1956) described the contact between the fresh and the saline zones in the El-Arish area. They determined the boundary between the two zones to be the line of 2,500 mg/l TDS, as shown in Figure 7. Paver and Jordan reported that any overpumping from the aquifer allowed the saline water to flow into the fresh water zone.

Using a map of the TDS, as shown in Figure 8, Geofizika (1963) divided the El-Arish area into two distinct zones, the western zone where the electrical conductivity (EC) is low (2,000 < EC < 4,000 μmhos/cm), and the eastern zone where the EC is high (4,000 < EC < 6,000 μmhos/cm). Geofizika attributed this lateral change in TDS to the higher hydraulic conductivity of the aquifer in the western zone and to the constant flushing of salts out of the

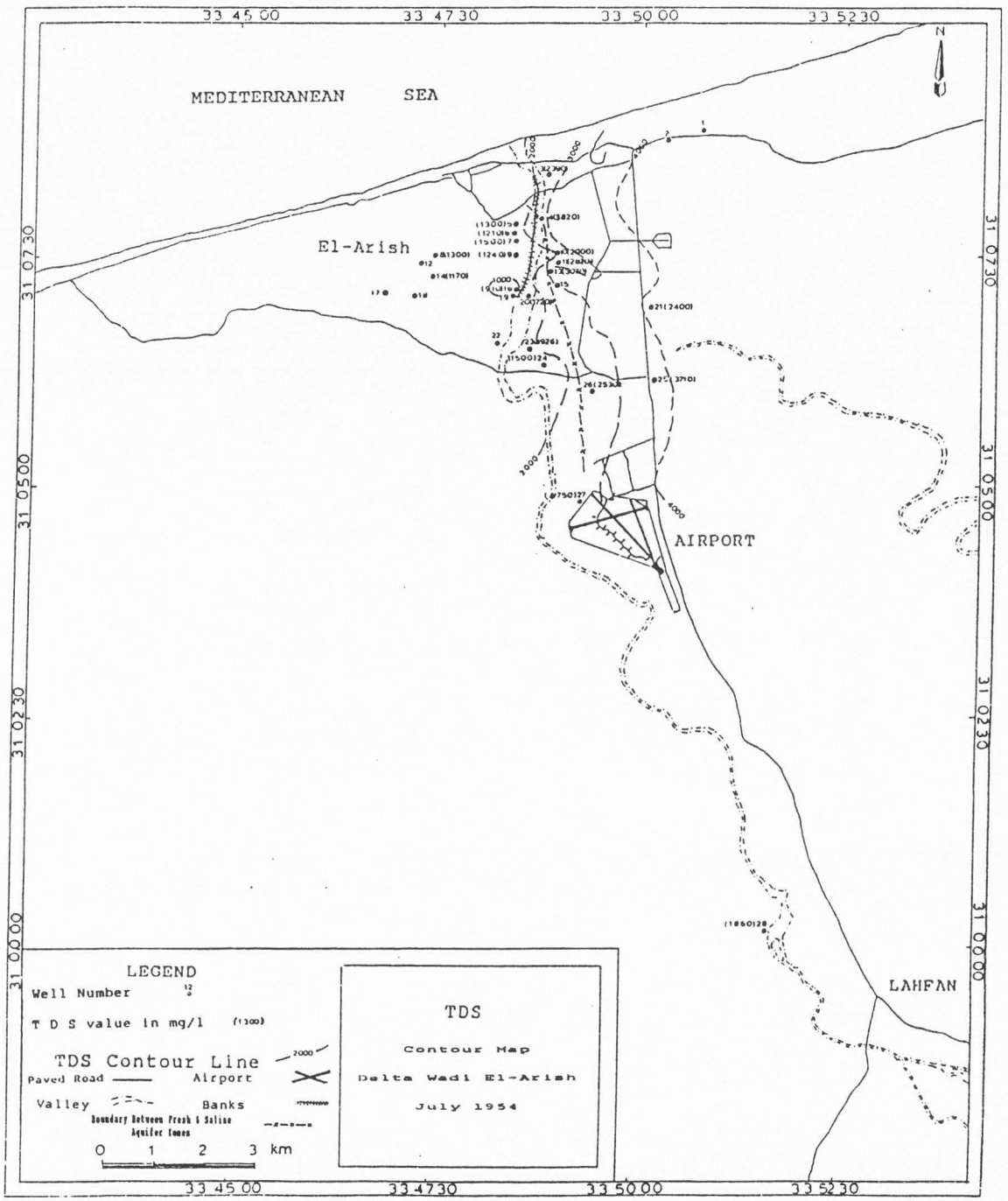

Fig. 7. TDS contour map, July 1954 (Paver and Jordan, 1956).

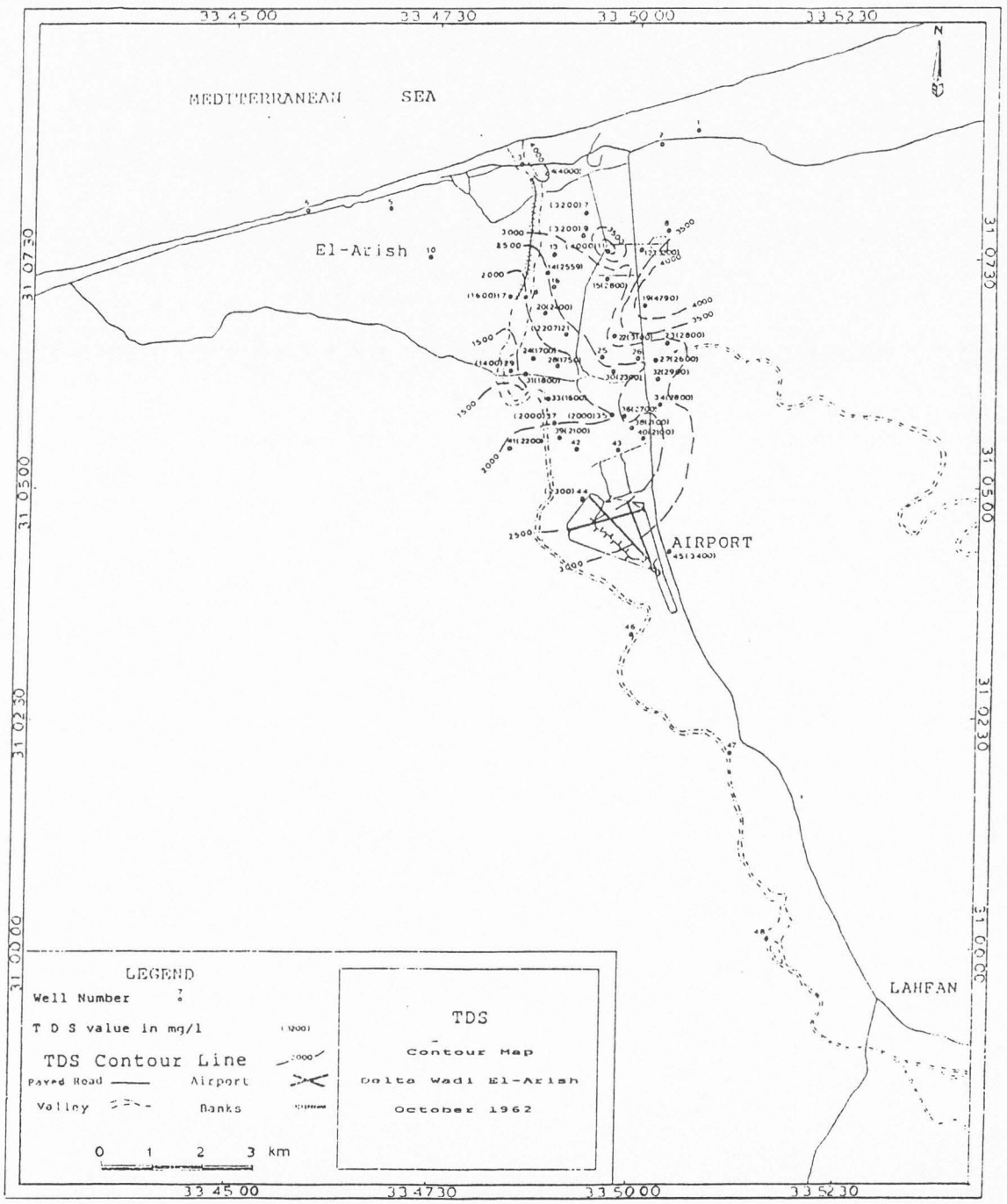

Fig. 8. TDS contour map, October 1962 (Geofizika, 1963).

aquifer along the direction of flow.

Based upon his TDS survey done in 1968, Taha reported that the changes in TDS are related to the rainy seasons, because the highest TDS occurs in July and the lowest TDS occurs in April. Taha attributed the low groundwater TDS in the western part of the El-Arish area to the continuous recharge from the sand dunes that cover most of the western surface area, and also to groundwater inflow through a number of buried channels under the sand dunes.

Dames and Moore (1984) noted that there is a similarity between the TDS map of the Quaternary aquifer in the El-Arish area prepared by them in 1981, as shown in Figure 9, and the 1962 map (Figure 8). The increase in TDS to the north of the El-Arish airport was attributed to the inflow of saline water into the aquifer by vertical movement from the deep aquifer along the Lahfan fault.

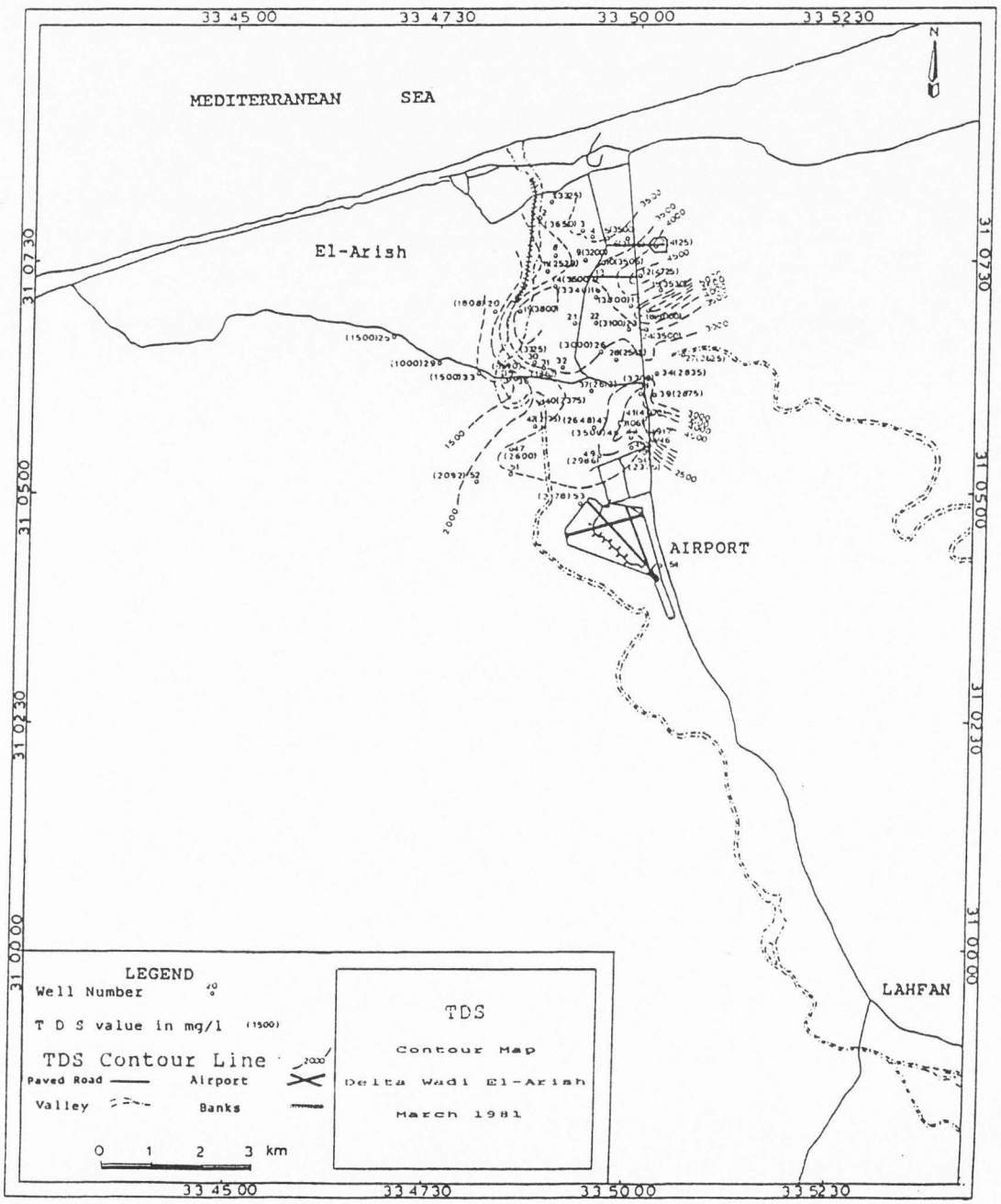

Fig. 9. TDS contour map, March 1981 (Dames and Moore, 1984).

CHAPTER III

HYDROGEOLOGY

Groundwater studies require that certain types of field data be collected in order to characterize the groundwater system, such as determining the direction of flow and estimating the hydraulic parameters of the water-bearing formations. To achieve these objectives, a field investigation was carried out. The information obtained during the field investigation is presented below.

Well Location and Numbering System

A field survey of the wells in the study area was carried out to determine well location coordinates, casing elevations, and ground surface elevations. The well field survey was performed by the Institute of Survey, Ministry of General Works and Water Resources, Egypt. One hundred seventy-six wells were surveyed; however, only 69 wells were used for the present study. Based upon a systematic well numbering system, a unique identification number was assigned for each well. In this numbering system, the area was divided into equal ten-by-ten-kilometer-square grids. These grids were sequentially numbered from the north to the south. The number of each well consisted of two numbers separated by a hyphen. The first number referred to the number of the grid in which the well was located. The second number was the well number inside each square grid,

also sequentially numbered from the west to the east. Figure 10 shows the location of the wells in the study area. Note that the topography affects the well distribution, as few wells have been drilled in the western portion of the area because it is covered with sand dunes.

The Aquifer System

The main aquifer system in the delta Wadi El-Arish area is comprised primarily of Quaternary deposits. The Quaternary aquifer in this area consists of two units: the upper Pleistocene alluvial gravel unit and the underlying lower Pleistocene calcareous sandstone (kurkar) unit. Most of the wells in the delta Wadi El-Arish area have been completed in both units of the Quaternary aquifer.

Four hydrogeologic cross sections were constructed, based on the hydrogeologic data (Table 1), to show the hydrogeology of the Quaternary deposits in the delta Wadi El-Arish area (RIWR, 1989). These cross sections, as shown in Figure 11, trend in different directions within the delta Wadi El-Arish area. Cross section I-I' (Figure 12) trends in a north-south direction and passes through wells 1-134, 1-128, 1-137, 1-136, G.D.D.0 29, G.D.D.0. (D), and G.D.D.0. (H) along the east side of the El-Arish--Lahfan road. Cross section II-II' (Figure 13) trends in a north-south direction and passes through wells 1-104, 1-98, 1-88, 1-78, 1-84, and 2-6. Cross section III-III' (Figure 14) trends in an east-west direction and passes through wells 1-141, 1-

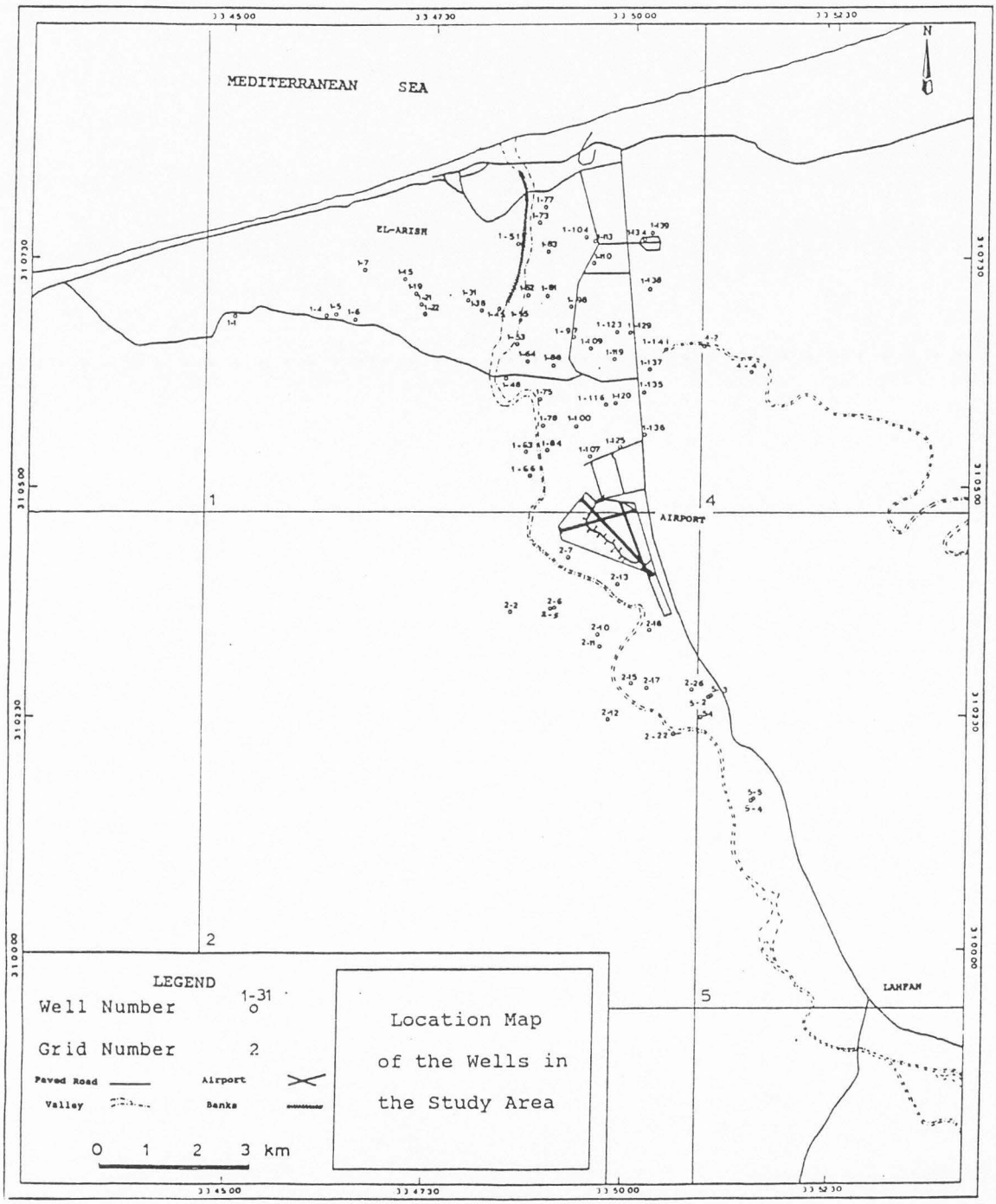

Fig. 10. Location map of the wells in the study area.

Table 1. Hydrogeologic Data from Delta Wadi El-Arish Wells (RIWR, 1989)

Well No.	Ground Elevation (m) a.MSL	Well Data Total Depth (m)	Screen Interval (m)	Water Level (m) a.MSL in June 1988	Alluvial Deposits Elevation (m) a.MSL Top	Alluvial Deposits Elevation (m) a.MSL Bottom	Kurkar Deposits Elevation (m) a.MSL Top	Kurkar Deposits Elevation (m) a.MSL Bottom
1-63	20.19	60	42-57	-1.59	8.2	-18.8	-18.8	
1-64	18.33	82		-2.18	-5.4	-20.6	-20.6	
1-78	18.95	55	35-50	-1.43	7.5	-22	-22	
1-84	20.33	55	40-50	0.0	8.3	-18.2	-18.2	
1-88	19.12	100		-2.01	-5.4	-45.4	-45.4	
1-98	20.02	54	40-50	-1.34	-14	-30	-30	
1-104	17.31	60	32-40	-2.47	10.3	-8.2	-8.2	
1-115	28.62	60	43-58		11.6	-15.4	-15.4	
1-119	23.37	62	43-58	-0.53	6.3	-13.2	-13.2	
1-128	20.6	54	30-42		1.6	-12	-12	
1-134	19.25	78	45-54	0.92	1.5	-24.2	-24.2	
1-136	27.88	66	45-60		10.4			
1-137	24.39	65	44-60	0.29	13.9	-28.1	-28.1	
1-141	23.75	64	46-61		15.2	-26.2	-26.2	
2-6	33.84	93	40-48	1.33	6.8	-3.6	-3.6	-33.6
GDDO (D)	40.7	77			36.5	0.7	0.7	-3.3
GDDO (H)	45.5	107			35.9	7.7		
GDDO 29	36.5	38			25			
Massaeid Piez. 82	25	114	35.5-45.5	0	-17.5	-27.5	-27.5	-43.5

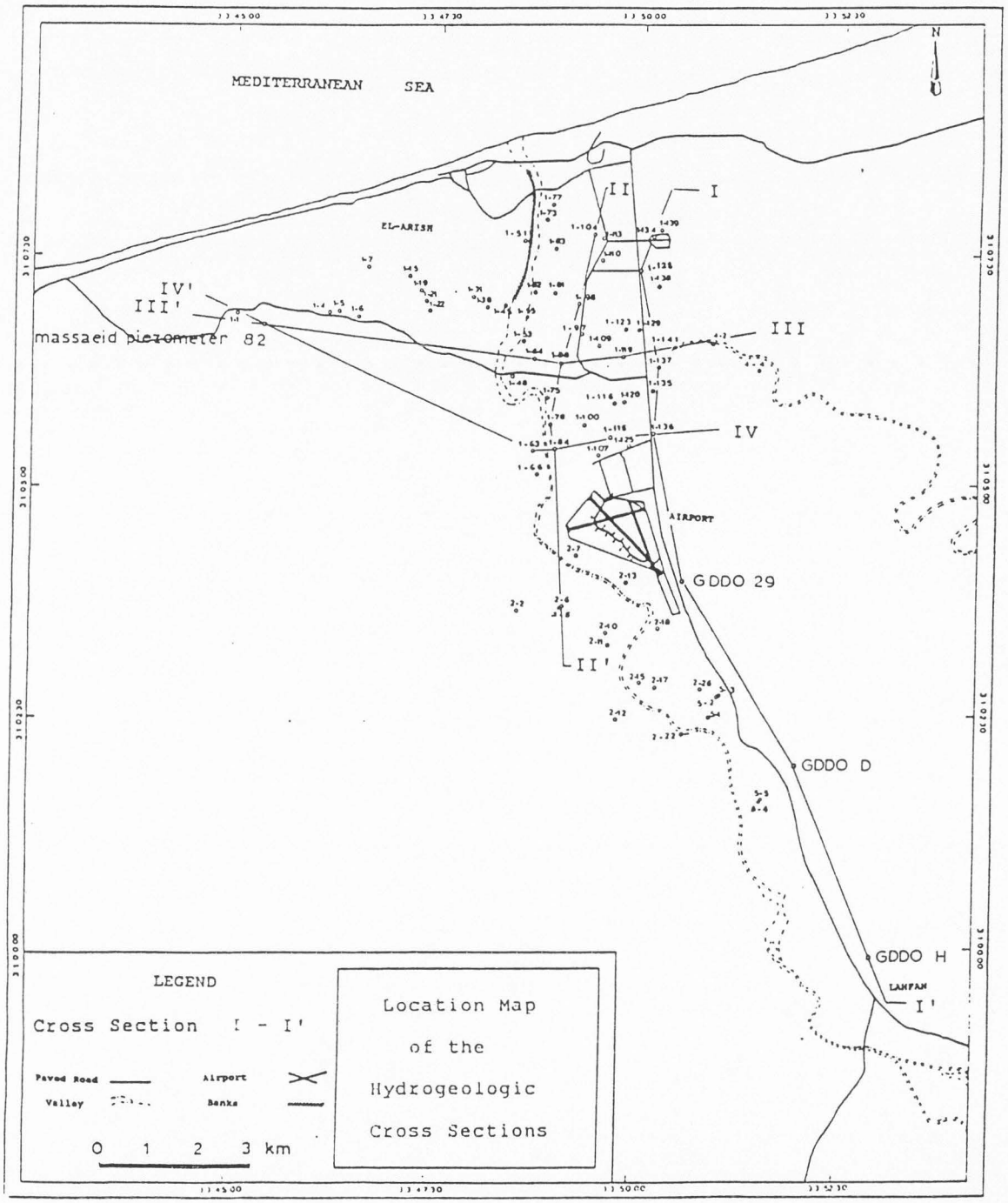

Fig. 11. Location map of the hydrogeologic cross sections (RIWR, 1989).

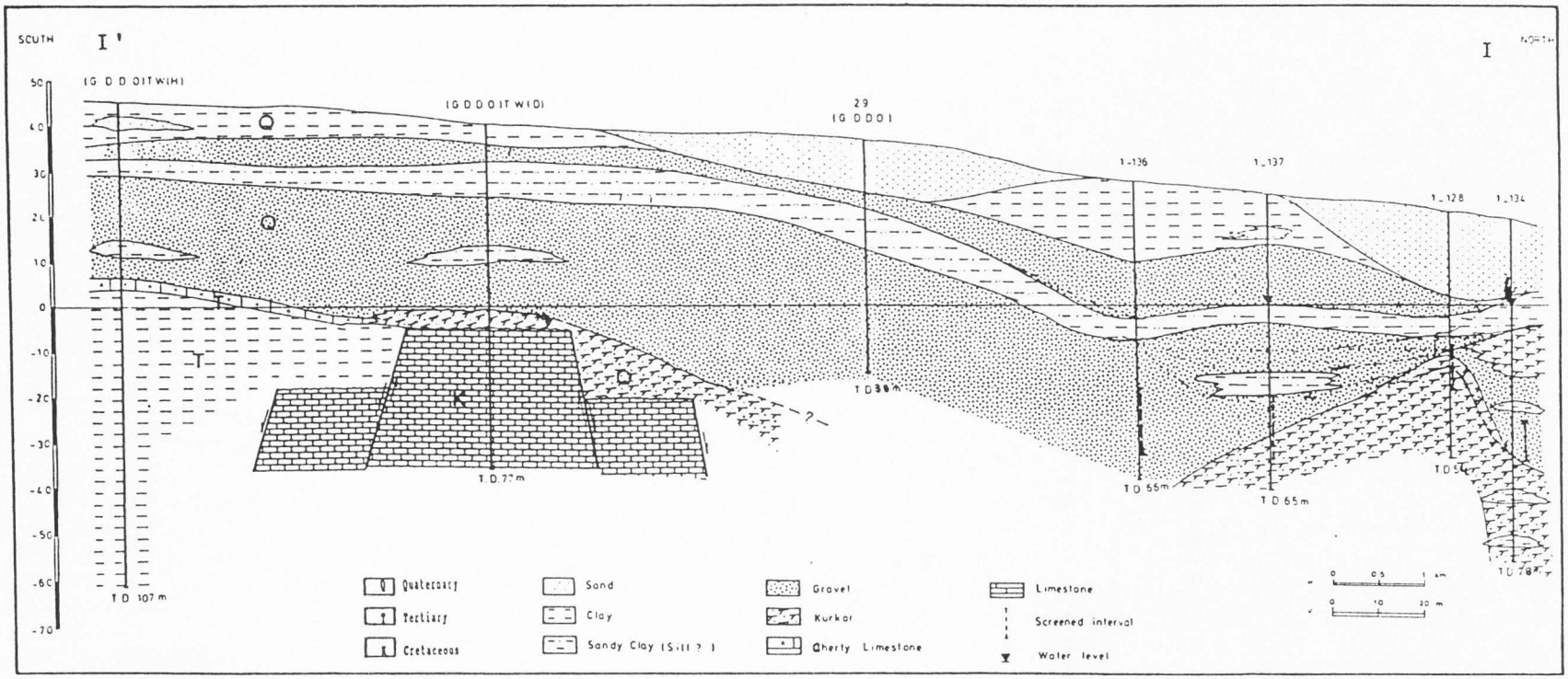

Fig. 12. Hydrogeologic cross section I - I′ (RIWR, 1989).

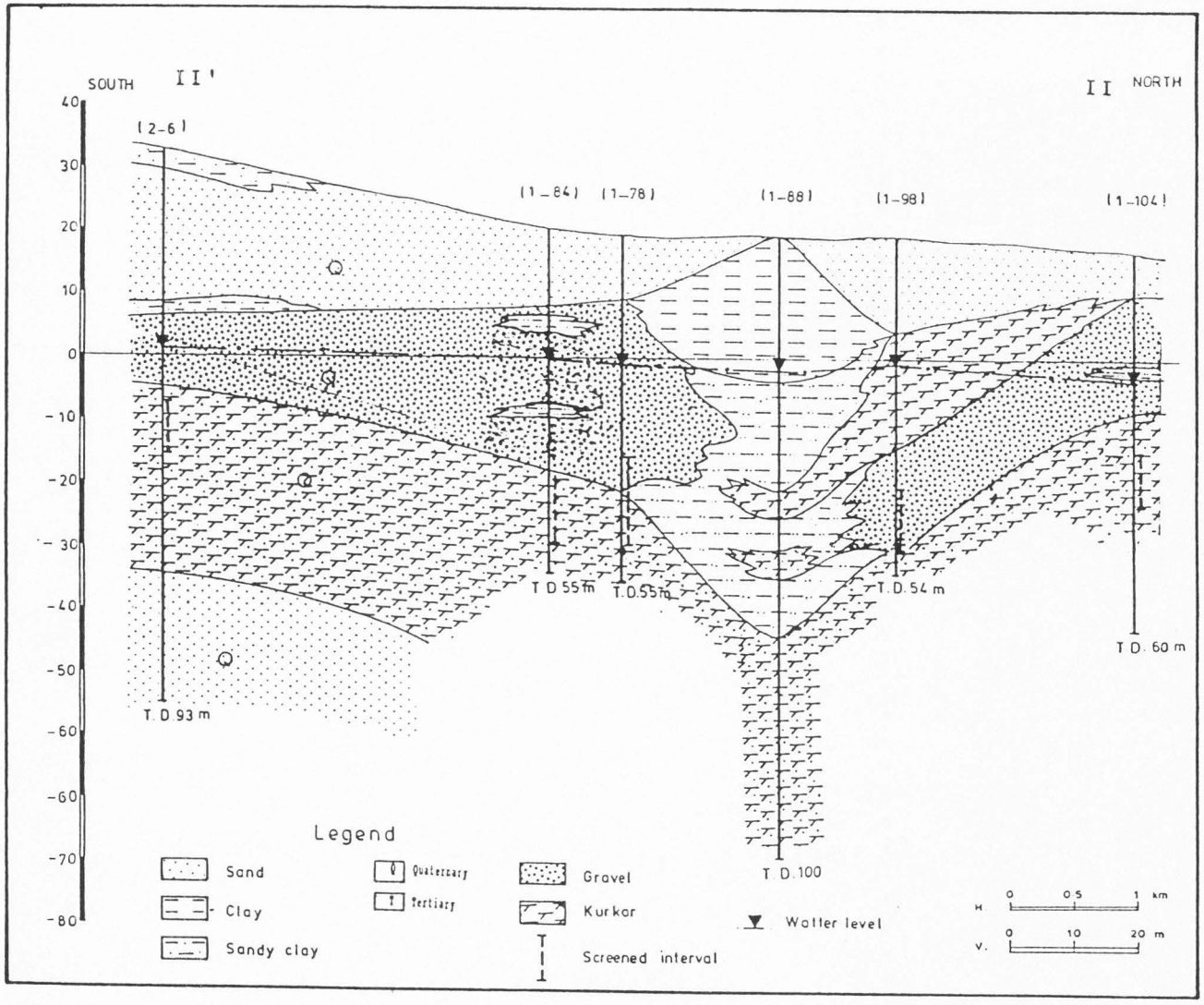

Fig. 13. Hydrogeologic cross section II - II' (RIWR, 1989).

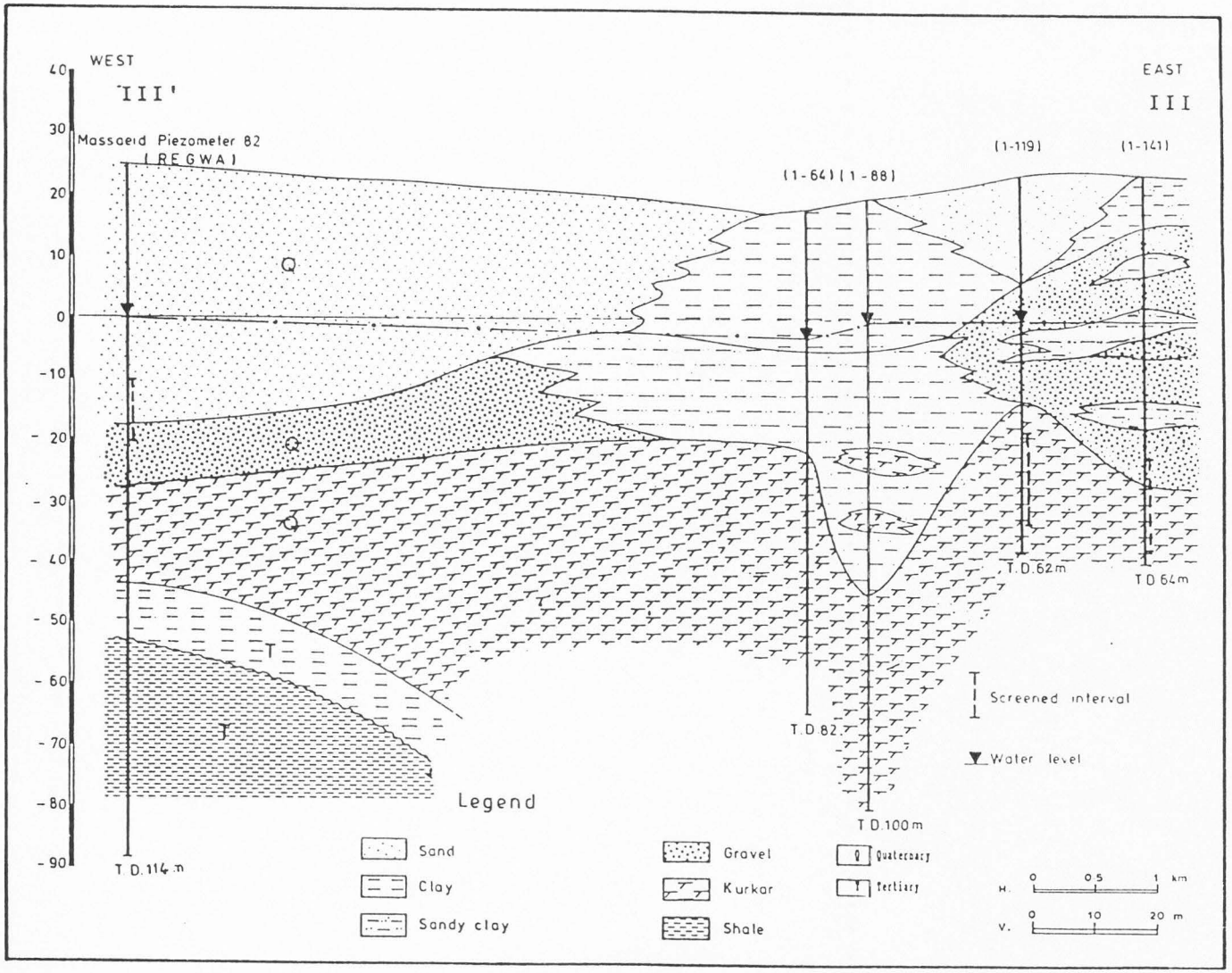

Fig. 14. Hydrogeologic cross section III - III' (RIWR, 1989).

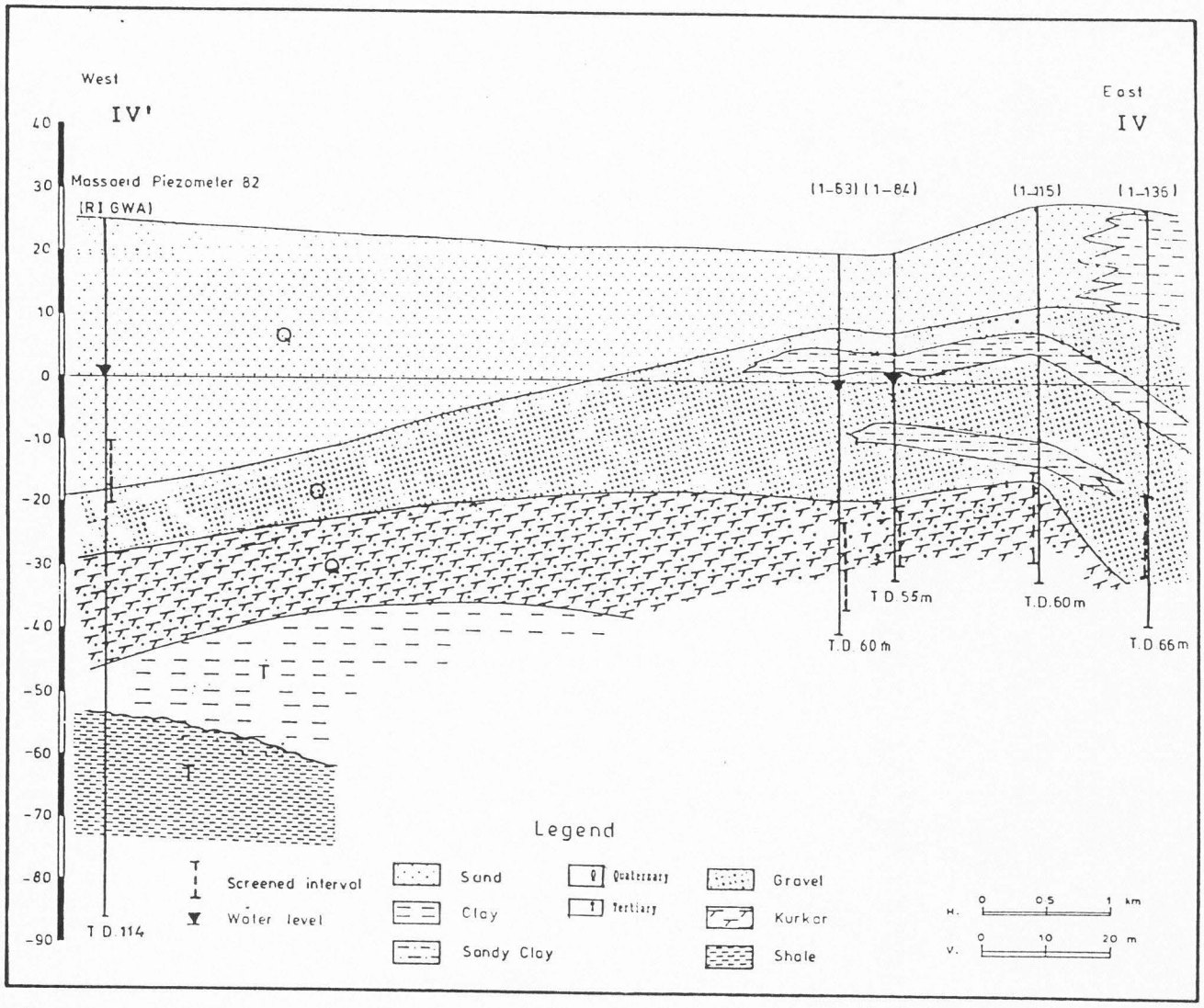

Fig. 15. Hydrogeologic cross section IV - IV' (RIWR, 1989).

119, 1-88, 1-64, and Massaeid piezometer 82. Cross section IV-IV' (Figure 15) also trends in an east-west direction and passes through wells 1-136, 1-115, 1-84, 1-63, and Massaeid piezometer 82. From the cross sections, shown in Figures 12 through 15, it can be seen that all the wells in the delta Wadi El-Arish area partially penetrate the Quaternary aquifer except for three deep wells, belonging to the Research Institute for Water Resources, which fully penetrate the Quaternary aquifer. These three wells and their associated piezometers are located in the southern part of the study area. Two wells, 5-2 and 5-4, and the corresponding two piezometers, 5-3 and 5-5, are located south of the El-Arish airport, while the third well, 2-5, and the associated piezometer, 2-6, are located southwest of the El-Arish airport. The lithologic units displayed in these sections, from youngest to oldest, are described below.

Holocene Deposits

Holocene deposits are predominantly clay, and vary in thickness from 10 to 18 m in cross section I-I'. This clayey layer changes into a quartz sand that ranges in thickness from 30 to 50 m north and east of the El-Arish airport.

In cross section II-II', Holocene deposits consist of quartz sand that changes into sandy clay and clay at wells 2-6 and 1-88, respectively.

In cross section III-III', Holocene deposits consist of quartz sand that decreases in thickness until it pinches out in the middle of the section at wells 1-64 and 1-88. The quartzose sandy layer changes into clay and sandy clay at wells 1-64 and 1-88, and at well 1-141 at the Wadi El-Mazzar in the eastern part of the section. Clay at wells 1-64 and 1-88 was deposited by the delta of Wadi El-Mazzar to the east of Wadi El-Arish at the same time as the quartz sand.

In cross section IV-IV', Holocene deposits are composed of quartz sand that decreases in thickness to the east. This quartz sand changes into a sandy clay layer at well 1-136 on the east side of the section.

Pleistocene Deposits

Pleistocene deposits consist of two distinct units; alluvial deposits and calcareous sandstone (kurkar).

Alluvial deposits. Alluvial deposits, which represent the upper Pleistocene unit, are composed of gravel interbedded with sandy-clay layers. This gravelly layer ranges in thickness from 30 to 50 m or more in cross section I-I'. At well 1-128 in the northern part of the section, there is a decrease in the thickness of the gravelly layer. This is attributable to the underlying structural high. The gravel is overlain by a continental calcareous sandstone in the northernmost portion of the section.

In cross section II-II', alluvial deposits consist of gravelly layers that increase in thickness to the north at

well 1-78. The gravel is overlain by a thin sandy clay layer at well 2-6, while at well 1-88 the gravel disappears and is replaced by a very thick clay and sandy clay unit interbedded with continental kurkar. This clay and sandy clay unit is directly underlain by calcareous sandstone (marine kurkar). This thick sandy clay at well 1-88 presumably was deposited in the early Pleistocene by the delta of Wadi El-Mazzar to the east of Wadi El-Arish, which became active at this location and deposited these clay materials at the same time as the calcareous sandstone (marine kurkar).

In cross section III-III', the alluvial deposits are composed of a gravelly layer that grades into sandy clay at wells 1-64 and 1-88. The gravelly layer is quite thick at well 1-141 on the easternmost edge of the section, and is interbedded with some sandy clay layers. This gravel is underlain by marine kurkar and is overlain by Holocene sandy clay.

In cross section IV-IV', the alluvial deposits consist of a gravelly layer that is continuously overlain by Holocene quartz sand. This gravelly layer increases in thickness and is interbedded with thin layers of sandy clay towards the east.

Calcareous sandstone. Calcareous sandstone, which represents the lower Pleistocene unit, was defined as a marine kurkar according to Taha (1968). The sandstone

(kurkar) unit is directly overlain by alluvial deposits and is fully penetrated at the G.D.D.O. well (D) in cross section I-I', where the unit is thinnest before pinching out to the south. At well (D), the kurkar unconformably overlies Cretaceous limestone, which has been structurally uplifted by a set of normal faults. These faults have been inferred from the depths of the lithologic units on both sides of well (D).

In cross section II-II', calcareous sandstone (marine kurkar) is overlain by alluvial deposits. The base of the marine kurkar unit is only penetrated by well 2-6.

In cross section III-III', calcareous sandstone (marine kurkar) exists across the entire section, and is overlain by alluvial deposits. The base of this unit was only penetrated near the western side of the section at Massaeid piezometer 82.

In cross section IV-IV', calcareous sandstone (marine kurkar) is present throughout most of the section. The bottom of the unit is only penetrated by one well, Massaeid piezometer 82, in the western part of the section.

The following can be concluded from the previous discussion:

1. The stratigraphic section in the delta Wadi El-Arish area consists of Holocene deposits comprised of quartz sand changing into sandy clay in some parts and leistocene deposits, which form the main aquifer in the delta Wadi El-

Arish area. The Pleistocene deposits can be divided into two distinct units: a) the upper Pleistocene alluvial unit, which consists of gravel interbedded with sandy clay layers, and with the continental calcareous sandstone in the northern part of the study area, and b) the lower Pleistocene calcareous sandstone unit (marine kurkar), which consists of sandstone with shell fragments that directly underlie the upper Pleistocene gravel. This marine kurkar unit disappears at well GDDO (H) in the southern part of the area. The Quaternary units unconformably overlie either Pliocene cherty limestone (conglomerate) in the southern part of the study area at well GDDO (H) or upper Cretaceous limestone at well GDDO (D).

2. In the area east of the El-Arish--Lahfan road and east of the Wadi El-Arish channel (as shown in Figures 12 and 14), the sandy clay layer found at the surface possibly prevents the infiltration of precipitation to the underlying layers. On the other hand, this sandy clay changes to quartz sand, particularly in the western portion of the study area, which possibly serves as a recharge area for the deeper aquifers.

3. The presence of the sandy clay layer overlying or interbedded with the gravel layer partially confines the underlying unit.

Hydrogeological Characteristics

Five sets of quarterly water-level measurements have been collected from the wells in the delta Wadi El-Arish area. These seasonal water-level measurements reflect the seasonal changes in the elevation of the potentiometric surface. Twenty-eight to thirty wells were monitored in the El-Arish area. These wells were monitored because their water levels could be measured with an electric sounder.

As previously mentioned, most of the wells where water levels were measured are completed into both the lower portion of the upper Pleistocene alluvial sand and gravel unit and the upper portion of the lower Pleistocene calcareous sandstone unit. Consequently, the measured water levels do not define the static water level of either one of the two units but represent a combined water level for both units.

The water-level measurements have been corrected to mean sea-level data. Measurements of water levels in the wells were made in June 1988, February 1989, July 1989, October 1989, and January 1990 (see Table 2).

Potentiometric Surface Map
June 1988

A potentiometric surface map has been constructed based upon the water-level measurements taken in June 1988 (Figure 16). The map shows that the zero potentiometric contour line surrounds a large area of the delta Wadi El-Arish.

Table 2. Potentiometric Level Data from Delta Wadi El-Arish Area

Well No.	June, 1988 Depth to Water (m)	June, 1988 Water Level (m) a.M.S.L.	February, 1989 Depth to Water (m)	February, 1989 Water Level (m) a.M.S.L.	July, 1989 Depth to Water (m)	July, 1989 Water Level (m) a.M.S.L.	October, 1989 Depth to Water (m)	October, 1989 Water Level (m) a.M.S.L.	January, 1990 Depth to Water (m)	January, 1990 Water Level (m) a.M.S.L.
1-1	8.86	0.12	8.36	0.62	8.46	0.52	8.61	0.37	8.32	0.66
1-4	13.24	-0.47	12.68	0.09	12.95	-0.18	13.00	-0.23	12.74	0.03
1-5	17.78	-0.20	17.90	-0.32	17.72	-0.14				
1-6	15.78	-0.35	14.92	0.51	14.8	0.63	15.12	0.31		
1-7	15.28	-0.22	15.19	-0.13	15.31	-0.25	15.28	-0.22	15.05	0.01
1-15	14.68	-1.33	14.62	-1.27	16.09	-2.74				
1-19	13.00	-1.57	12.38	-0.95	12.67	-1.24	12.90	-1.47	12.27	-0.84
1-21	9.62	-1.39	9.58	-1.35						
1-22	17.12	-1.32	17.20	-1.40					17.00	-1.20
1-48			18.10	-0.52	18.95	-1.37	16.36	1.22	18.20	-0.62
1-63	21.90	-1.59	21.74	-1.43	22.48	-2.17	22.12	-1.81	21.90	-1.59
1-64	20.80	-2.18	19.25	-0.63	20.90	-2.28	19.65	-1.03	19.24	-0.62
1-66	23.32	-1.34	22.95	-0.97	24.05	-2.07				
1-73			6.75	0.96			6.64	1.07	6.20	1.51
1-75			21.70	-2.87	21.80	-2.97	21.33	-2.50	21.05	-2.22
1-77					6.45	0.83	6.41	0.87	6.25	1.03
1-83			14.93	-0.20	15.40	-0.67	15.18	-0.45	14.85	-0.12
1-88	21.20	-2.01			21.30	-2.11	21.50	-2.31	20.10	-0.91
1-100	26.31	0.04	26.59	-0.24	26.80	-0.45	26.50	-0.15	26.20	0.15
1-104	20.35	-2.47	20.95	-3.07	21.45	-3.57	21.17	-3.29	20.70	-2.82
1-107	27.80	0.55	27.75	0.60			28.20	0.15	28.19	0.16
1-110	20.83	-0.07	20.85	-0.09	21.61	-0.85				
1-116	26.65	0.30								
1-119	24.05	-0.53	23.82	-0.30	24.22	-0.70			23.89	-0.37
1-120	25.34	-0.77	24.75	-0.18	25.50	-0.93	25.43	-0.86	25.05	-0.48
1-123	19.64	-0.14							19.23	0.27
1-125	27.72	1.54	27.65	1.61			28.85	0.41		
1-129			22.80	0.12	23.84	-0.92				

(Table 2 continued)

1-134	18.33	0.92	18.40	0.85	18.95	0.30	18.74	0.51	19.10	0.15
1-135	25.50	0.21							23.80	1.91
1-137	24.10	0.29	23.86	0.53			24.85	-0.46	24.08	0.31
1-138					20.60	-0.31	20.20	0.09	20.00	0.29
1-141			23.25	0.50	23.95	-0.20				
2-6	33.11	1.33	33.30	1.14			33.43	1.01	33.41	1.03
2-10							34.08	-0.30	34.30	-0.52
2-18					30.60	1.39	32.78	-0.79	31.43	0.56
2-26	39.81	1.57			40.12	1.26	41.05	0.33		
4-2	22.82	-0.79	22.83	-0.80	22.91	-0.88	22.92	-0.89	22.96	-0.93
5-1	40.95	1.85			41.08	1.72	42.00	0.80	41.70	1.10
5-3			37.35	2.39	37.50	2.24			37.71	2.03
5-5	43.91	2.56			44.04	2.43	44.11	2.36	43.93	2.54

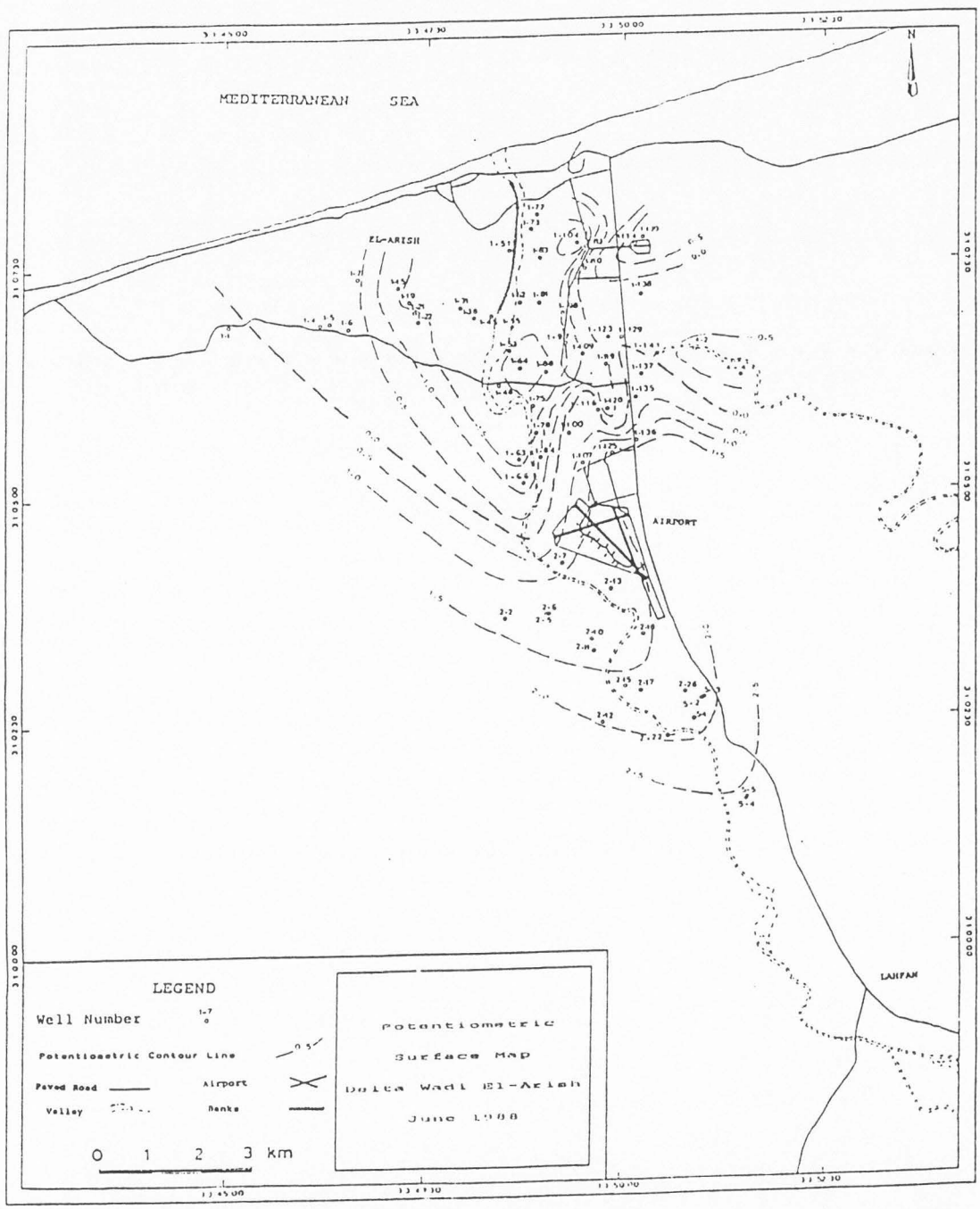

Fig. 16. Potentiometric surface map, June 1988.

This area is bounded by the airport to the south, the coastal road to the north, the El-Massaeid suburb to the west, and the El-Arish--Lahfan road to the east. The water levels in this area have dropped below sea level, with elevations ranging between -0.5 and -2.0 m. In the area south of the El-Arish airport, the map shows that the potentiometric surface lies above sea level, with water level elevations ranging between +0.5 and +2.5 m.

The potentiometric contour lines indicate that groundwater flows towards the Wadi El-Arish channel. In the area north of the airport and southeast of the town of El-Arish, the potentiometric contour lines are closely spaced, indicating that the gradient is steeper, and they are elongated in the north-south and northeast-southwest directions. The map shows that the lowest potentiometric surface elevations in the entire delta Wadi El-Arish region occur in this area. Two separate potentiometric depressions are present within this area; one is located in the northeastern corner of the area around well 1-104, where the elevation of the potentiometric surface was -2.47 m, while the other is located near the bend of the Wadi El-Arish channel around wells 1-64 and 1-88, where the elevations of the potentiometric surface were -2.18 and -2.01 m, respectively. These two groundwater depressions are attributable to the relatively heavy pumping in these two areas since 1980. In addition, there is a facies change of

the upper Pleistocene unit from a gravelly layer to a sandy clay layer interbedded with continental sandstone lenses (kurkar). Consequently, the aquifer transmissivity is less, resulting in deeper cones of depression.

In the area north of the airport and east of the El-Arish--Lahfan road, two areas where the potentiometric surface elevations are high can be found. One is located near well 1-134, where the water level elevation was +0.92 m. The other is located near wells 1-135 and 1-137, where the water-level elevations were +0.21 m and +0.29 m, respectively. These two water level highs are separated by an area of low potentiometric surface elevations extending east-west along Wadi El-Mazzar. The two high groundwater elevation areas can be explained as resulting from an increase in the aquifer thickness in both areas. Consequently, the aquifer transmissivity is high, resulting in smaller cones of depression. In addition, the deep percolation of return flow through the irrigated lands would cause a rise in groundwater elevation.

Potentiometric Surface Map
February 1989

The potentiometric surface map shown in Figure 17 was constructed using the water-level elevations measured in February 1989. The map shows that the zero potentiometric

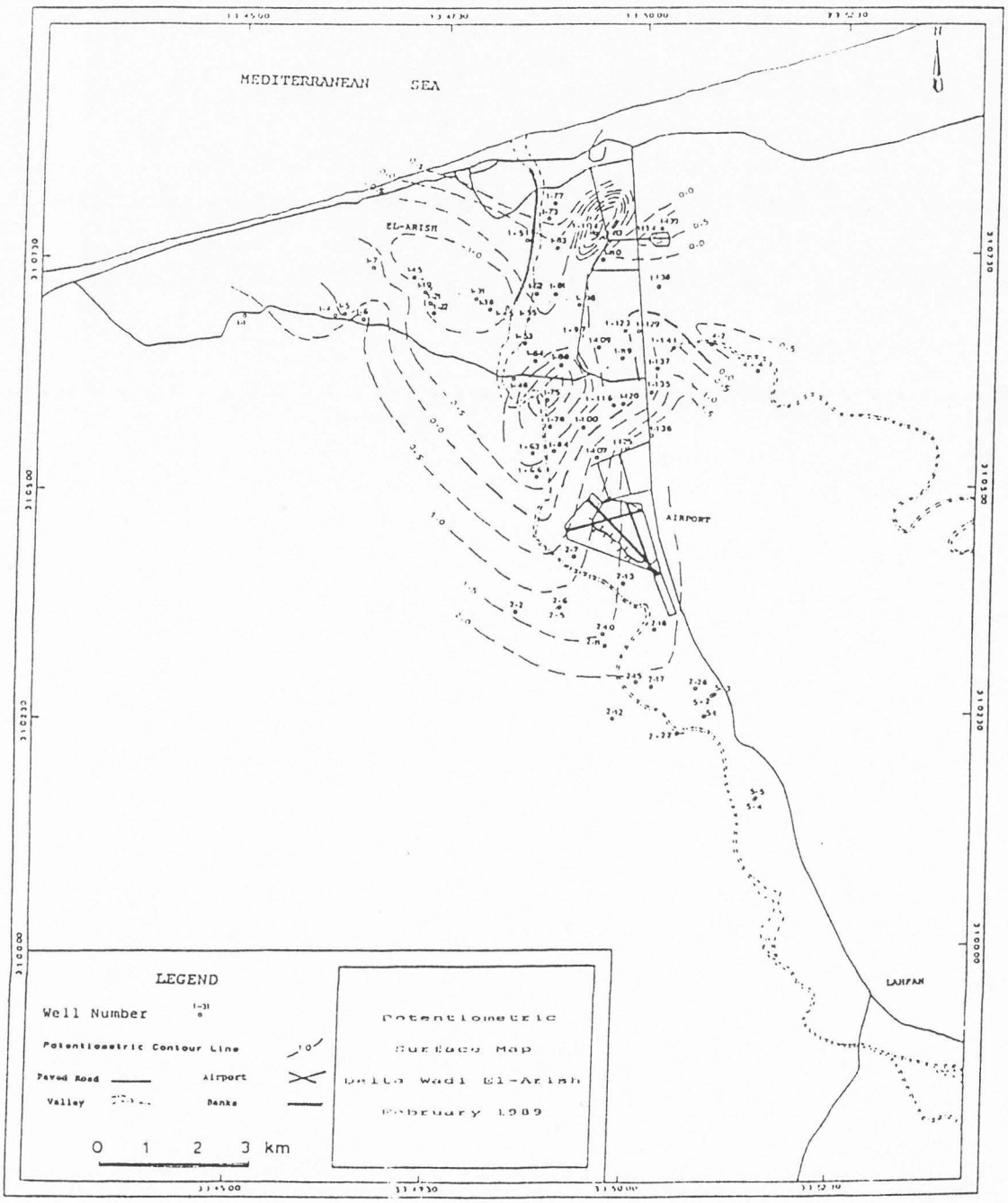

Fig. 17. Potentiometric surface map, February 1989.

contour line surrounds a smaller area than that in June 1988. This is because of the decrease in the pumping rate during the winter. South of the coastal road, a small area of high potentiometric surface elevations is shown. This is because of the lower pumping rate of the coastal wells, which is reduced by 25 m^3/h, and the fact that they are pumped only for three hours every other day.

Potentiometric Surface Map
July 1989

The potentiometric surface map based on the water-level measurements taken in July 1989 (Figure 18) shows a general decline of groundwater elevations, which is clearly evident from the zero potentiometric contour line in the central portion of the study area. The zero potentiometric contour line encompasses a larger area than that in February 1989. This is due to the increase in the pumping rate during the summer. In the northwest corner of the study area, a small potentiometric low is present around well 1-15, where the potentiometric surface elevation was -2.74 m. South of the coastal road and west of the El-Arish--Lahfan road, a small potentiometric low can be seen near well 1-104, where the potentiometric surface elevation was -3.57 m.

Potentiometric Surface Map
October 1989

A potentiometric surface map was produced based on the water-level measurements taken in October 1989 (Figure 19).

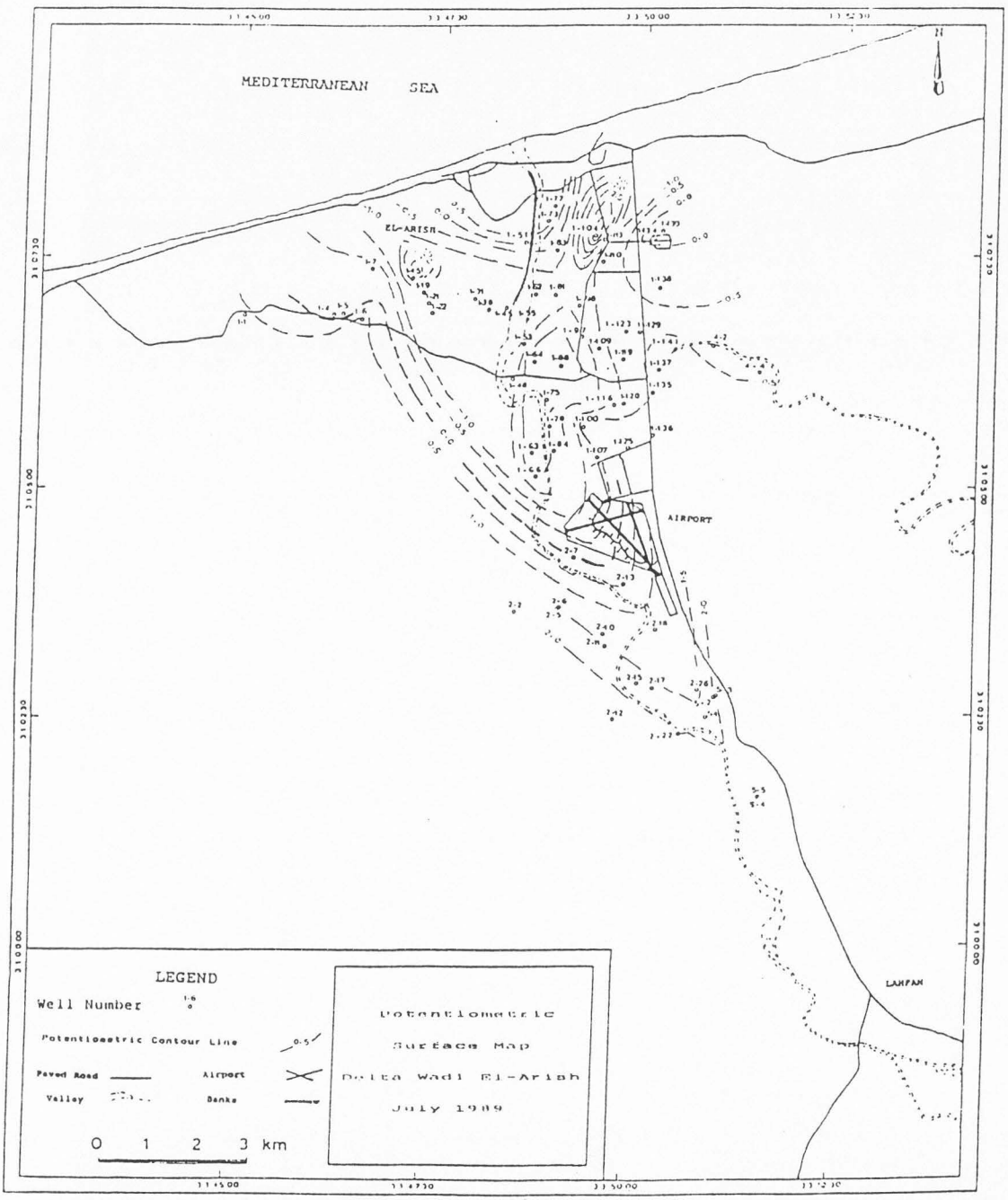

Fig. 18. Potentiometric surface map, July 1989.

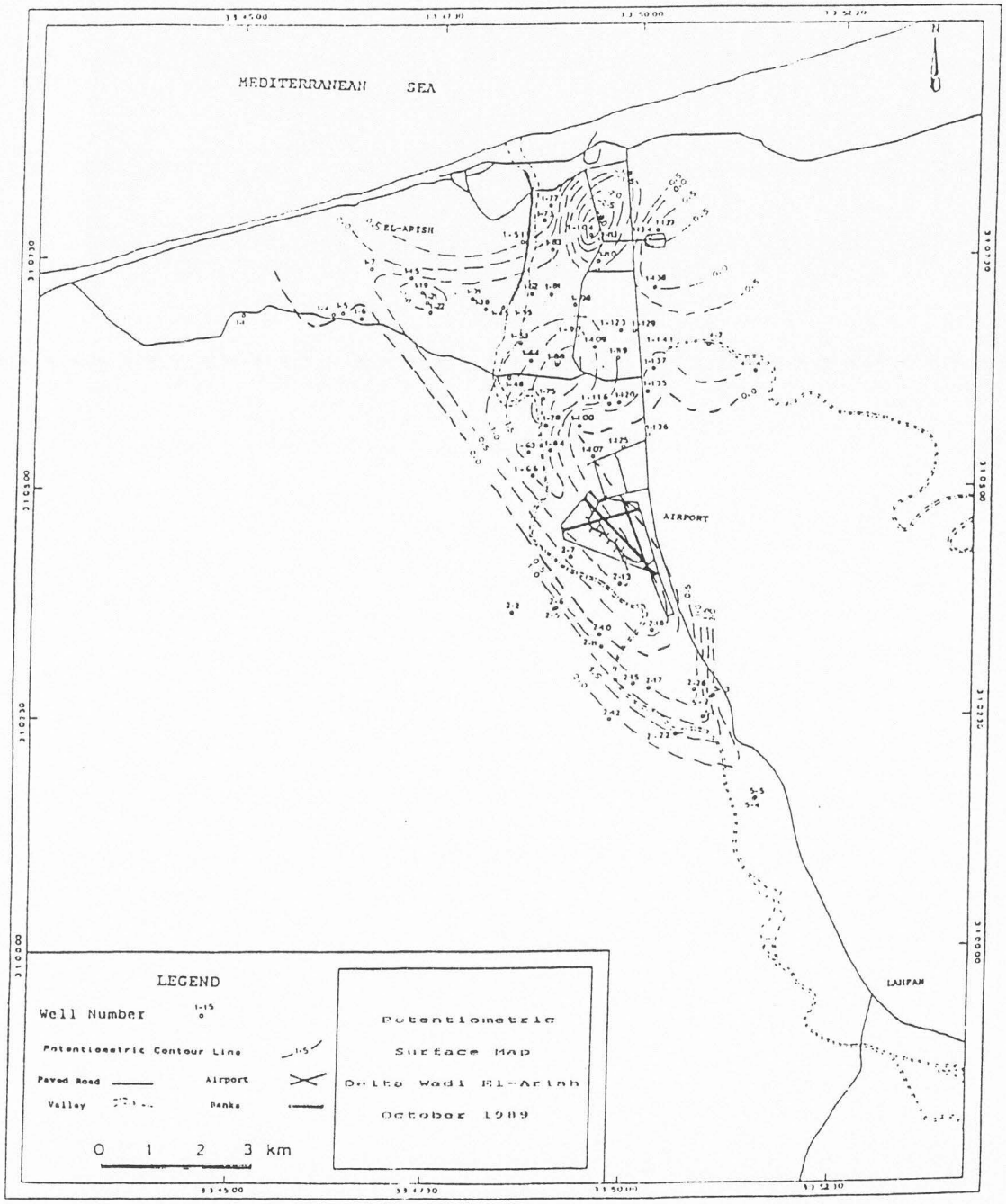

Fig. 19. Potentiometric surface map, October 1989.

The map shows that the potentiometric contour lines, to some extent, are similar to those in July 1989. The most significant difference between the two maps is that the -1.0 m potentiometric contour line in the central portion of the study area encompasses a smaller area and is divided into three zones. This is due to the decrease in the pumping rate at the beginning of winter. The first of these three zones is located north of the El-Arish airport along the Wadi El-Arish channel around wells 1-75 and 1-88, where the potentiometric surface elevations were -2.50 m and -2.31 m, respectively. The second is located in the northwest corner of the area north of the middle road around well 1-19, where the potentiometric surface elevation was -1.47 m. The third is located south of the coastal road and west of the El-Arish--Lahfan road around well 1-104, where the potentiometric surface elevation was -3.29 m.

Potentiometric Surface Map
January 1990

A potentiometric surface map was produced based on the water-level measurements taken in January 1990 (Figure 20). The map shows that the zero potentiometric contour line in the central part of the study area encompasses a relatively small area compared to that in October 1989. The three zones in the central part of the study area within the -1.0 m potentiometric contour line are similar to those in October 1989 but have smaller areas, especially the zone

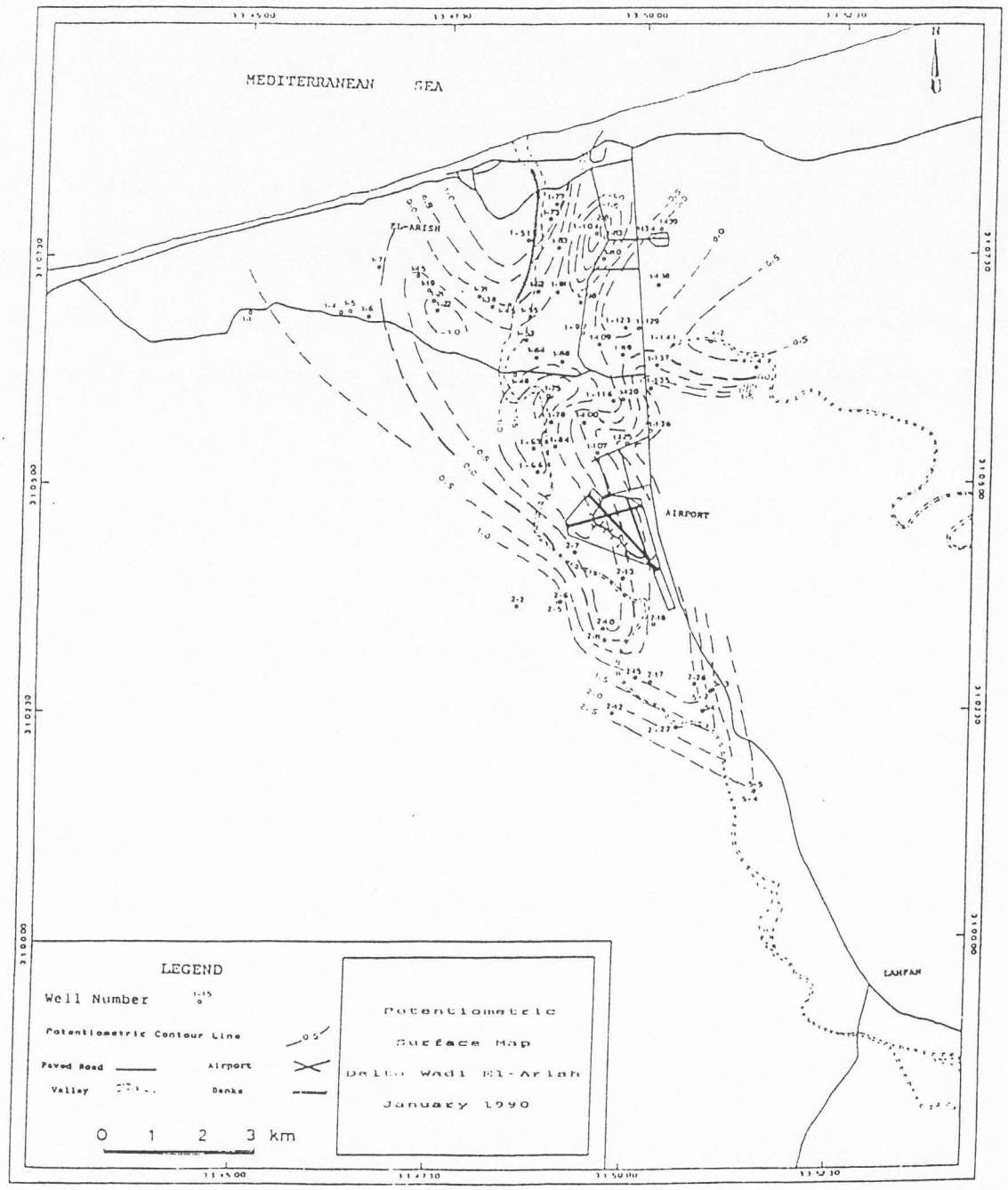

Fig. 20. Potentiometric surface map, January 1990.

located north of the airport along the Wadi El-Arish channel. This is due to an even greater decrease in the pumping rate during the winter.

Groundwater Extraction in the Delta Wadi El-Arish Area

The groundwater extraction rates are useful in demonstrating the relationship between the extraction rate and the potentiometric level. The measured groundwater extraction rate was 51,700 m^3/day in June 1988 from 145 wells completed within the Quaternary aquifer in the delta Wadi El-Arish area. A total of 25,000 m^3/day was used for domestic purposes, while 26,700 m^3/day was used for irrigation purposes (RIWR, 1989).

Paver and Jordan (1956) stated that according to his inventory in the delta Wadi El-Arish area, the extraction rate was 5,600 m^3/day from 24 wells in 1954. Geofizika (1963), during water studies in the northern Sinai peninsula in 1962, stated that the extraction rate was 21,400 m^3/day from 34 wells. Dames and Moore (1984) estimated that the extraction rate was 25,000 m^3/day in 1981 from the 50 wells that were producing at that time.

The historical groundwater extraction rates in the delta Wadi El-Arish area are presented in the form of an extraction histogram in Figure 21. The histogram shows rapidly increasing groundwater extraction rates from 1954 to

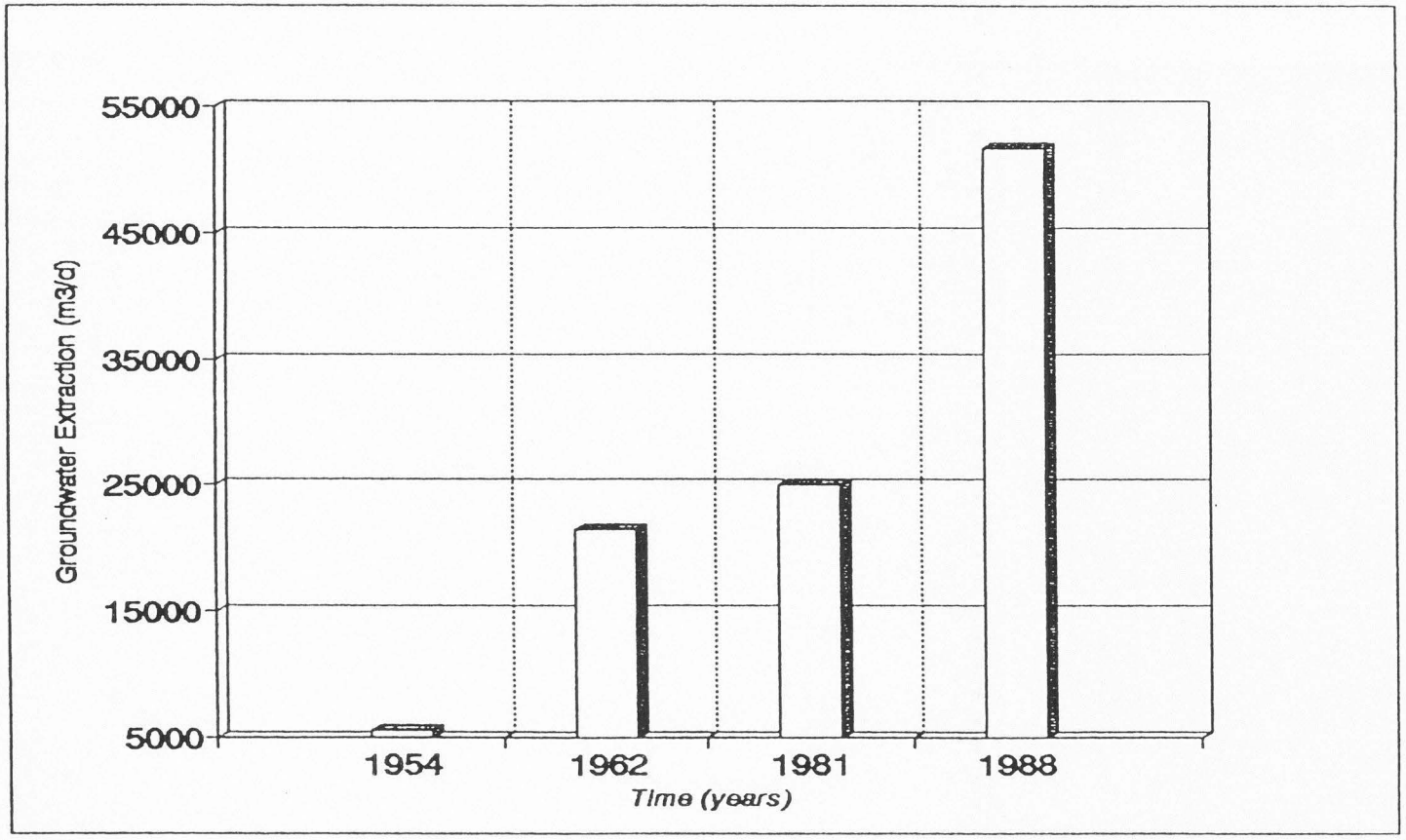

Fig. 21. Extraction histogram.

1962 and again from 1981 to 1988. The measured extraction rates were about ten times greater in 1988 than in 1954.

Based upon the groundwater extraction rate measured in years 1954, 1962, 1981, and 1988 (Figure, 21) and the corresponding potentiometric surface maps (Figures, 4, 5, 6, and 16), it can be concluded that the greater the ground water extraction rate the lower the potentiometric level.

Hydraulic Parameters of the Quaternary Aquifer

The measurements of the hydraulic parameters for the Quaternary aquifer in the delta Wadi El-Arish area give a better picture of groundwater behavior within the study area. These hydraulic parameters are transmissivity (T) and storativity (S). Transmissivity is defined as the rate of flow per unit width of the aquifer per unit change in hydraulic gradient through the complete thickness of the aquifer (Fetter, 1988). Storativity is defined as the volume of water released from, or added to, the aquifer per unit area and per unit change of head (Fetter, 1988).

The hydraulic parameters were determined by conducting pumping tests. Pumping tests have been conducted on three test wells (2-5, 5-2, and 5-4) belonging to the Research Institute for Water Resources. Test well 2-5 is completed in the calcareous sandstone (kurkar) unit (Figure 13), while the other two test wells, 5-2 and 5-4, are completed in

alluvium (Appendix A). These pumping tests were long-duration (720 to 1,440 minutes) constant-discharge tests. In addition, step-drawdown tests were performed on the three test wells listed above and also on 21 other wells in the delta Wadi El-Arish area.

The drawdown data from the long-duration constant-discharge tests (Appendix B) were analyzed to determine the aquifer transmissivity and storativity. The step-drawdown test data were used to determine the well efficiencies and specific capacities.

Analysis of Constant Discharge Test Data

Two different methods were used to analyze the constant discharge test data. These methods are the Stallman (1963) method and the Hantush and Jacob (1955) method. These two methods were used, rather than other methods, because the flattening of the drawdown curves (Figures 22-27) is evidence that there must be some source of water other than the aquifer itself, either a positive (recharge) boundary or leakage from an overlying aquifer through the intervening aquitard.

Stallman Method

The Stallman (1963) method has been developed to analyze constant discharge test data when the wells are located near a boundary such as a fault. The method of images is used to determine the nature and location of

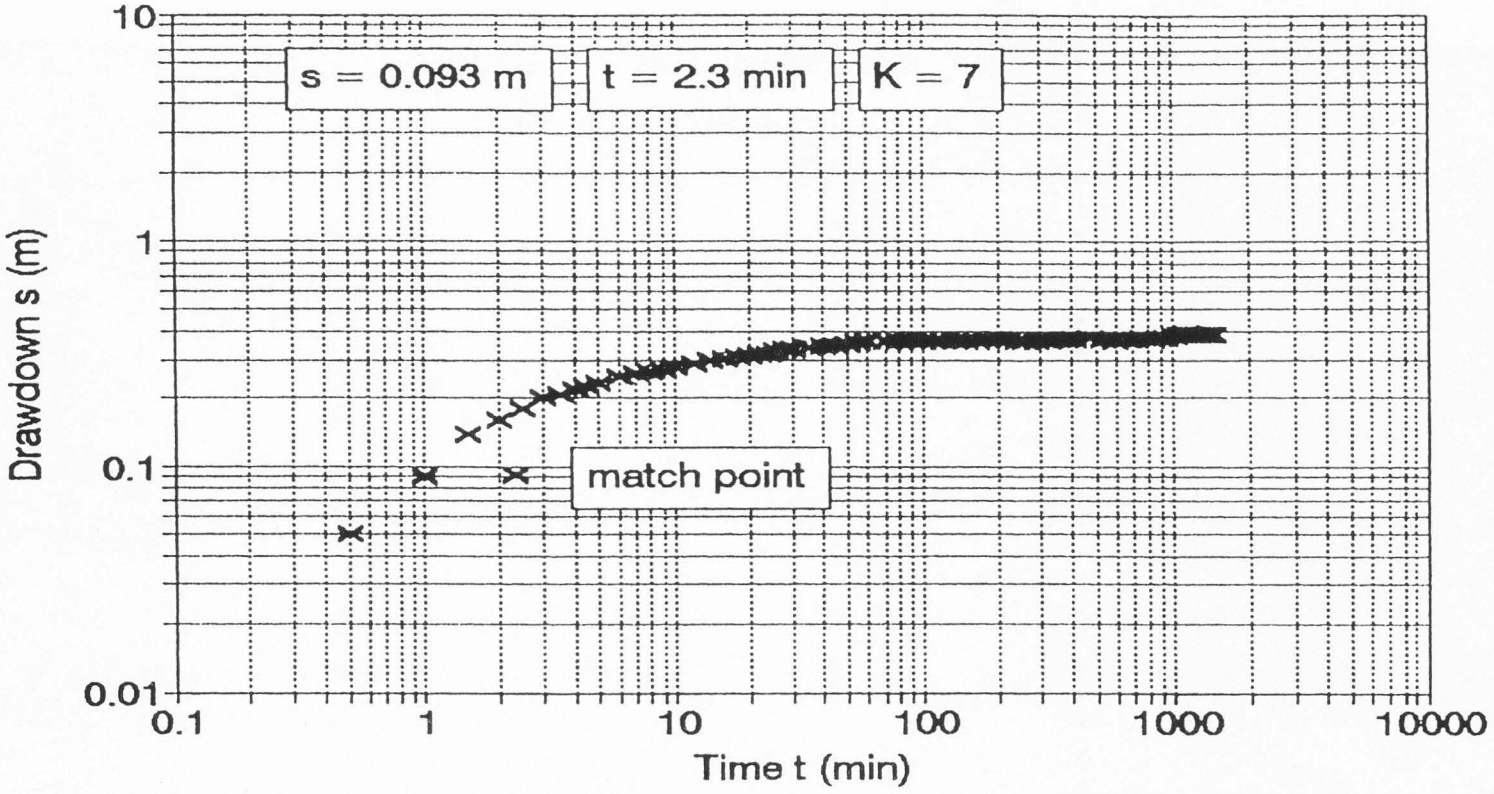

Fig. 22. Pumping well 2-5.

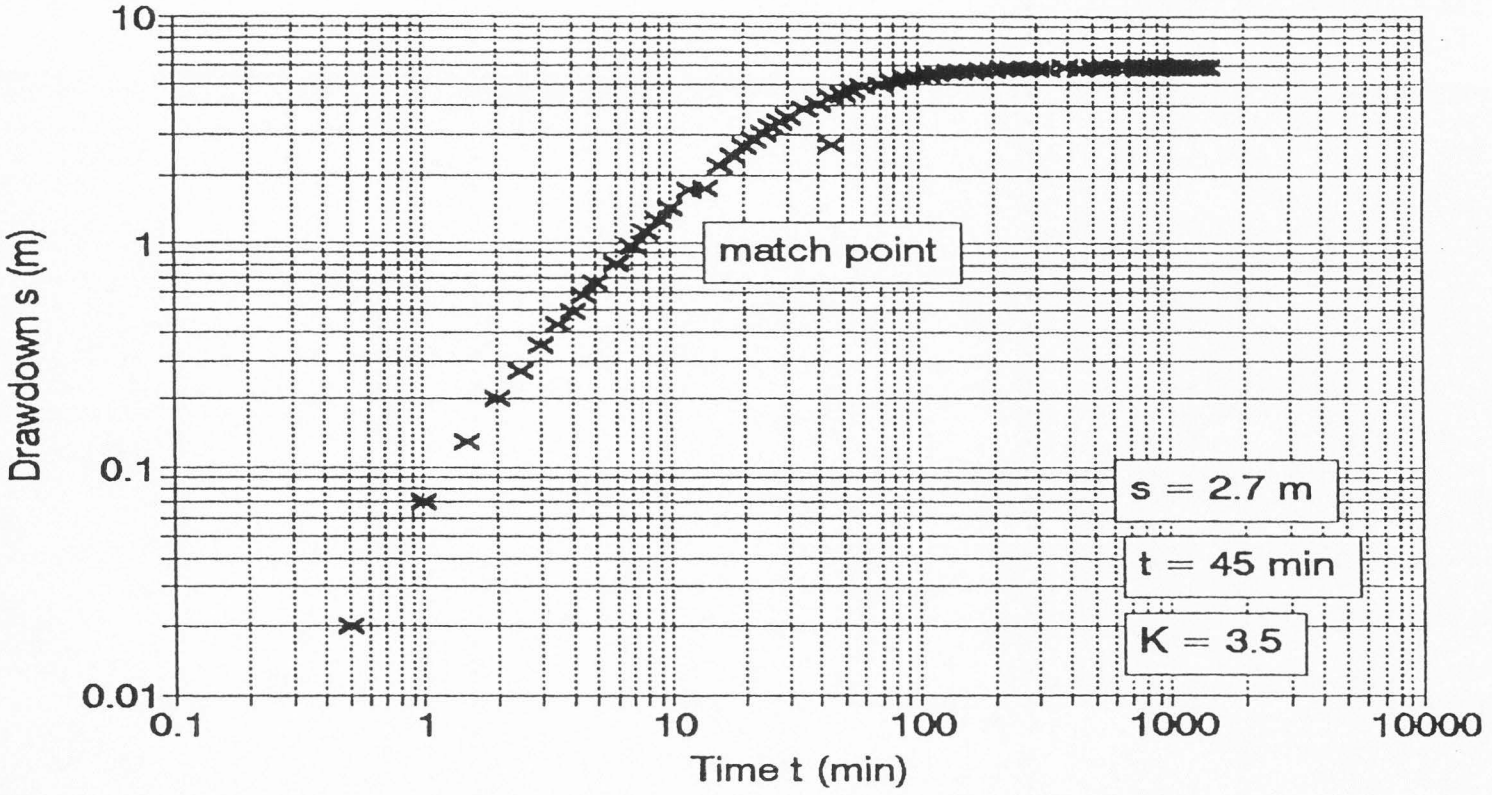

Fig. 23. Pumping well 5-2.

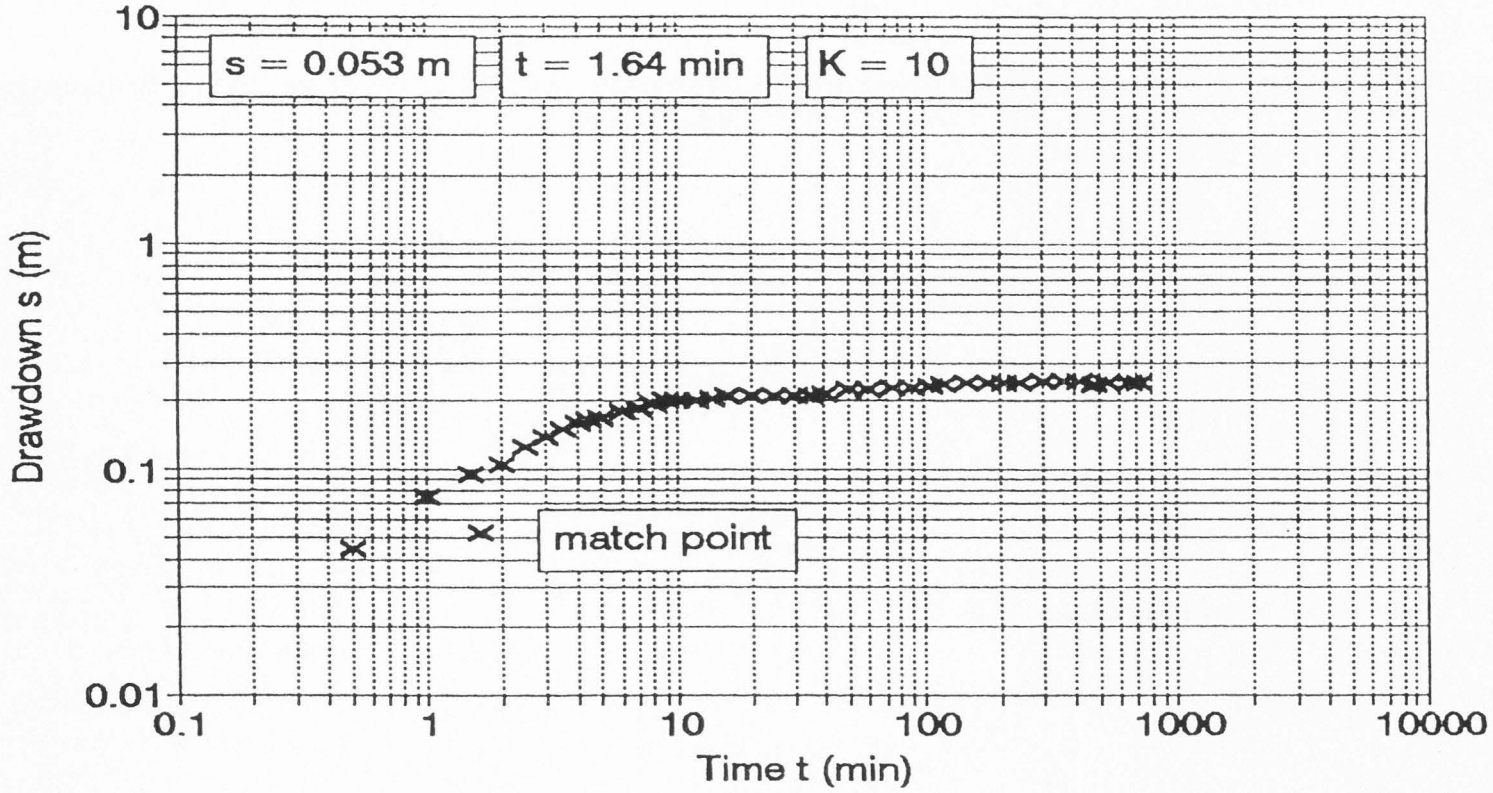

Fig. 24. Pumping well 5-4.

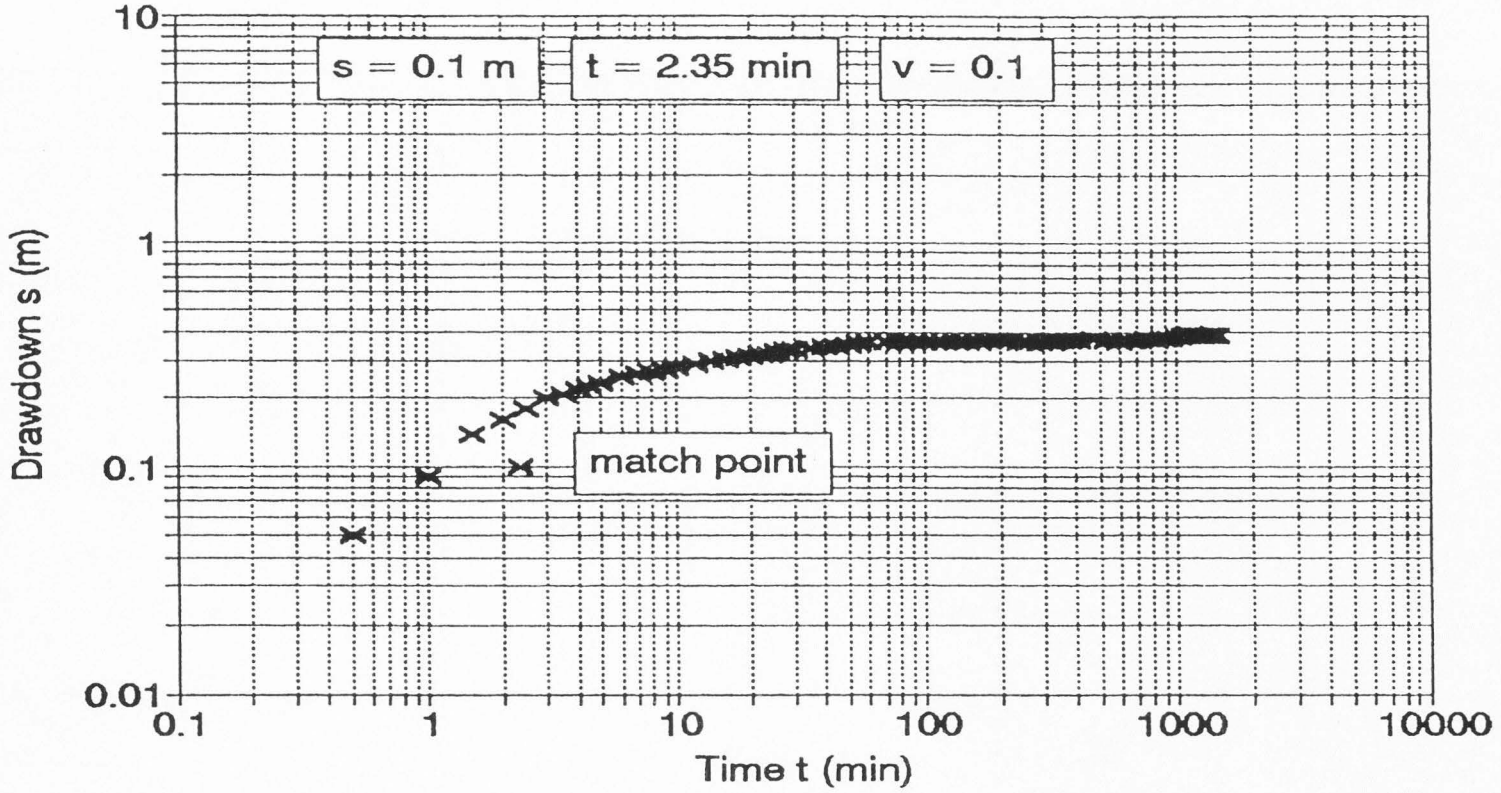

Fig. 25. Pumping well 2-5.

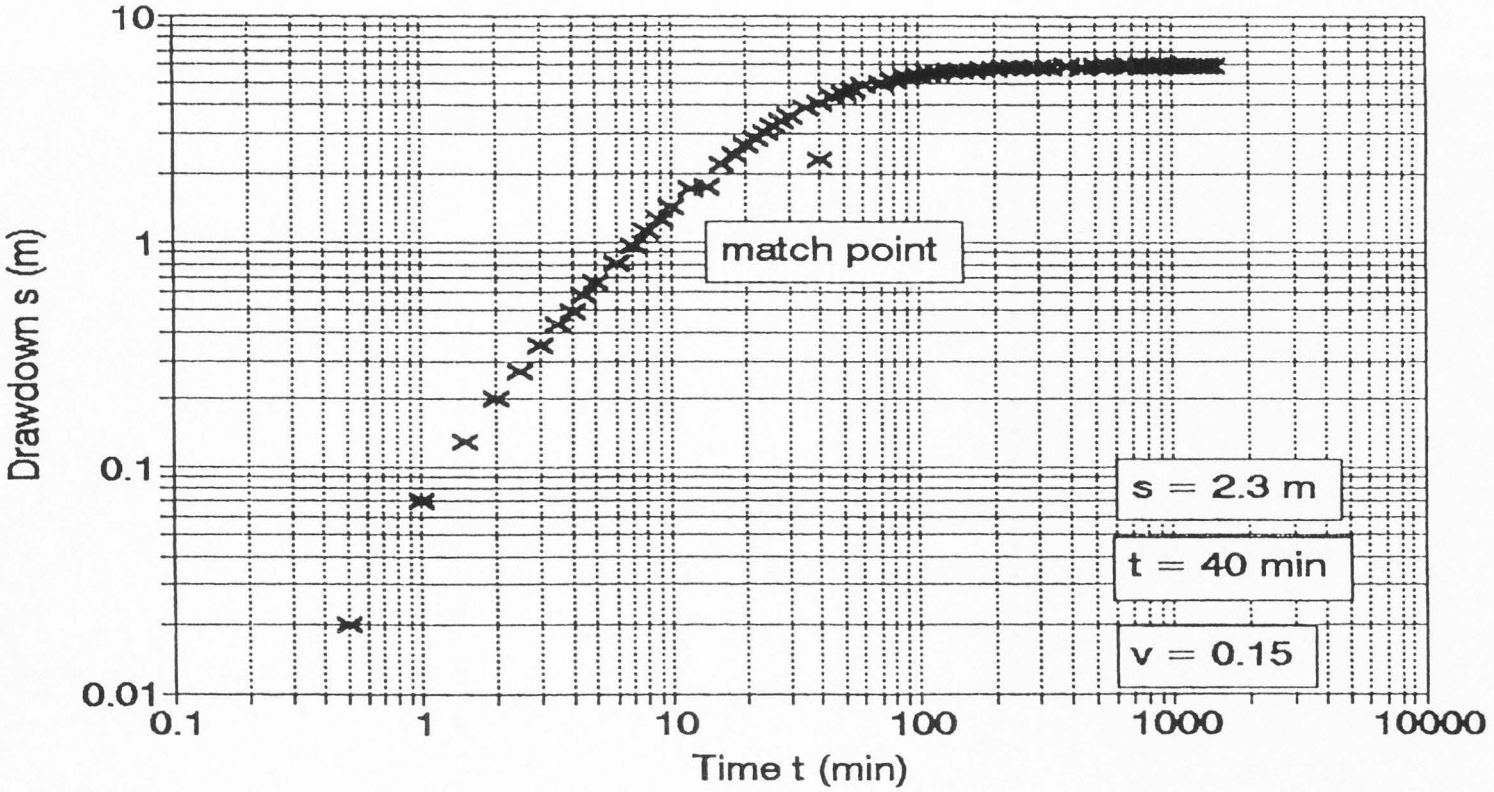

Fig. 26. Pumping well 5-2.

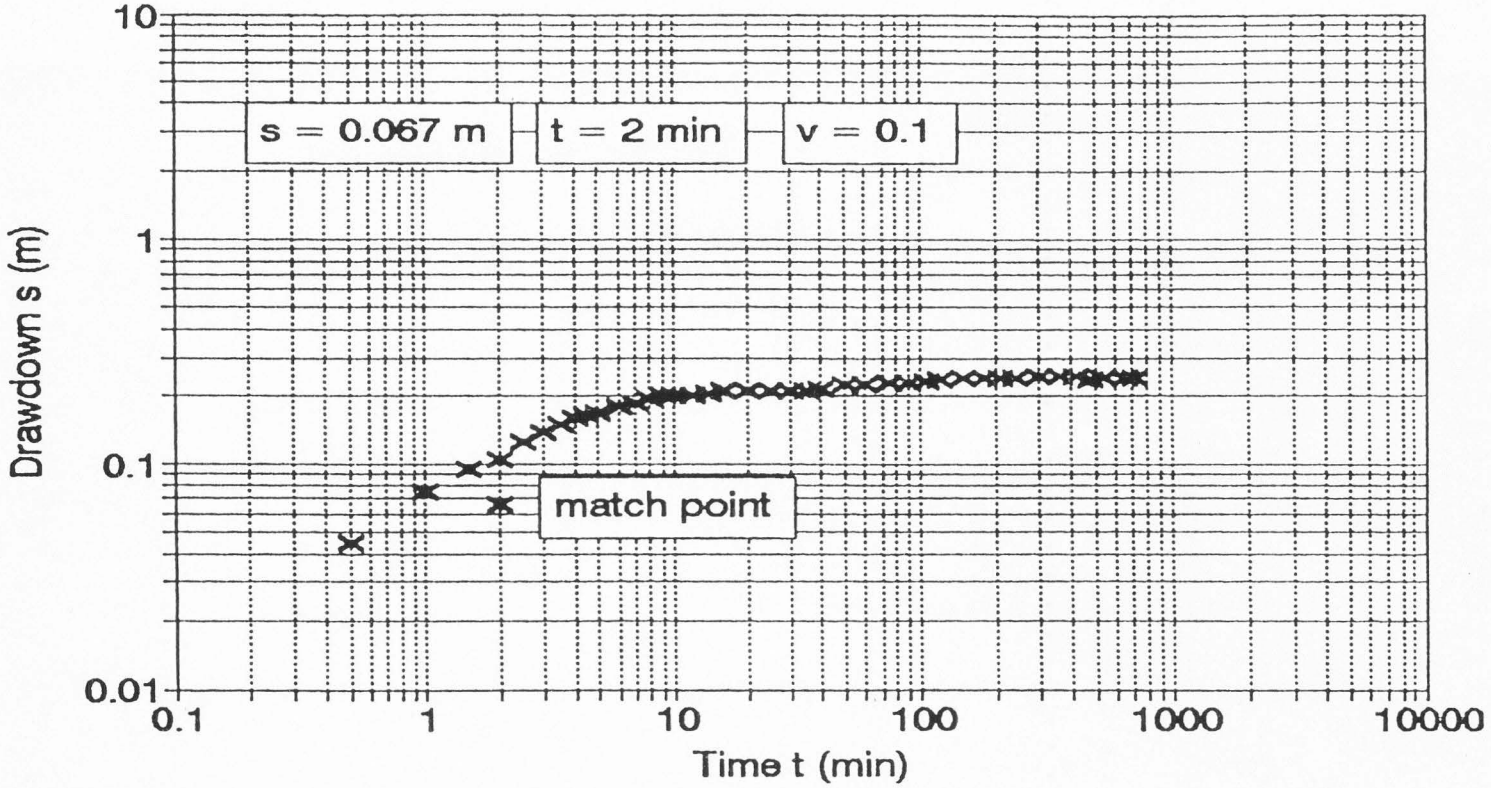

Fig. 27. Pumping well 5-4.

aquifer boundaries. The effect of an imaginary well located at a distance of twice the distance to the actual boundary is superimposed on the drawdown produced by the actual pumping well. The imaginary well may be either a discharging image well (discharge boundary) or a recharging image well (recharge boundary), depending on the type of the boundary. In this method, the values of drawdown (s_o) versus the corresponding time (t) in each observation well located at a distance (r_p) from the pumping well are plotted on fully logarithmic paper of the same scale as that used for the Stallman-type curves. Figures 22 through 24 show the time-drawdown curves for the test wells 2-5, 5-2, and 5-4, respectively. The Stallman-type curves are constructed by plotting Σ W(u) versus $1/u_p$ (where Σ W(u) is the well function for both the pumping well and the imaginary recharge well, while $u_p = \frac{Sr_p^2}{4Tt}$ for the pumping well) for many values of $K = r_i/r_p$ (see below) on fully logarithmic paper. The data plot is matched with the type curves until the data plot closely fits one of the type curves and a match point can be chosen. The match point chosen was at the intersection of Σ W(u) = 1, and $1/u_p = 10$. From this match point, the values of drawdown (s_o) and time (t) corresponding to the Σ W(u) = 1 and $1/u_p = 10$ can be determined. Using the values of Σ W(u) and (s_o) from the match point, the transmissivity (T) of the aquifer can be calculated using the following equation:

$$T = \frac{Q}{4\pi s_o} \Sigma W(u) \quad (1)$$

where Q is the constant discharge rate of the pumping well. Using the calculated value of T along with the values of $1/u_p$ and t chosen from the match point, the storativity (S) of the aquifer can be calculated using the following equation:

$$S = \frac{4Tt}{r_p^2} u_p \quad (2)$$

where r_p is the distance from the pumping well to the observation well. The distance from the pumping well to an imaginary pumping or recharging well can be calculated using the following equation:

$$K = \frac{r_i}{r_p} \quad (3)$$

where K is the value of the particular type curve which most closely fits the data and r_i is the distance from the pumping well to the imaginary pumping or recharging well. The coordinates of the match points of the field data with the type curves and the values of K using the Stallman method are shown in Figures 22-24.

Hantush and Jacob Method

The Hantush and Jacob (1955) method has been used to analyze the constant discharge test data in addition to the Stallman (1963) method. This method is used for aquifers that obtain water from leakage from an overlying aquifer

without storage in the intervening aquitard. In this method, the values of drawdown (s) versus the corresponding time (t) in each observation well located at a distance (r) from the pumping well are plotted on fully logarithmic paper of the same scale as that used for the Hantush and Jacob-type curves. Figures 25 through 27 show the time-drawdown curves for test wells 2-5, 5-2, and 5-4, respectively. The type curves are constructed by plotting L(u,v) versus 1/u (where L(u,v) is the well function of u and v, and $u = \frac{Sr^2}{4Tt}$) for many values of v on fully logarithmic paper. The data plot is matched with the type curves until the data plot closely fits one of the type curves and a match point can be chosen. The match point chosen was at the intersection of L(u,v) = 1, and 1/u = 10. From this match point, the values of the drawdown (s) and time (t) corresponding to L(u,v) = 1 and 1/u = 10 can be determined. Using the values of L(u,v) and (s) from the match point, the transmissivity (T) of the aquifer can be calculated using the following equation:

$$T = \frac{Q}{4\pi s} L(u,v) \qquad (4)$$

where Q is the constant discharge rate of the pumping well. Using the calculated value of T along with the values of 1/u and t chosen from the match point, the storativity (S) of the aquifer can be calculated using the following equation:

$$S = \frac{4Tt}{r^2} u \qquad (5)$$

where r is the distance from the pumping well to the observation well. The ratio of $\frac{K'}{b'}$ can be calculated using the following equation:

$$\frac{K'}{b'} = T\ (2v/r)^2 \qquad (6)$$

where K' and b' are the hydraulic conductivity and the thickness of the confining layer, respectively, while v is the value of the particular type curve that most closely fits the data. Using the Hantush and Jacob method, the coordinates of the match points of the field data with the type curves and the values of v are shown in Figures 25-27.

Table 3 presents the calculated values of transmissivity and storativity of the Quaternary aquifer using both methods. Table 3 also presents the distances from the pumping well to the recharge boundary (= 1/2 r_i) for the three wells using the Stallman method, and the calculated values of the hydraulic conductivities of the confining layer using the thickness of the confining layer (b') measured from hydrogeologic cross section II-II' (Figure 13) and the lithologic well logs (Appendix A) for the three wells using the Hantush and Jacob method.

As shown in Table 3, the distances from the pumping well to a hypothetical recharge boundary for the three wells

Table 3. Analysis of Constant Discharge Test Data

Well Number	Stallman method			Hantush and Jacob method				
	T m^2/day	S	Distance to recharge boundary m	T m^2/day	S	$\frac{K'}{b}$ 1/sec	b m	K' m/sec
2-5	1160	0.007	35.7	1100	0.007	4.9×10^{-6}	2	10^{-5}
5-2	6	0.0008	17.5	7	0.0008	7.2×10^{-8}	1.5	10^{-7}
5-4	270	0.001	50	210	0.001	9.7×10^{-7}	4.5	4×10^{-6}

are small values, suggesting that the flattening of the drawdown curves observed during the pumping tests probably was not the result of a positive (recharge) boundary. Consequently, it seems more likely that the flattening of the drawdown curves during the pumping tests was caused by leakage of water from the overlying Holocene sand deposits through the intervening sandy clay aquitard with no water being obtained from storage within the sandy clay aquitard. Using the Hantush and Jacob method, the transmissivity of the aquifer at well 2-5 is approximately 1100 m^2/day, while the transmissivity is approximately 210 and 7 m^2/day at wells 5-4 and 5-2, respectively. The lower transmissivity values of the aquifer at wells 5-4 and 5-2 indicate that the transmissivity of the alluvial deposits is lower than that of the calcareous sandstone (kurkar). The low transmissivity value of alluvium relative to the sandstone

(kurkar) is the result of fact that the alluvium is more poorly sorted than the sandstone (kurkar) unit. The very low transmissivity value of the aquifer at well 5-2 is attributable to the decrease in thickness of the alluvial deposits at this location.

The estimates of the storativity of the aquifer are approximately 7×10^{-3}, 8×10^{-4}, and 1×10^{-3} for the three wells 2-5, 5-2, and 5-4, respectively, using the Hantush and Jacob method. Table 3 also presents the values of the hydraulic conductivity of the confining layer at the three well locations. These values are 10^{-5} m/sec, 10^{-7} m/sec, and 4×10^{-6} m/sec for wells 2-5, 5-2, and 5-4, respectively. These hydraulic conductivity values for the confining layer (K') are reasonable for a sandy clay (Freeze and Cherry, 1979, Table 2.2, p. 29). From the storativity values, it can be concluded that the Quaternary aquifer behaves as a semi-confined aquifer at all three well locations.

Analysis of Step-Drawdown Test Data

Step-drawdown tests were also conducted on wells 2-5, 5-2, 5-4, and 21 other wells in the delta Wadi El-Arish area in order to calculate the specific capacities of these wells and also to estimate aquifer losses and well losses, and thus well efficiencies. The aquifer loss (BQ) is that portion of the drawdown in the pumping well resulting from groundwater being removed from the aquifer at the well. The

Table 4. Analysis of Step-Drawdown Test Data

Well No.	Step No.	Step Drawdown Test Q m^3/day	s (m)	Aquifer Loss Constant (B)	Well Loss Constant (C)	Aquifer Losses (m)	Well Losses (m)	Well Eff. (E)	Specific Capacity Q/s
	1	969.6	3.15	B_1 = 0.00252	C_{12} = 0.0000007483	2.4465	0.7035	77.67	308
1-1	2	1154.4	3.91	B_2 = 0.00136		0.2511	0.5089	33.04	295
	3	1286.4	4.53	B_3 = 0.00019	C_{23} = 0.0000018447	0.0256	0.5934	4.14	284
	1	640.8	4.55	B_1 = 0.00343	C_{12} = 0.0000057311	2.1967	2.3533	48.28	141
1-4	2	787.2	6.25	-----		---	---	---	126
	3	933.6	8.56	-----	C_{23} = 0.0000142304	---	---	---	109
	1	624	5.2	B_1 = 0.00435	C_{12} = 0.0000063844	2.7141	2.4859	52.19	120
1-5	2	744	6.77	-----		---	---	---	110
	3	880.8	9.12	-----	C_{23} = 0.0000159464	---	---	---	97
	1	870	2.27	B_1 = 0.00177	C_{12} = 0.0000009604	1.5431	0.727	67.98	383
1-48	2	1175	3.41	-----	-----	---	---	---	345
	3	1535	4.7	-----	-----	---	---	---	327
	1	905	2.27	B_1 = 0.00168	C_{12} = 0.00000091	1.5247	0.7453	66.16	399
1-63	2	1390	4.1	B_2 = 0.00053		0.258	1.572	14.1	339
	3	1735	5.95	-----	C_{23} = 0.0000019146	---	---	---	292
1-64	1	905	1.08	B_1 = 0.00060	C_{12} = 0.0000006534	0.5448	0.5352	50.45	838
	2	1340	1.98	B_2 = 0.00125		0.5447	0.3553	60.52	677
	3	1725	2.8	B_3 = 0.00190	C_{23} = 0.0000000743	0.7324	0.0876	89.31	616
1-75	1	905	1.08	B_1 = 0.00060	C_{12} = 0.0000006534	0.5448	0.5352	50.45	838
	2	1340	1.98	B_2 = 0.00125		0.5447	0.3553	60.52	677
	3	1725	2.8	B_3 = 0.00190	C_{23} = 0.0000000743	0.7324	0.0876	89.31	616
	1	1550	6.82	B_1 = 0.00291	C_{12} = 0.00000096	4.5135	2.3065	66.18	227
1-78	2	1865	8.77	B_2 = 0.00447		1.4065	0.5435	72.13	213
	3	2180	10.73	B_3 = 0.00602	C_{23} = 0.0000000504	1.8958	0.0642	96.72	203
	1	870	6.48	B_1 = 0.00668	C_{12} = 0.0000008791	5.8146	0.6654	89.73	134
1-83	2	1104	8.45	-----	-----	---	---	---	131
	3	1425	11	-----	-----	---	---	---	130
	1	870	6.3	B_1 = 0.00390	C_{12} = 0.0000038393	3.3941	2.9059	53.87	138
1-84	2	1170	9.82	B_2 = 0.00366		1.0995	2.4205	31.23	119
	3	1380	12.72	B_3 = 0.00343	C_{23} = 0.000004071	0.72	2.18	24.83	108
	1	1420	4.55	B_1 = 0.00066	C_{12} = 0.0000017891	0.9424	3.6076	20.71	312
1-88	2	1780	6.85	-----		---	---	---	260
	3	2090	9.55	-----	C_{23} = 0.0000034639	---	---	---	219
	1	905	1.74	B_1 = 0.00186	C_{12} = 0.0000000667	1.6854	0.0546	96.86	520
1-104	2	1160	2.25	B_2 = 0.00158		0.4023	0.1077	78.87	516
	3	1470	2.93	B_3 = 0.00129	C_{23} = 0.0000003426	0.4007	0.2792	58.93	502
	1	1033	2.07	B_1 = 0.00111	C_{12} = 0.0000008641	1.148	0.922	55.46	499
1-107	2	1445	3.41	B_2 = 0.00158		0.6495	0.6905	48.47	424
	3	1930	5.2	B_3 = 0.00204	C_{23} = 0.0000004886	0.9802	0.7998	55.32	371
	1	905	2.95	B_1 = 0.00195	C_{12} = 0.0000014502	1.7622	1.1877	59.74	307
1-109	2	1250	4.7	-----	-----	---	---	---	266
	3	1660	6.75	-----	-----	---	---	---	246

(Table 4 continued)

	1	905	2.65	B_1 = 0.00199	C_{12} = 0.000001037	1.8007	0.8493	67.95	342
1-119	2	1355	4.6	B_2 = 0.00124		0.5567	1.3933	28.55	295
	3	1725	6.72	B_3 = 0.00048	C_{23} = 0.0000017029	0.1793	1.9407	8.46	257
	1	830	6.79	B_1 = 0.00733	C_{12} = 0.000001019	6.088	0.702	89.66	122
1-123	2	1060	8.92	B_2 = 0.00813		1.8707	0.2593	87.83	119
	3	1320	11.35	B_3 = 0.00893	C_{23} = 0.000000174	2.3223	0.1077	95.57	116
	1	1087	6.92	B_1 = 0.00526	C_{12} = 0.0000010153	5.7204	1.1996	82.66	157
1-125	2	1420	9.52	B_2 = 0.00087		0.2907	2.3093	11.18	149
	3	1773	13.37	-----	C_{23} = 0.0000045171	---	---	---	133
	1	1350	5.65	B_1 = 0.00185	C_{12} = 0.0000017308	2.4956	3.1544	44.17	239
1-135	2	1720	8.3	B_2 = 0.00059		0.2169	2.4331	8.19	207
	3	2110	11.85	-----	C_{23} = 0.0000025532	---	---	---	178
	1	1080	3.52	B_1 = 0.00238	C_{12} = 0.0000008113	2.5737	0.9463	73.12	307
1-136	2	1500	5.4	-----	-----	---	---	---	278
	3	1950	7.4	-----	-----	---	---	---	264
	1	935	1.48	B_1 = 0.00120	C_{12} = 0.0000004144	1.1177	0.3623	75.52	632
1-137	2	1320	2.3	B_2 = 0.00149		0.5774	0.2426	70.42	574
	3	1625	2.98	B_3 = 0.00180	C_{23} = 0.0000001444	0.5503	0.1297	80.93	545
	1	905	3.27	B_1 = 0.00335	C_{12} = 0.000000294	3.0292	0.2408	92.64	277
1-141	2	1200	4.44	B_2 = 0.00151		0.4441	0.7259	37.96	270
	3	1535	6.2	-----	C_{23} = 0.0000020439	---	---	---	248
	1	844.8	2.28	B_1 = 0.00111	C_{12} = 0.0000018769	0.9405	1.3395	41.25	371
2-5	2	1116	3.58	-----	-----	---	---	---	312
	3	1584	5.48	-----	-----	---	---	---	289
	1	148.8	5.29	B_1 = 0.03050	C_{12} = 0.0000339226	4.5389	0.7511	85.8	28
5-2	2	218.4	8.28	B_2 = 0.02940		2.0465	0.9435	68.45	26
	3	253.2	9.92	B_3 = 0.02830	C_{23} = 0.0000399106	0.985	0.655	60.06	26
	1	85.2	0.95	B_1 = 0.00505	C_{12} = 0.0000715397	0.4307	0.5193	45.34	90
5-4	2	140.8	2.13	B_2 = 0.00393		0.2184	0.9616	18.51	66
	3	299.3	8.26	B_3 = 0.00280	C_{23} = 0.0000815136	0.444	5.686	7.24	36

well loss (CQ^2) is that portion of the drawdown resulting from head losses across the well screen, through the casing and due to non-Darcian flow (Jacob, 1947).

In the step-drawdown tests, three two-hour long steps were conducted for each of these wells. The drawdown (s) and the corresponding discharge (Q) of each step were recorded, and are shown in Table 4.

In the analysis of the step-drawdown test data, the values of the aquifer loss constant (B) and the well loss constant (C) can be calculated using the following equations (Jacob, 1947):

$$\Delta s_1 = B_1 Q_1 + C_1 Q_1^2 \tag{7}$$

$$\Delta s_2 = B_2 (Q_2 - Q_1) + C_2 (Q_2^2 - Q_1^2) \tag{8}$$

$$\Delta s_3 = B_3 (Q_3 - Q_2) + C_3 (Q_3^2 - Q_2^2) \tag{9}$$

$$C_{12} = \frac{\frac{\Delta s_2}{\Delta Q_2} - \frac{\Delta s_1}{\Delta Q_1}}{\Delta Q_1 + \Delta Q_2} \tag{10}$$

$$C_{23} = \frac{\frac{\Delta s_3}{\Delta Q_3} - \frac{\Delta s_2}{\Delta Q_2}}{\Delta Q_2 + \Delta Q_3} \tag{11}$$

where s_1, s_2, s_3, Q_1, Q_2, and Q_3 are the drawdowns and the corresponding discharges, and B_1, B_2, B_3, C_1, C_2, and C_3 are the aquifer loss constants and the well loss constants, for the three steps. C_{12} and C_{23} represent the values of the well loss constant using the drawdown and discharge data for

steps 1 and 2, and steps 2 and 3, respectively. The values of the well loss constant for step 1 (C_1) and step 3 (C_3) have been taken as C_{12} and C_{23}, respectively, while the value of the well loss constant for step 2 has been estimated as the arithmetic mean of the well loss constants for steps 1 and 3.

The results of the analysis of the step-drawdown test data are shown in Table 4. In addition to the aquifer losses, the well losses for each of the three steps for each well, are provided in Table 4. The estimates of the aquifer losses range from 0.0277 m in well 1-1 to 6.0839 m in well 1-123. The estimates of the well losses range from 0.0546 m in well 1-104 to 5.6851 m in well 5-4.

Well Efficiency

The well efficiency (E) is determined by the following equation (Jacob, 1947):

$$E = \frac{BQ}{s} \times 100 \qquad (12)$$

where BQ is that portion of drawdown due to aquifer loss and s is the total drawdown in the well. The efficiency of each well for each of the three steps has been calculated as a percentage and is shown in Table 4. Table 4 shows that the well efficiency generally decreases with increasing discharge.

Specific Capacity

The specific capacity of a well is defined as the well discharge per unit decline of water level (Q/s). The specific capacity of each well at each pumping rate during the step-drawdown tests is shown in Table 4. The estimates of the specific capacity range from 26 m^2/day in well 5-2 to 838 m^2/day in wells 1-64 and 1-75. The distribution of the values of specific capacity shows that high values were measured for wells completed in either kurkar or kurkar and alluvium in the northern part of the study area, while low values were measured for wells completed in alluvium in the southern part of the area. This could be attributed to the higher transmissivity of the kurkar unit relative to the alluvium as documented by the constant discharge pumping tests.

CHAPTER IV

HYDROCHEMISTRY

Five sets of water samples have been collected from the wells in the delta Wadi El-Arish area, as shown in Appendix C. The five water sample sets were collected in October 1987, April 1988, July 1989, October 1989, and January 1990, and show the seasonal variation in groundwater chemistry. The number of wells sampled ranged from 32 to 45. The water samples were analyzed in the laboratory of the Groundwater Research Institute, Water Research Center in Cairo, except the last water sample set, in January 1990, which was analyzed in the laboratory of the Drainage Research Institute, Water Research Center. The analyses included pH, electrical conductivity, total dissolved solids, and the concentrations of the major inorganic ions (Ca^{++}, Mg^{++}, Na^{+}, K^{+}, HCO_3^{-}, SO_4^{--} and Cl^{-}). The concentrations of the major inorganic ions are presented in parts per million (ppm) and milliequivalents per liter in addition to percentages of total meq/l (see Appendix C).

The results of the chemical analyses of the groundwater samples have been used to evaluate the suitability of groundwater in the Wadi El-Arish area for irrigation. In addition, the hydrochemical analyses have been used to prepare:

1. TDS contour maps to show the spatial distribution of groundwater TDS.

2. TDS profiles to demonstrate the changes in TDS with time.

3. Ion concentration maps to show the distribution of the major ions in the study area.

4. A Piper (trilinear) diagram to determine groundwater types based on the dominant cation(s) and anion(s).

5. A table of $\frac{Na}{Cl}$ ratio to evaluate the degree of mixing between river water and sea water.

6. Sulin's (1948) graph for classification of groundwater genesis to deduce the origin of the well samples.

Groundwater TDS

TDS Contour Map of October 1987

The TDS contour map of October 1987, as shown in Figure 28, exhibits a general increase in TDS from the west to the east, and also from the northwestern to the southeastern part of the study area. The total dissolved solids (TDS) concentrations range from 1,500 ppm along the western margin to 4,500-5,500 ppm along the southeastern and northern margins of the area. The area can be divided into two distinct zones as follows:

1. Low TDS zone: This zone is located to the west of the Wadi El-Arish channel in the western part of the study

area, and in the middle part of the area south of the middle road between the Wadi El-Arish channel and the El-Arish--Lahfan road (Figure 28). The TDS concentrations generally range between about 1,500 and 2,500 ppm in this zone.

2. High TDS zone: This zone is located in two areas; the first occupies the eastern part of the area east of the El-Arish--Lahfan road to the north of the El-Arish airport, and along both sides of the El-Arish--Lahfan road north of the middle road. The second occupies the northern part of the study area to the south of the coastal road. The TDS concentrations in this zone generally range from about 2,500 to 5,500 ppm.

The explanation for the high TDS of the Quaternary aquifer throughout most of the second zone is that the wells tap the lower Pleistocene (marine kurkar) unit, as shown in Figures 14 and 15. This lower calcareous sandstone (kurkar) is a slightly more saline water-bearing unit than the units that overlie it because it does not receive recharge directly from Wadi El-Arish. In addition, deep percolation of return flow through irrigated lands with high salt contents might explain the saline nature of the kurkar, and also the rise in groundwater levels in this zone, as shown in Figure 16. The high TDS contents are due to sea water intrusion from the Mediterranean Sea in the northern part of this zone.

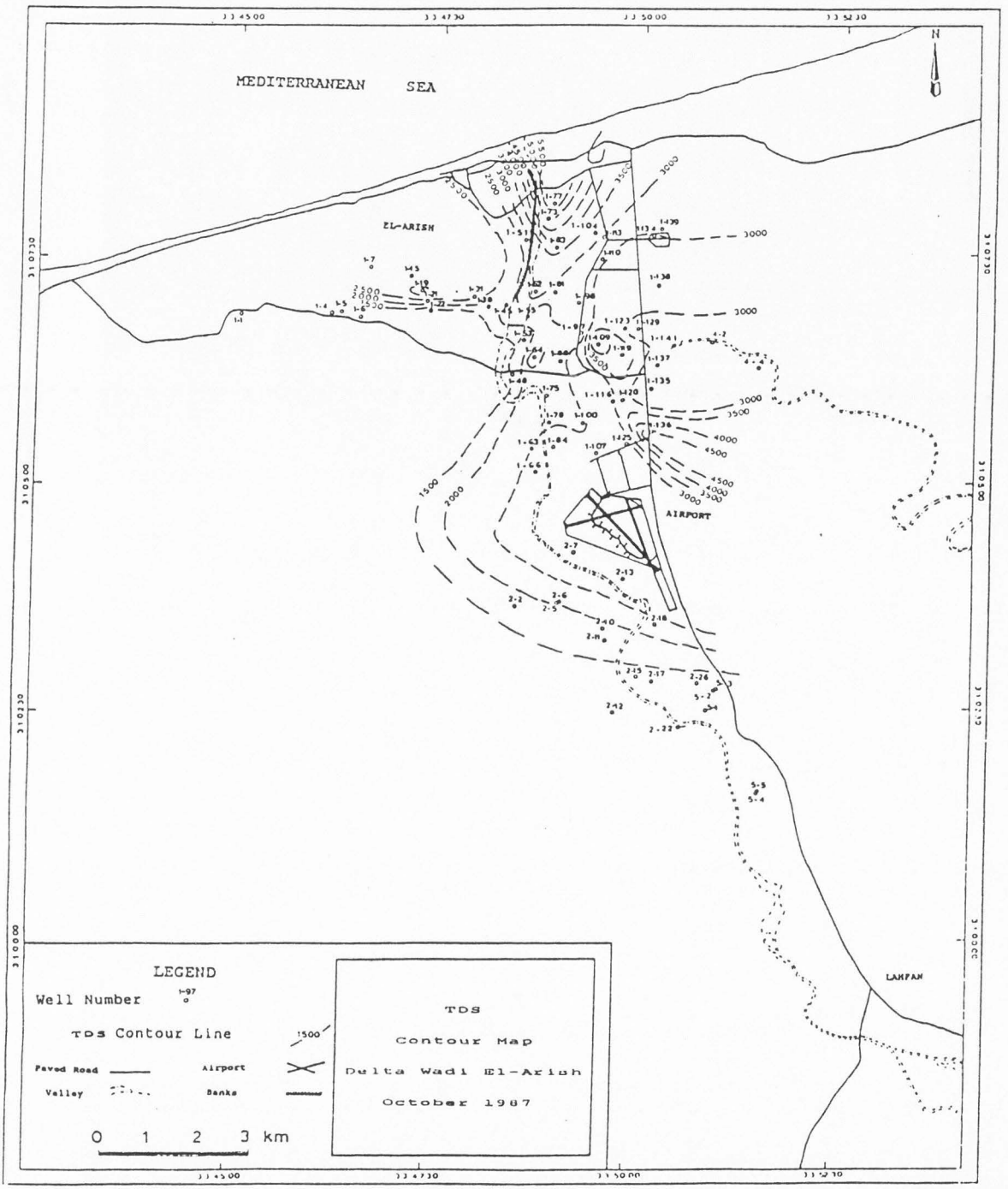

Fig. 28. TDS contour map, October 1987.

TDS Contour Map of April 1988

The TDS contour map of April 1988, as shown in Figure 29, shows that the distribution of TDS was quite similar to that in October 1987, except that there was a general increase in TDS in the two zones.

The low TDS zone located in the western and south-central parts increased from a minimum of 1,500 ppm up to 2,000 ppm, and from a maximum of 2,500 ppm to 3,500 ppm. In the area south of the El-Arish airport, the only TDS value recorded was 1,580 ppm at well 5-1.

The high TDS zone along the eastern and northern sides of the study area showed an increase in the maximum TDS up to 5,000 ppm around well 1-136 and up to more than 6,000 ppm at well 1-77.

TDS Contour Map of July 1989

The TDS contour map of July 1989, as shown in Figure 30, shows a remarkable decrease in TDS from the map of April 1988 in the western part of the area, particularly to the north of the El-Arish--El-Massaeid middle road where the TDS values generally ranged from about 1,500 to 2,000 ppm. The TDS decrease in this zone is attributable to wells 1-1 to 1-6 not having been used since 1988. Shut down of these wells caused a decrease in the extraction rate in this zone and a corresponding decrease in TDS. These wells were shut down because of the completion of the Nile water pipeline to El-Arish. The completion of the Nile water pipeline to El-

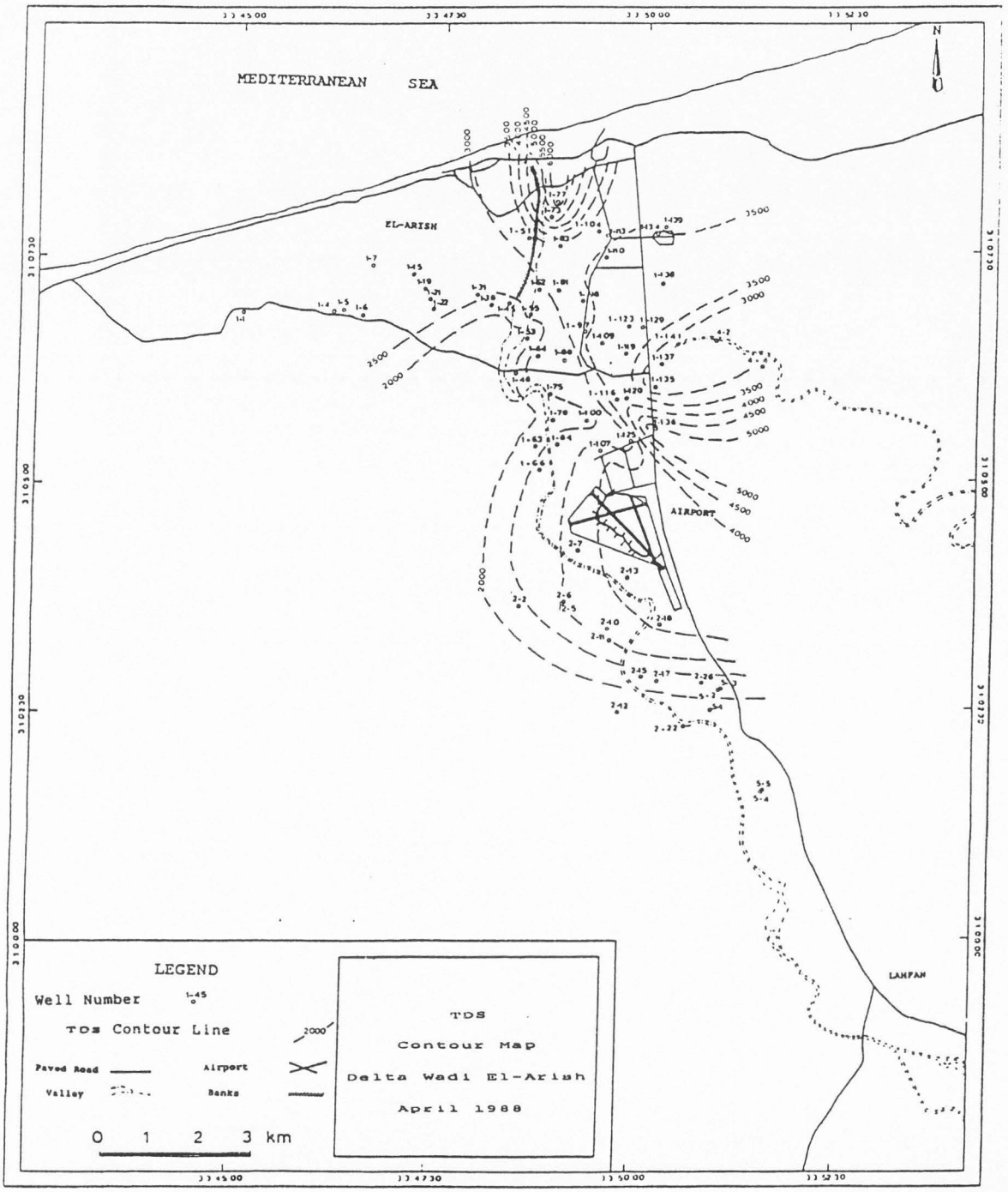

Fig. 29. TDS contour map, April 1988.

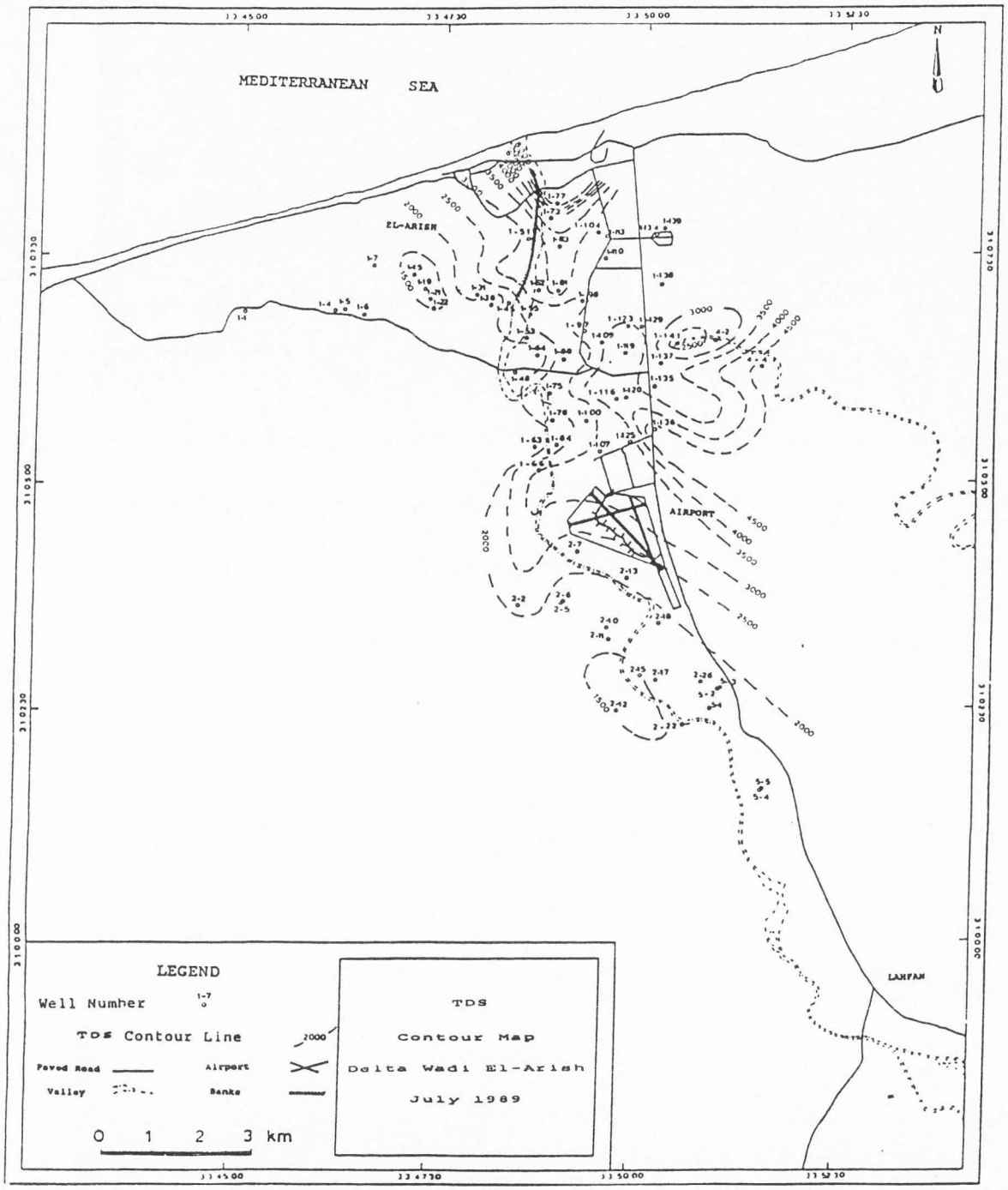

Fig. 30. TDS contour map, July 1989.

Arish also caused a decrease in TDS in the eastern area, where the maximum TDS recorded was less than 4,700 ppm. This is because waste water returning from domestic uses may recharge the aquifer and reduce TDS contents. On the other hand, higher TDS values were recorded in the northern part of the area, where TDS generally increased up to more than 8,000 ppm at well 1-77. South of the El-Arish airport, the TDS values generally were in the 1,500 to 2,000 ppm range.

TDS Contour Map of October 1989

The TDS contour map of October 1989, as shown in Figure 31, shows a decrease in TDS in the northern part of the area, where the TDS generally ranged from about 2,500 to 5,000 ppm. This is due to the decrease in the pumping rate at the beginning of winter, which caused a decrease in sea water intrusion from the Mediterranean Sea. In the southern part of the area, there was a slight increase in TDS. This increase in TDS is due to the increase in the pumping rate due to increasing water requirements for more irrigated lands. The TDS in this area generally was in the 2,000 to 2,500 ppm range. The TDS values in the western and eastern parts of the study area were almost identical to those in July 1989.

TDS Contour Map of January 1990

The TDS contour map of January 1990, as shown in Figure 32, is virtually identical to the map of October 1989.

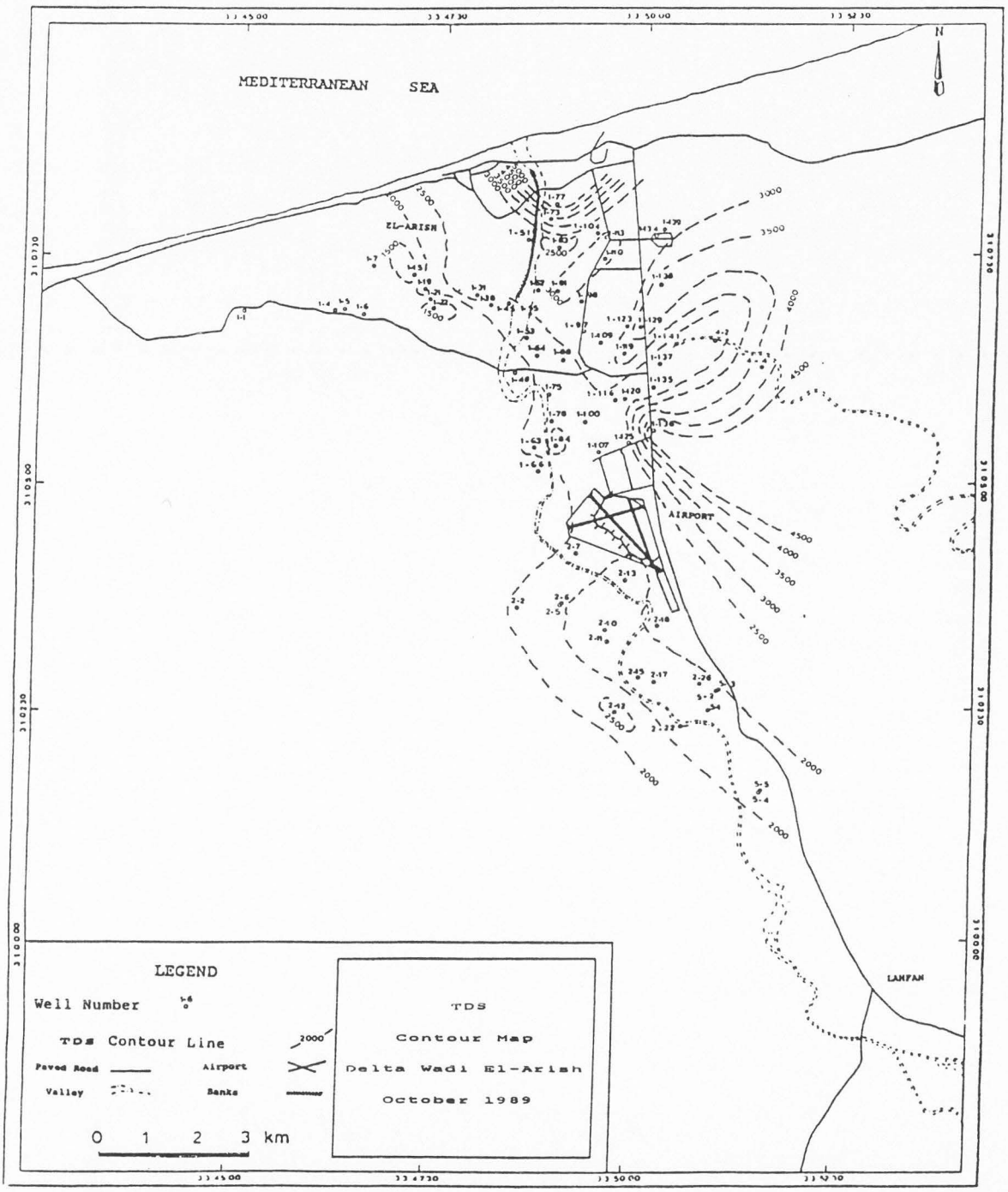

Fig. 31. TDS contour map, October 1989.

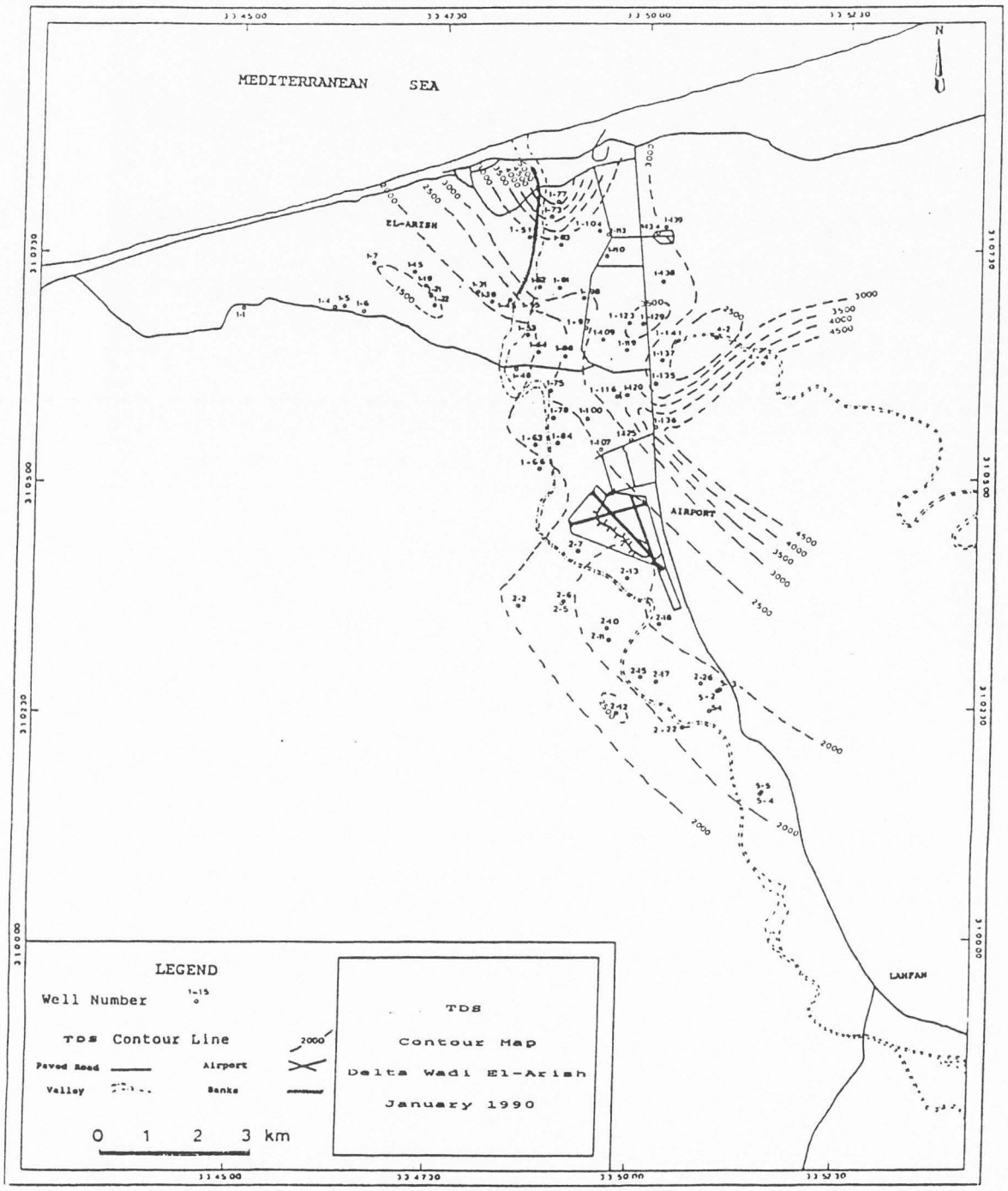

Fig. 32. TDS contour map, January 1990.

Change in Groundwater TDS 1962-1990

The two TDS contour maps of the delta Wadi El-Arish area in 1962 (Figure 8) and in 1990 (Figure 32) were used to prepare two pairs of TDS profiles, as shown in Figure 33. The 1962 TDS contour map was used rather than the 1954 TDS map, because the 1954 TDS map does not have enough data points to prepare the profiles.

The first pair of profiles trends in a north-south direction and passes through wells 1-77, 1-73, 1-83, 1-98, 1-88, 1-100, 1-107, 2-18, and 5-1. The profiles show a general TDS increase during the period from 1962 to 1990. The profiles also display a gradual decrease in TDS from north to south in both 1962 and 1990. The TDS ranged from 3,500 ppm in the northern part to about 2,500 ppm in the central part in 1962; TDS ranged from 5,000 ppm in the northern part to 1,500 ppm in the southern part in 1990. The higher TDS in the northern part was caused by sea water intrusion from the Mediterranean Sea.

The second pair of profiles trends in an east-west direction, passing through wells 4-4, 1-135, 1-75, 1-64, 1-22, and 1-7. The profiles also show a TDS increase during the period from 1962 to 1990. The profiles display a gradual decrease in TDS from east to west in both 1962 and 1990. The higher TDS in the eastern part caused by the fact that most of the wells tap the kurkar unit, which is slightly more saline than the alluvium. In 1962, the TDS

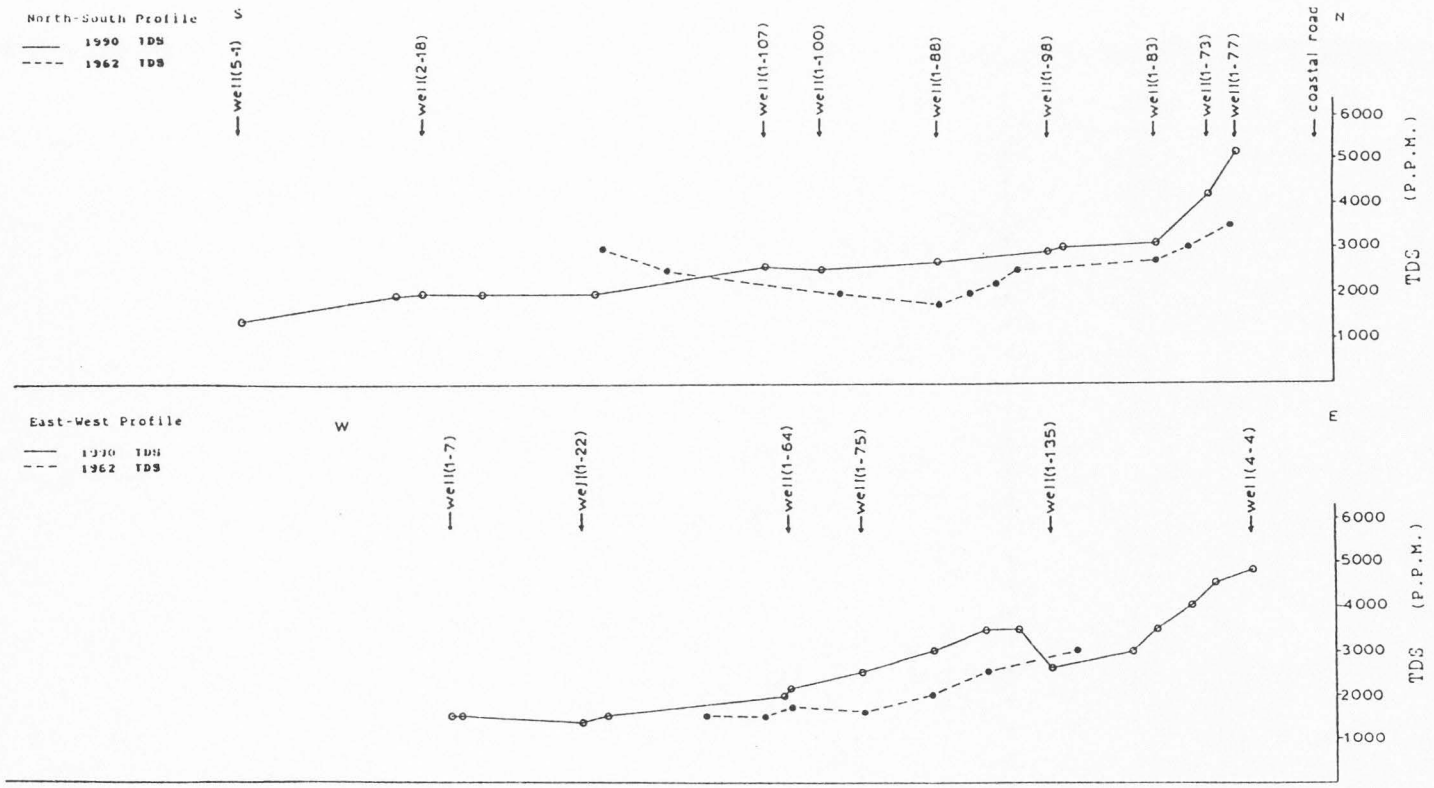

Fig. 33. TDS profiles showing change in groundwater TDS in delta Wadi El-Arish area from 1962 to 1990.

ranged from 3,000 ppm in the east to 1,500 ppm in the central part, while it ranged from 5,000 ppm in the east to 2,000 ppm in the west in 1990. The increase in groundwater extraction during the period from 1962 to 1990 caused a general increase in TDS because of the upward leakage of water from the more saline deep Cretaceous aquifer. Deep percolation of more saline return flow through irrigated lands also caused a general increase in TDS.

Distribution of Major Inorganic Ions

The concentrations of the major inorganic ions in groundwater samples from the Quaternary aquifer for the October 1989 set have been mapped, as shown in Figures 34 to 39, to show the distribution of each of these ions within the study area. The major inorganic ions are Na^{+}, K^{+}, Mg^{++}, Ca^{++}, SO_4^{--}, HCO_3^{-}, and Cl^{-}. The January 1990 set has not been used because this set of samples was the only one to be analyzed in the laboratory of the Drainage Research Institute; therefore, it may not be as reliable.

Sodium Plus Potassium Ions

The distribution of sodium plus potassium in the study area is shown in Figure 34. The distribution of the sum of these two ions coincided to some degree with the TDS distribution (Figure 31). The map also shows that the concentration of sodium plus potassium was lowest in the western and southern parts, where values of 145 ppm and 207

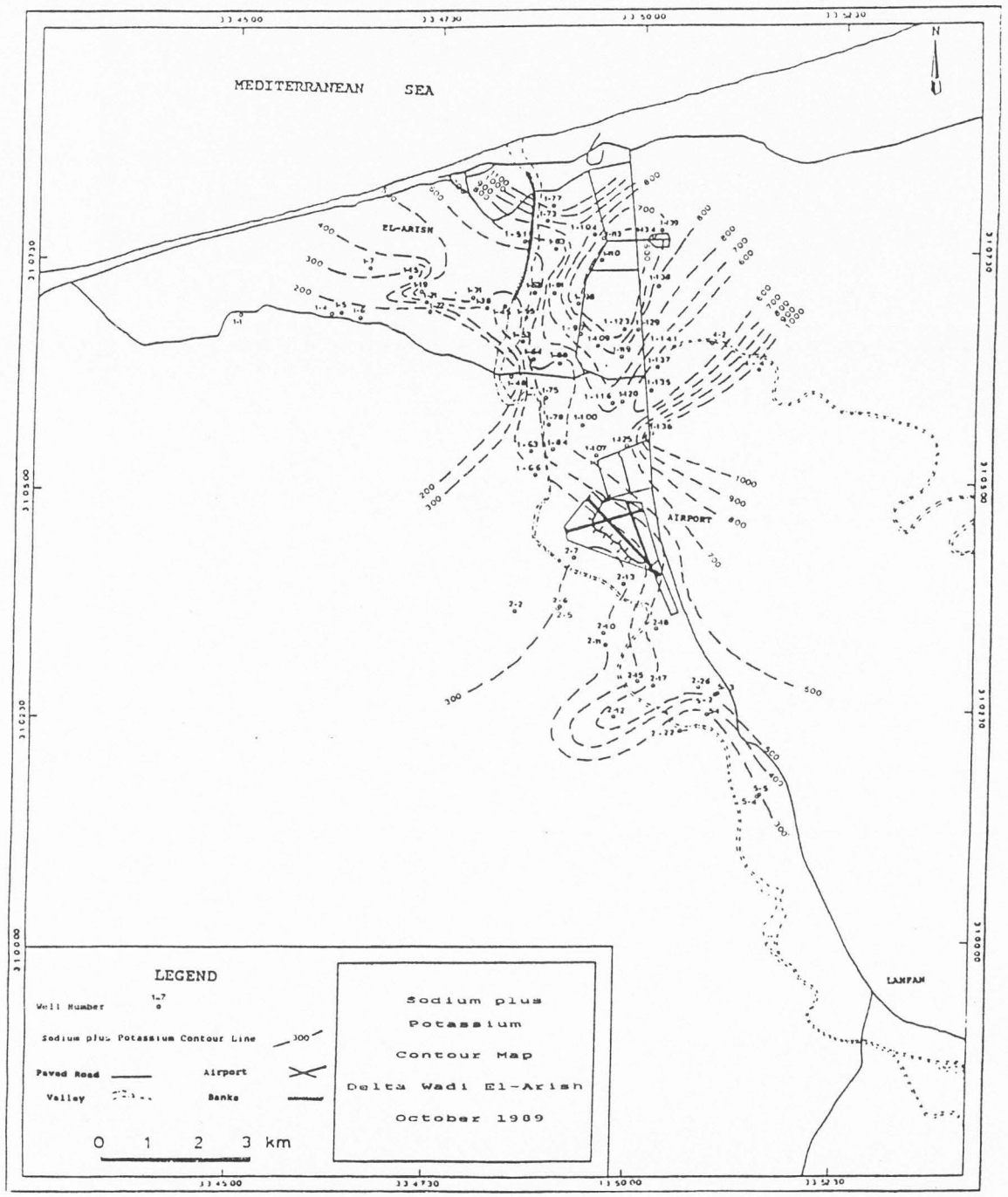

Fig. 34. Sodium plus potassium contour map, October 1989.

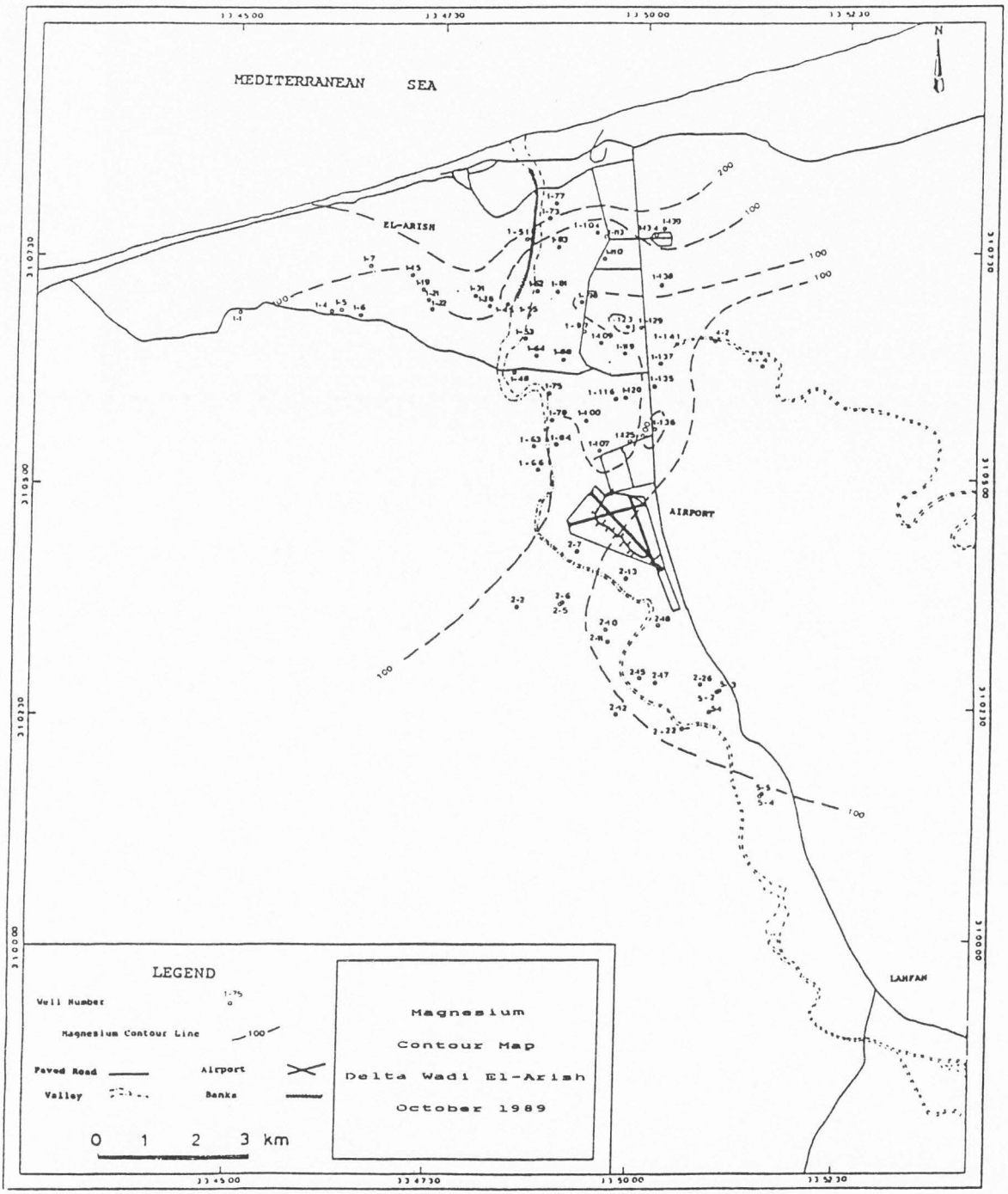

Fig. 35. Magnesium contour map, October 1989.

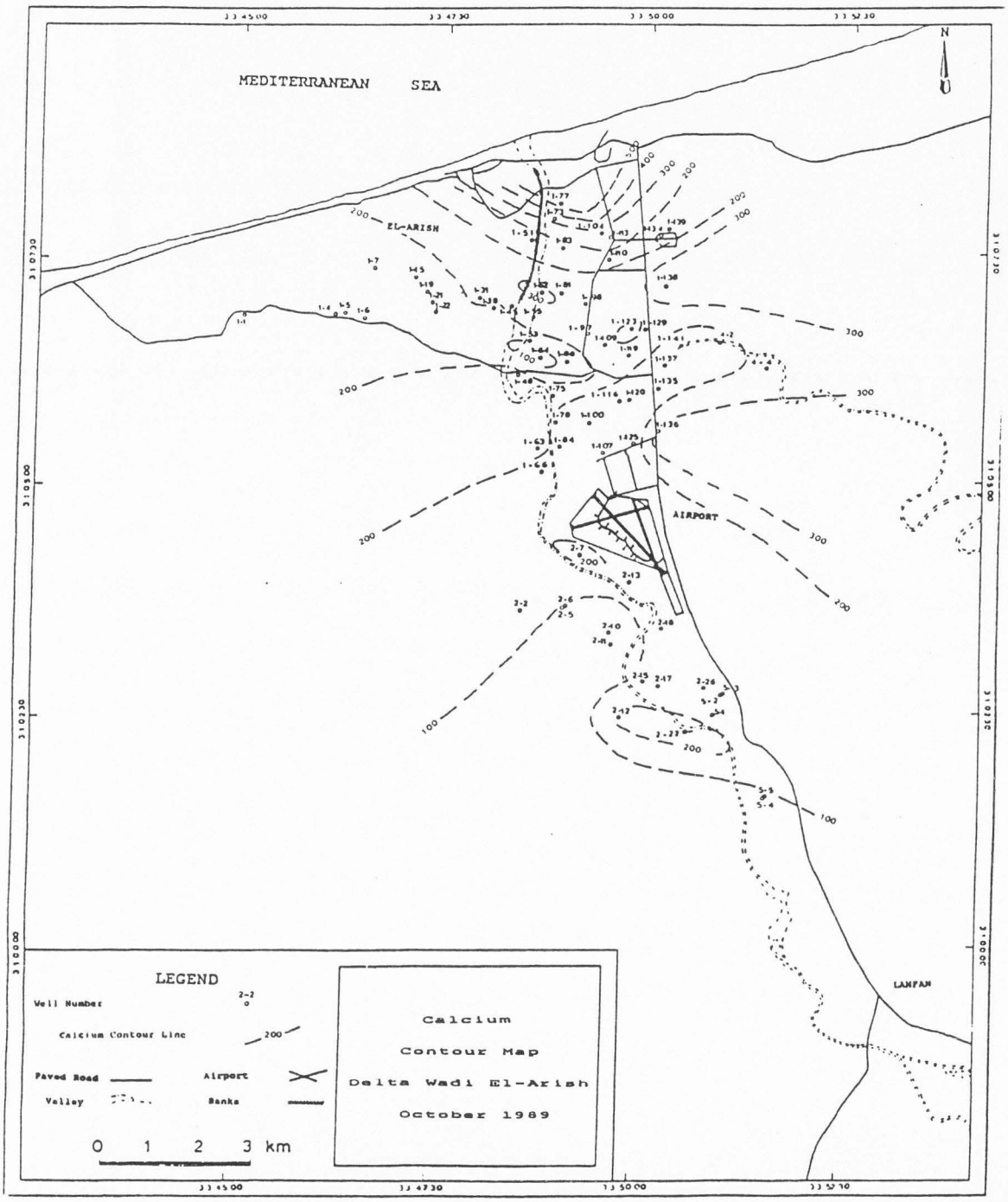

Fig. 36. Calcium contour map, October 1989.

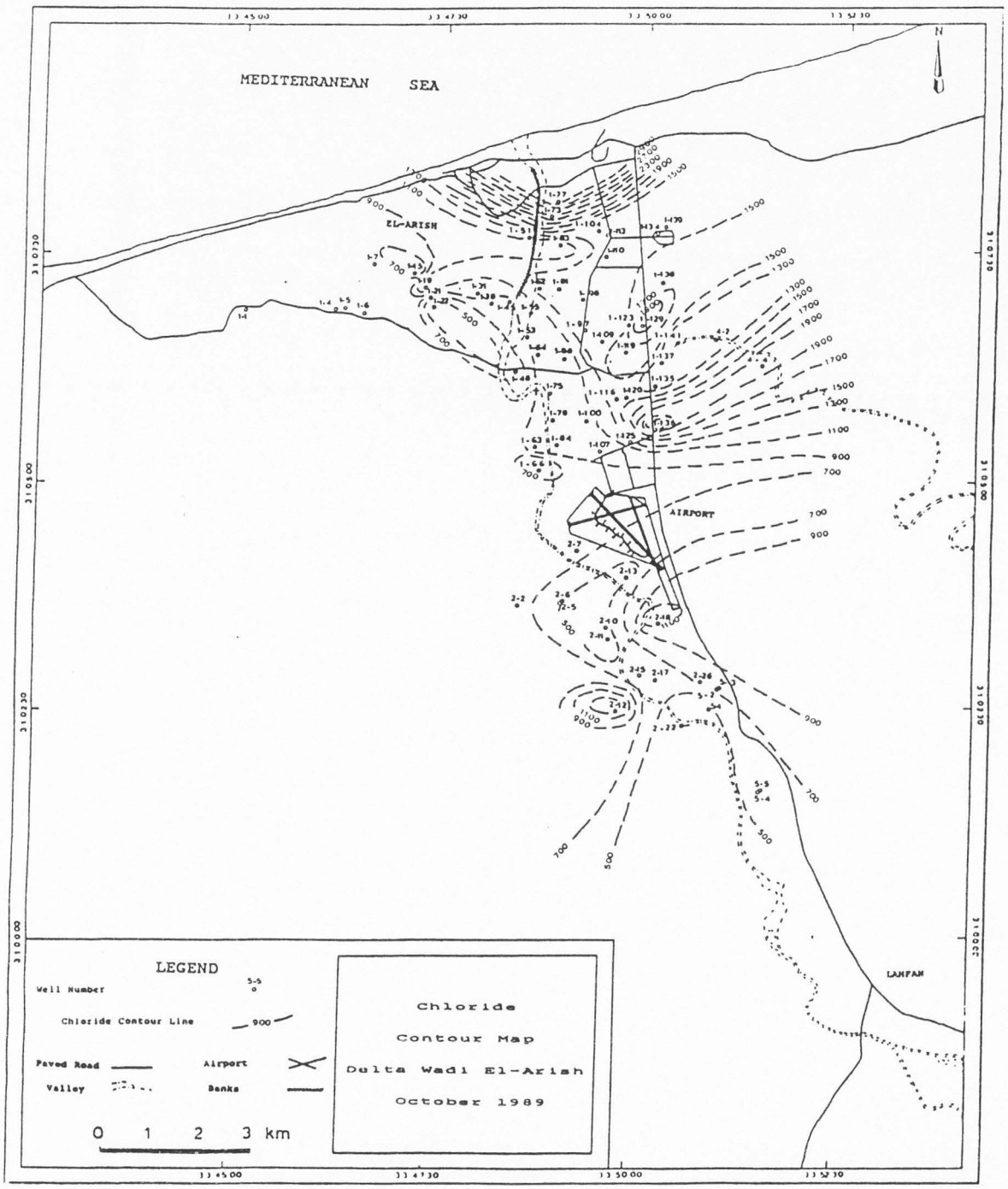

Fig. 37. Chloride contour map, October 1989.

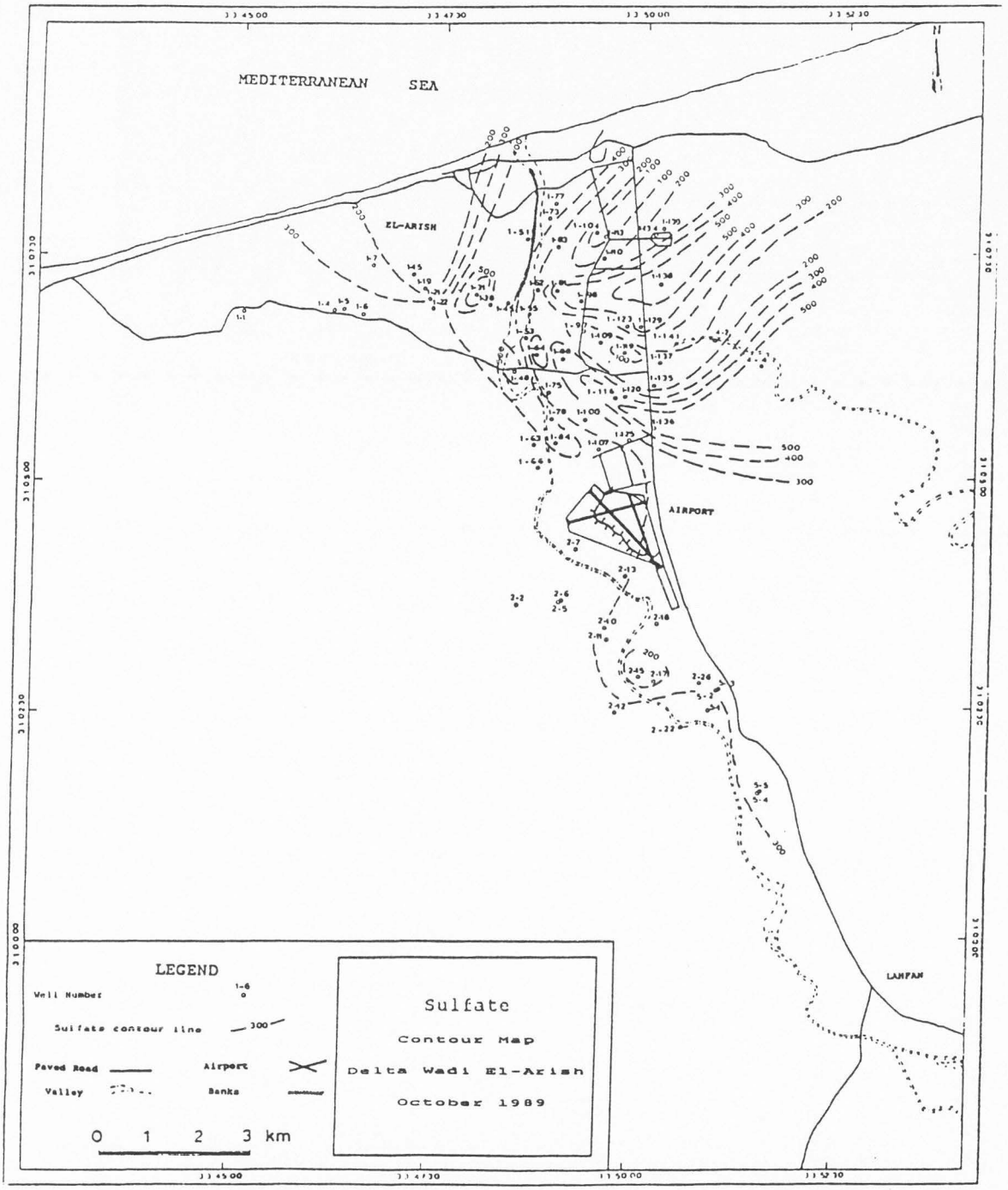

Fig. 38. Sulfate contour map, October 1989.

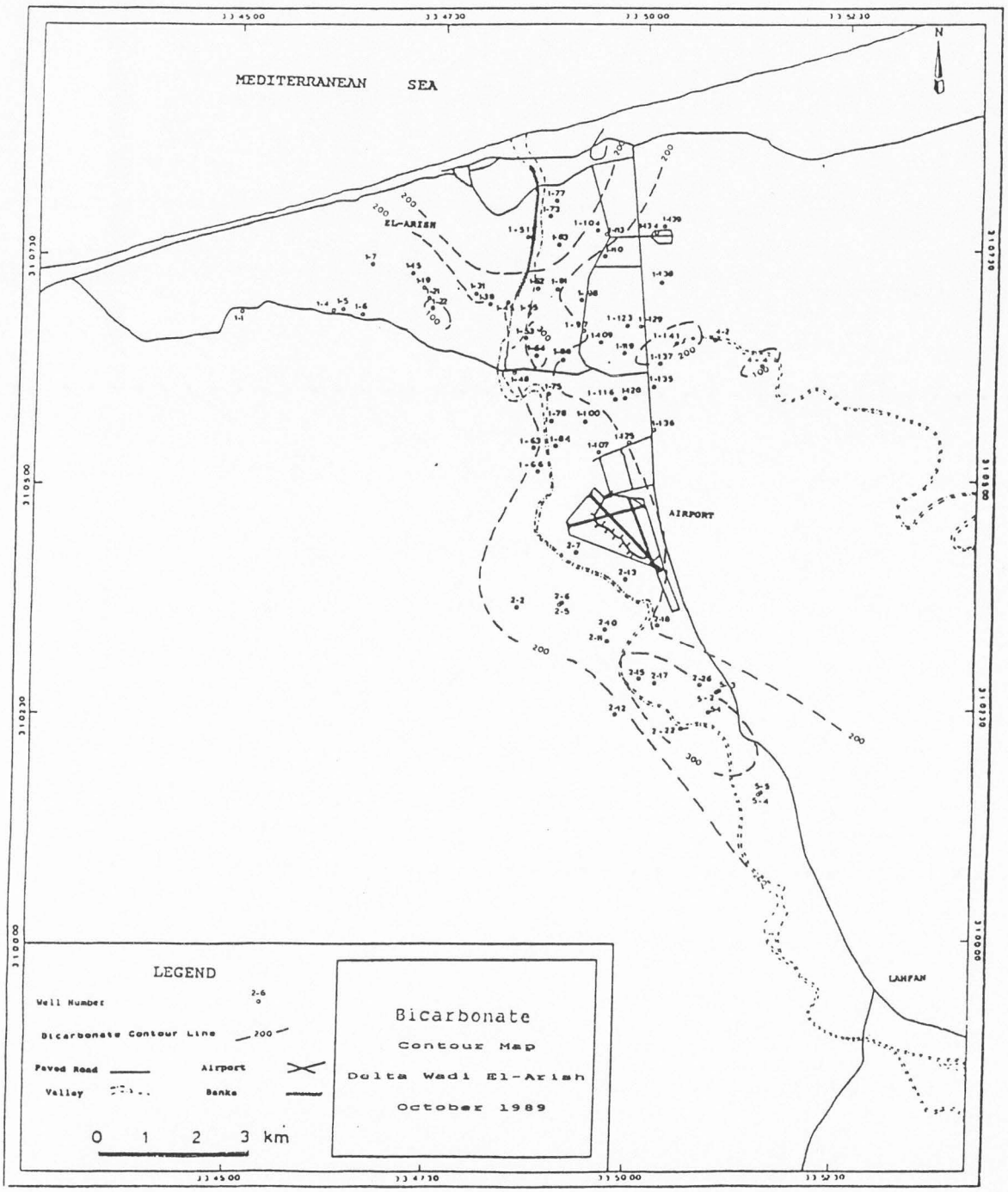

Fig. 39. Bicarbonate contour map, October 1989.

ppm were recorded at wells 1-22 and 2-22, respectively. On the other hand, the maximum values were measured in the northern part, where a value of 1,116 ppm was recorded at well 1-77, and in the eastern part, where a value of 1,093 ppm was recorded at well 1-136. The high sodium plus potassium concentrations in the northern part are due to sea water intrusion from the Mediterranean Sea, while the high concentrations in the eastern part are due to pumping from the kurkar unit, which is slightly more saline than the alluvium.

Magnesium Ion

The magnesium contour map (Figure 35) shows that the highest magnesium concentrations were measured in the northern and eastern parts of the study area, where values of 252, 235, and 227 ppm were recorded at wells 1-77, 1-123, and 1-136, respectively. The lowest concentrations were measured along the western side of the El-Arish--Lahfan road, where values of 2 and 5 ppm were recorded at wells 1-109 and 1-104, respectively. The high magnesium concentrations in the northern and in the eastern parts are due to sea water intrusion and pumping from the kurkar unit, respectively.

Calcium Ion

The calcium contour map (Figure 36) shows a general increase in calcium concentrations from the south to the

north. Concentrations ranged from 48 ppm at well 2-11 south of the El-Arish airport to 505 ppm at well 1-77 in the northern part of the area. Relatively high calcium concentrations also were measured in the eastern part of the area, where values of 323 and 327 ppm were recorded for wells 1-136 and 1-138, respectively. The high calcium concentrations in the northern and eastern parts are due to sea water intrusion and pumping from the kurkar unit, respectively.

Chloride Ion

The chloride contour map, as shown in Figure 37, shows that chloride concentrations are the highest of all the major inorganic ions. The map also shows that the highest chloride concentrations were measured in the northern part and in the eastern part, north of the El-Arish airport and east of the El-Arish--Lahfan road. These high chloride concentrations can be explained by sea water intrusion and pumping from the kurkar unit in the northern and eastern parts, respectively. The lowest chloride concentrations were measured along the western side of the Wadi El-Arish channel to the north of the El-Arish--El-Massaeid middle road, and also south of the El-Arish airport. The low chloride concentrations in both the western and southern parts are due to direct recharge from the sand dunes that cover most of the western surface area and to inflow of groundwater through a number of buried channels in the

The chloride concentrations ranged from about 500 to 2,900 ppm.

Sulfate Ion

The sulfate contour map, as shown in Figure 38, shows that sulfate concentrations generally fell between chloride and bicarbonate concentrations. The highest sulfate concentrations were measured in the northwestern and eastern parts of the area, where values ranged from 696 ppm at well 1-31 to 555 and 546 ppm at wells 1-136 and 1-138, respectively. The lowest sulfate concentrations were measured in samples from wells along the western side of the El-Arish--Lahfan road, where values ranged from 62 ppm at well 1-119 to 96 ppm at well 1-104. The low sulfate concentrations along the western side of the El-Arish--Lahfan road are due to the continuous flushing of the aquifer along the Wadi El-Arish channel.

Bicarbonate Ion

The bicarbonate contour map, as shown in Figure 39, when compared to Figures 37 and 38, shows that bicarbonate concentrations are the lowest among all the major anions. The low bicarbonate concentrations could be attributed to the absence of shallow meteoric water that is directly recharged by rainfall in the wells completed in the Pleistocene units. The map shows no real trend in the bicarbonate concentrations. The bicarbonate concentrations

ranged from a high of 384 ppm at well 5-1 to a low of 49 ppm at well 1-22. The map shows that the highest bicarbonate concentrations were measured in the southern part of the area, south of the El-Arish airport near the bend in the Wadi El-Arish channel. The lowest bicarbonate concentrations were measured along the western and eastern margins, and to the north of the El-Arish--El-Massaeid middle road.

From the previous discussion it can be concluded that the increase in TDS and also the increase in major inorganic ion concentrations in the northern part of the study area are due to sea water intrusion from the Mediterranean Sea. In addition, the increases in TDS and major inorganic ion concentrations in the eastern part of the area are due to the fact that the wells tap the lower Pleistocene (kurkar) unit, which is more saline than the alluvium because it does not receive recharge directly from Wadi El-Arish. The kurkar unit receives recharge from the more saline deep Cretaceous aquifer. Deep percolation of return flow through irrigated lands with high salt contents might also contribute to the saline nature of the kurkar.

pH Values

The pH values measured for groundwater samples from the wells, as shown in Appendix C, show the water to be neutral to slightly alkaline. The pH values ranged from 7.1 to 8.8,

except for well 1-137, which had a measured pH of 7.0 in July 1989.

Hydrochemical Water Types

A Piper (trilinear) diagram (Piper, 1944) has been used to determine the water type for the samples collected from wells in the delta Wadi El-Arish area (Figure 40).

A Piper diagram contains three areas; two triangles, one for cations and the other for anions, are displayed in the lower left and the lower right corners of the diagram, respectively, and a central diamond-shaped area is displayed between and above the two triangles. Each vertex represents 100 percent of the total milliequivalents per liter being comprised of a certain ion. The percentage of the total milliequivalents per liter of the three major cations is plotted as a single point on the lower left triangle, while the percentage of the total milliequivalents per liter of the three major anions is plotted on the lower right triangle. A third point is plotted on the central diamond-shaped area at the intersection of the two lines projected from the two points on the triangles.

Chemical analyses of groundwater samples collected from wells in the delta Wadi El-Arish area in October 1989, as shown in Appendix C, have been plotted on Figure 40. The diagram shows that three main water types are present. The

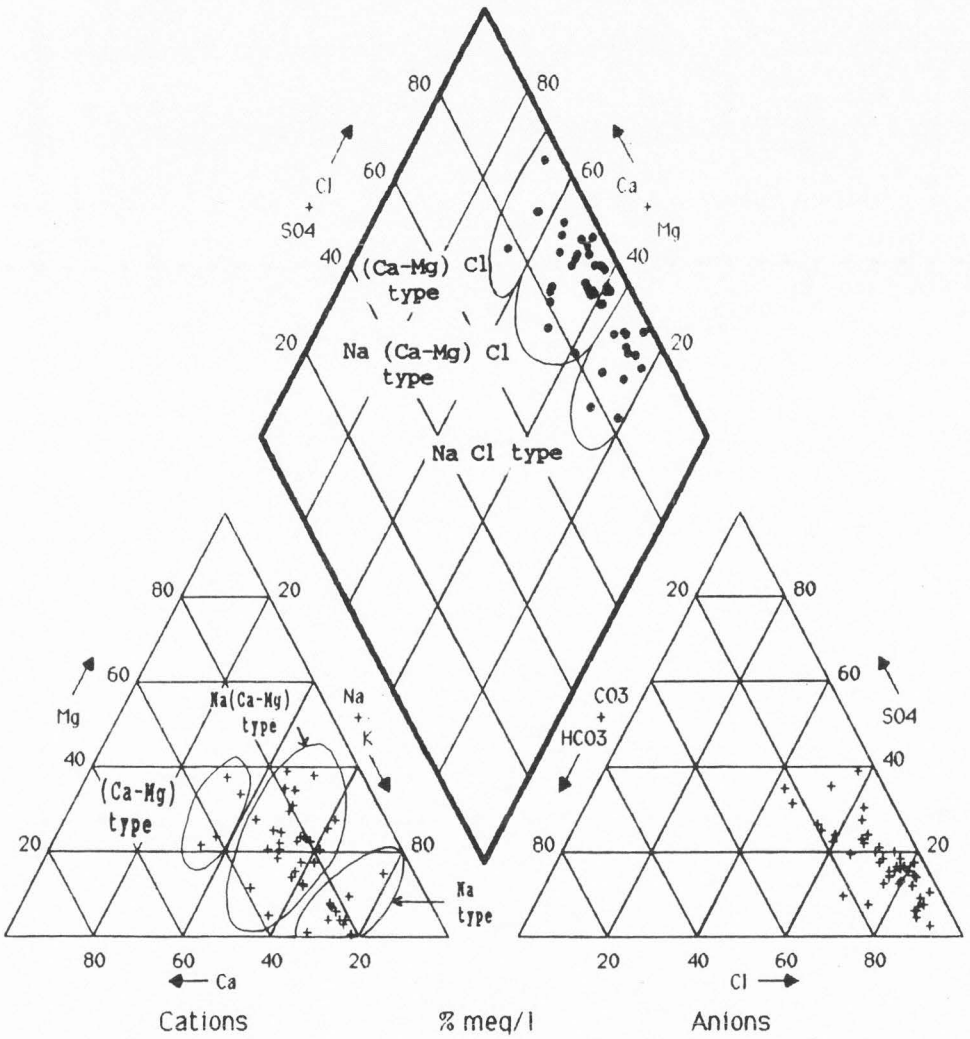

Fig. 40. Piper (trilinear) diagram (after Piper, 1944).

first water type is a sodium-chloride type and is represented by the water samples from twelve wells, nine of which are located in the north-central part of the area (wells 1-64, 1-81, 1-83, 1-97, 1-100, 1-104, 1-109, 1-119, 1-125, 2-15, 4-4 and 5-2). Chloride and sodium are still the dominant anion and cation, respectively, for the second water type, but some calcium and/or magnesium is present in significant concentrations in addition to sodium. This water type is found in most of the water wells, particularly the wells located in the northwestern and eastern parts of the study area and along the Wadi El-Arish channel (wells 1-7, 1-15, 1-19, 1-31, 1-38, 1-45, 1-62, 1-63, 1-66, 1-75, 1-77, 1-84, 1-88, 1-98, 1-123, 1-129, 1-135, 1-136, 1-138, 1-139, 1-141, 2-2, 2-11, 2-12, 2-13, 2-18, 4-2, 5-1, 5-4). The third water type is represented by four wells, 1-22, 1-48, 2-7, and 2-22, located in the western part of the area. Chloride is still the dominant anion in this water type, but calcium and/or magnesium, rather than sodium, are the dominant cations.

Figure 41 shows that the sodium-chloride water type is concentrated in the north-central part of the study area, and the second water type is concentrated in the northwestern and eastern parts of the study area, while the third water type is concentrated in the western part of the study area. The most likely reasons that the groundwater is dominated by chloride and sodium are 1) many of the wells

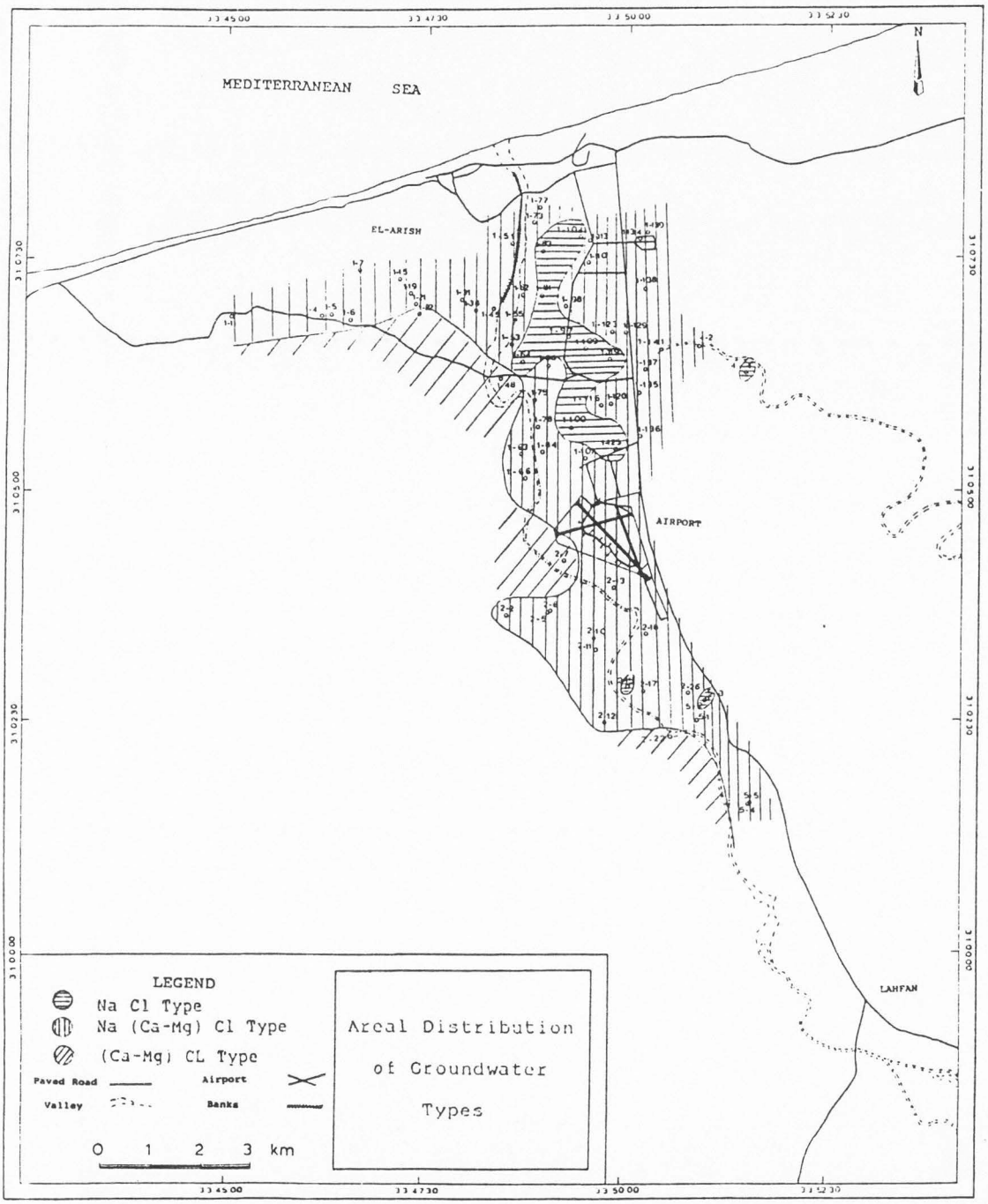

Fig. 41. Areal distribution of groundwater types.

pump from the kurkar, and 2) the proximity of the Mediterranean Sea. The presence of Na Cl water in the north-central area is due to the extremely high extraction rates, which caused sea water intrusion from the Mediterranean Sea. The existence of (Ca-Mg) Cl water in the western area and Na (Ca-Mg) Cl water throughout the rest of the study area is due to Na Cl water from the Mediterranean and the kurkar being diluted by meteoric water moving into the area from sand dunes in the southwest and from the Wadi El-Arish channel.

Ratios of Major Inorganic ions

The ratio of $\frac{Na}{Cl}$ was determined for groundwater samples from the wells in the study area using the data collected in October 1989 (Appendix C). The ratio was determined for concentrations measured in meq/l (Table 5). Sea water has a value of 0.85 for $\frac{Na}{Cl}$ while river water has a value of 1.79 (Al-Ruwaih, 1984). These sea water and river water values were taken as end members for comparison with the ratios determined for the water samples collected from the wells to evaluate the degree of mixing between sea water and river water. A few wells have a $\frac{Na}{Cl}$ ratio higher than the value for sea water but less than the standard river water value; however, the ratios of $\frac{Na}{Cl}$ in most of the water samples show that they are lower than the value for

Table 5. Groundwater Hydrochemical Ratios and Origins in the Delta Wadi El-Arish Area

Well No.	Hydrochemical Ratios $\frac{Na}{Cl}$	$\frac{Cl-(Na+K)}{Mg}$	$\frac{(Na+K)-Cl}{SO4}$	Ground Water Origin
1-7	0.66	0.78		Old Marine
1-15	0.69	0.87		Old Marine
1-19	0.68	1.04		Marine
1-22	0.54	0.66		Old Marine
1-31	0.63	0.69		Old Marine
1-38	0.68	0.50		Old Marine
1-45	0.85	1.74		Marine
1-48	0.66	0.71		Old Marine
1-62	0.62	2.53		Marine
1-63	0.79	1.08		Marine
1-64	1.03		0.40	Deep Meteoric
1-66	0.80	0.43		Old Marine
1-75	0.75	1.17		Marine
1-77	0.58	1.63		Marine
1-81	0.88	1.05		Marine
1-83	0.96	0.56		Old Marine
1-84	0.77	0.69		Old Marine
1-88	0.80	0.71		Old Marine
1-97	0.82	2.52		Marine
1-98	0.70	1.19		Marine
1-100	0.98	0.33		Old Marine

(Table 5 continued)

1-104	0.77	22.12		Marine
1-109	0.89	20.00		Marine
1-119	0.76	3.03		Marine
1-123	0.63	0.76		Old Marine
1-125	0.94	0.42		Old Marine
1-129	0.69	1.08		Marine
1-135	0.64	1.28		Marine
1-136	0.70	1.08		Marine
1-138	0.79	1.30		Marine
1-139	0.73	1.06		Marine
1-141	0.72	0.87		Old Marine
2-2	0.68	0.57		Old Marine
2-7	0.54	0.90		Old Marine
2-11	1.11		0.26	Deep Meteoric
2-12	0.62	0.98		Old Marine
2-13	0.86	0.31		Old Marine
2-15	1.02		0.26	Deep Meteoric
2-18	0.76	1.48		Marine
2-22	0.77	0.40		Old Marine
4-2	0.67	1.54		Marine
4-4	0.95	0.78		Old Marine
5-1	1.11		0.19	Deep Meteoric
5-2	1.05		0.23	Deep Meteoric
5-4	0.80	0.32		Old Marine

sea water (Table 5). The low ratios of $\frac{Na}{Cl}$ in most of the water samples collected could be attributed to the adsorption of sodium from sea water onto the fine-grained sediments comprising much of the subsurface geologic materials (El-Kiki, 1981). The high $\frac{Na}{Cl}$ ratio for a few of the wells could be explained by receiving recharge from water of meteoric origin.

Groundwater Genesis

The origin of the samples collected from wells in the delta Wadi El-Arish area (Figure 42) has been deduced using Sulin's (1948) graph for classification of groundwater genesis.

Sulin's graph contains two quadrangles connected together at only a single point. At the transitional point, the concentration of sodium plus potassium is equal to the chloride concentration. The upper quadrangle represents a marine water origin while the lower quadrangle represents a meteoric water origin. The upper quadrangle is divided into two equal triangles. The hypotenuse for both triangles is represented by the line described by:

$$\frac{Cl^- - (Na^+ + K^+)}{Mg^{++}} = 1$$

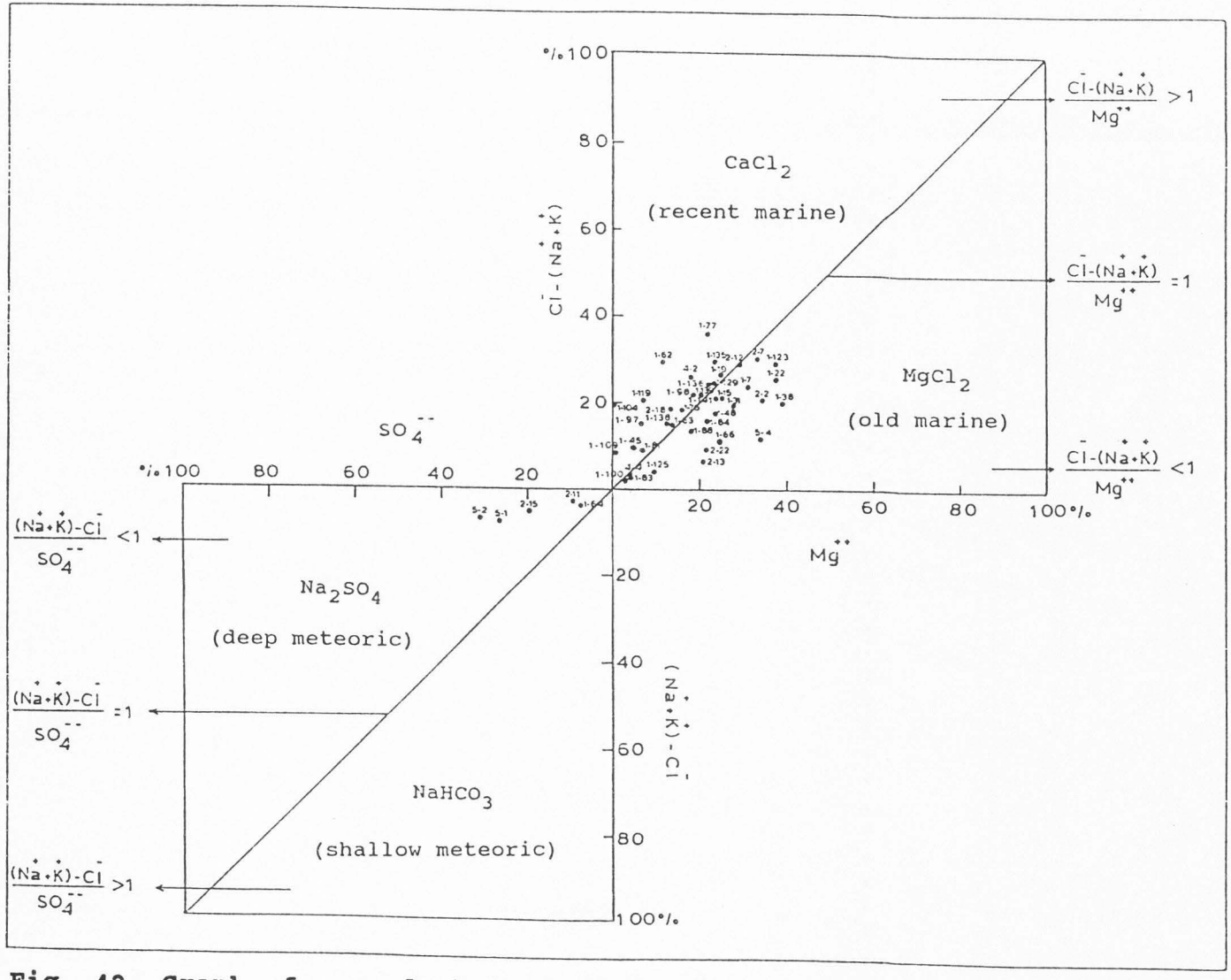

Fig. 42. Graph of groundwater genesis (Sulin, 1948).

Thus, the ratio of $\frac{Cl^- - (Na^+ + K^+)}{Mg^{++}}$ in the lower triangle is less than one, while the ratio in the upper triangle is greater than one. The hydrochemical composition of the lower triangle represents a Mg Cl_2 type of water that reflects an old marine origin (connate water), while the upper triangle represents a Ca Cl_2 type of water that reflects a young marine origin.

The lower quadrangle is also divided into two equal triangles, where the hypotenuse for both triangles is represented by the line described by:

$$\frac{(Na^+ + K^+) - Cl^-}{SO_4^{--}} = 1$$

Thus, the ratio of $\frac{(Na^+ + K^+) - Cl^-}{SO_4^{--}}$ in the lower triangle is greater than one, while the ratio in the upper triangle is less than one. The hydrochemical composition of the lower triangle represents a Na HCO_3 water type that reflects a shallow meteoric origin, while the hydrochemical composition of the upper triangle represents a Na SO_4 water type that reflects a deep meteoric origin.

The ratios of the major inorganic ions in the groundwater samples collected from wells in the delta Wadi El-Arish area, as shown in Table 5, are plotted on Figure 42 to determine their probable origins. The graph shows that there are three principal origins for the groundwater. The

first two are of marine origin where the concentration of chloride is greater than the concentration of sodium plus potassium. The third is of deep meteoric origin where the concentration of sodium plus potassium is higher than the concentration of chloride. The graph shows the absence of Na HCO_3 water of shallow meteoric origin.

The Ca Cl_2 water type is represented by samples collected from wells 1-19, 1-45, 1-62, 1-63, 1-75, 1-77, 1-81, 1-97, 1-98, 1-104, 1-109, 1-119, 1-129, 1-135, 1-136, 1-138, 1-139, 2-18, and 4-2. This type of water reflects young marine (Mediterranean) water, but the proximity of the data points to the $\frac{Cl^- - (Na^+ + K^+)}{Mg^{++}} = 1$ line suggests that the water in these wells may have been old marine (connate) water originally that has been largely replaced by recent marine water from the Mediterranean Sea.

The Mg Cl_2 water type is represented by samples collected from wells 1-7, 1-15, 1-22, 1-31, 1-38, 1-48, 1-66, 1-83, 1-84, 1-88, 1-100, 1-123, 1-125, 1-141, 2-2, 2-7, 2-12, 2-13, 2-22, 4-4, and 5-4. This type of water reflects old marine (connate) water; however, once again, the proximity of the data points to the $\frac{Cl^- - (Na^+ + K^+)}{Mg^{++}} = 1$ line suggests that it may have mixed with some marine water from the Mediterranean Sea. The Na_2 SO_4 water type is represented by samples collected from wells 1-64, 2-11, 2-15, 5-1, and 5-2, and reflects a deep meteoric origin.

The Ca CL_2 (recent marine) and Mg Cl_2 (old marine) water samples were collected from most of the wells in the delta Wadi El-Arish area, while the Na_2 SO_4 (deep meteoric) water samples were collected in the southern part of the area south of the El-Arish airport, suggesting that such water is being recharged by deep percolation of meteoric water in this area, possibly through the fault at Lahfan (Figure 43). Figure 43 shows that the Mg Cl_2 (old marine) type is found throughout most of the study area. The Ca Cl_2 (recent marine) type is concentrated in the northern part of the area and also near the bend in the Wadi El-Arish channel around wells 1-63 and 1-75. The presence of young marine water in the northern part of the area is due to sea water intrusion from the Mediterranean Sea, while the existence of old marine water in most of the rest of the area is due to the fact that most of the wells have been completed in the marine calcareous sandstone (kurkar) unit.

Suitability of Groundwater for Irrigation

The suitability of groundwater in the Quaternary aquifer in the delta Wadi El-Arish area for irrigation purposes has been evaluated using the hydrochemical data from the water samples collected in October 1989. The hydrochemical composition of groundwater affects both the fertility of the soil and plant growth. Because of the wide

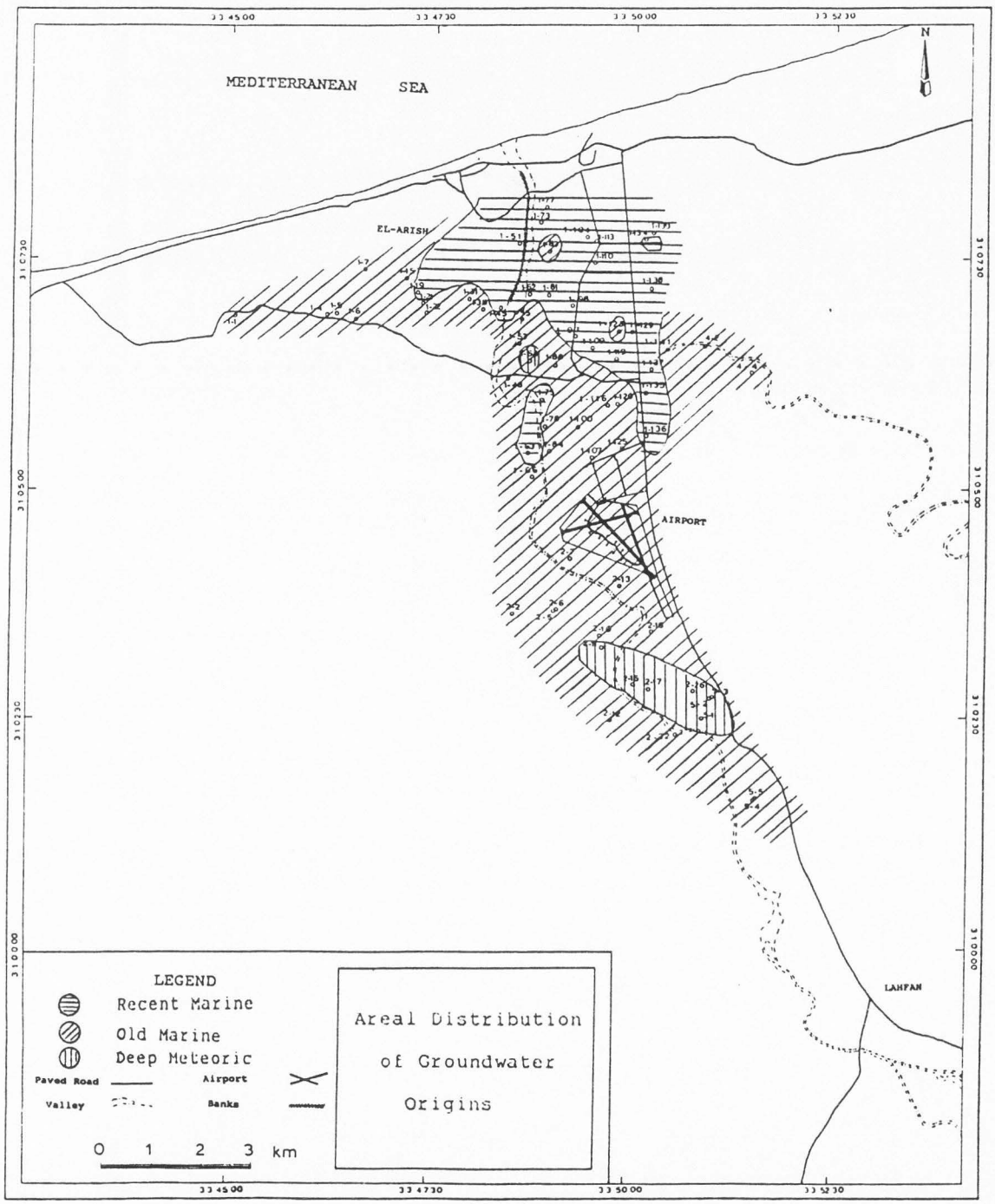

Fig. 43. Areal distribution of groundwater origins.

range in the salinity tolerances of different plants, absolute limits for the salinity of groundwater cannot be defined.

The sodium concentration is significant when evaluating the suitability of groundwater for irrigation because sodium may cause an increase in the hardness of the soil as well as a reduction in its permeability. The U.S. Salinity Laboratory (1954) has defined the sodium adsorption ratio (SAR) by the following relationship:

$$SAR = \frac{Na^{+}}{\sqrt{(Ca^{++} + Mg^{++})/2}} \qquad (13)$$

where all concentrations are expressed in milliequivalents per liter.

Table 6 shows the calculated SAR for all water samples in the delta Wadi El-Arish area collected in October 1989 and the electrical conductivity for each water sample.

Based on the data presented in Table 6, a classification diagram for irrigation water, recommended by the U.S. Salinity Laboratory (1954) has been prepared (Figure 44). The diagram is based on the electrical conductivity (EC) of water in micromhos per centimeter (μmhos/cm) at 25°C versus the sodium adsorption ratio (SAR). The electrical conductivity is plotted on a logarithmic scale, and reflects the water salinity hazard. The SAR is plotted on an arithmetic scale and reflects the sodium

Table 6. Sodium Adsorption Ratio (SAR), Electrical Conductivity (EC), Percent Sodium, and Classes in the El-Arish Wells in October 1989

Well No.	EC μmhos/cm at 25°C	SAR	Percent Sodium	Classes
1-7	2800	5.24	50	C4S2
1-15	2100	4.61	49	C3S2
1-19	3900	8.33	60	C4S3
1-22	1600	2.31	31	C3S1
1-31	4200	5.03	43	C4S2
1-38	3000	4.87	44	C4S2
1-45	3800	7.18	47	C4S2
1-48	2500	3.36	36	C4S1
1-62	4500	6.64	50	C4S2
1-63	3500	7.45	58	C4S2
1-64	3200	13.44	78	C4S4
1-66	2600	4.84	48	C4S2
1-75	3500	7.64	58	C4S2
1-77	8100	9.9	51	C5S4
1-81	5000	12.65	69	C5S4
1-83	3500	12.69	75	C4S4
1-84	4000	7.4	55	C4S3
1-88	3600	7.64	58	C4S2
1-97	4600	13.27	71	C4S4
1-98	4500	7.45	52	C4S3
1-100	3500	12.92	75	C4S4
1-104	4500	11.25	68	C4S3

(Table 6 continued)

Well No.	EC µmhos/cm at 25°C	SAR	Percent Sodium	Classes
1-109	4500	15.79	78	C4S4
1-119	5000	12.83	70	C5S4
1-123	4500	7.24	51	C4S3
1-125	4000	12.45	73	C4S4
1-129	5800	9.85	57	C5S3
1-135	4100	7.53	55	C4S3
1-136	7000	11.27	58	C5S4
1-138	5500	10.78	61	C5S4
1-139	4600	9.54	61	C4S3
1-141	3800	7.49	56	C4S2
2-2	3100	5.14	46	C4S2
2-7	3400	3.76	36	C4S2
2-11	2000	6.22	61	C3S2
2-12	200	6.67	49	C4S2
2-13	300	4.74	49	C4S2
2-15	300	8.96	71	C4S3
2-18	3600	8.27	61	C4S3
2-22	2100	2.91	32	C3S1
4-2	3500	7.99	59	C4S3
4-4	4500	15.51	74	C4S4
5-1	2600	5.41	52	C4S2
5-2	3000	9.77	69	C4S3
5-4	2400	4.73	48	C4S2

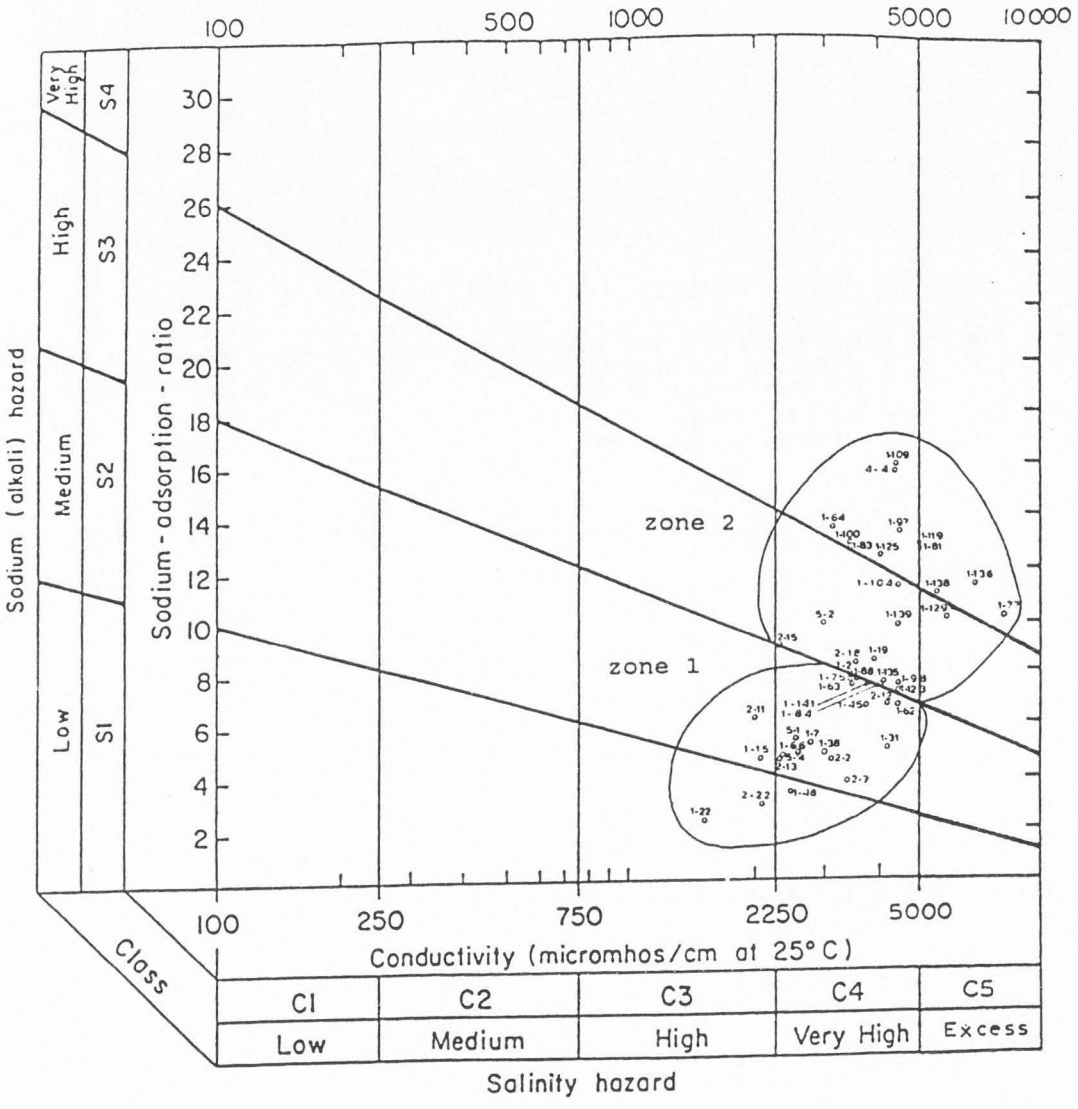

Fig. 44. Diagram for studying suitability of groundwater for irrigation purposes (U.S. Salinity Laboratory, 1954).

hazard. The diagram indicates that groundwater in the delta Wadi El-Arish area includes eight irrigation suitability classes, which are C_3 S_1, C_4 S_1, C_3 S_2, C_4 S_2, C_4 S_3, C_5 S_3, C_4 S_4, and C_5 S_4, as shown in Table 6. The eight irrigation suitability classes can be divided into two zones.

Zone 1

This zone is located along the western side of the Wadi El-Arish channel, including the area to the south of the El-Arish airport, as shown in Figure 45. The characteristics of groundwater in this zone are:

EC = 1600 - 4500 μmhos/cm

SAR = 2.31 - 7.64

These groundwater characteristics are included in classes C_3 S_1, C_3 S_2, C_4 S_1, and C_4 S_2, which are suitable for high to very high salt-tolerant crops without unfavorable effects on plant growth.

Zone 2

This zone is located in the eastern and central parts of the area, more or less along the eastern side of the Wadi El-Arish channel, and also in the southeastern part of the study area (Figure 45). The characteristics of groundwater in this zone are:

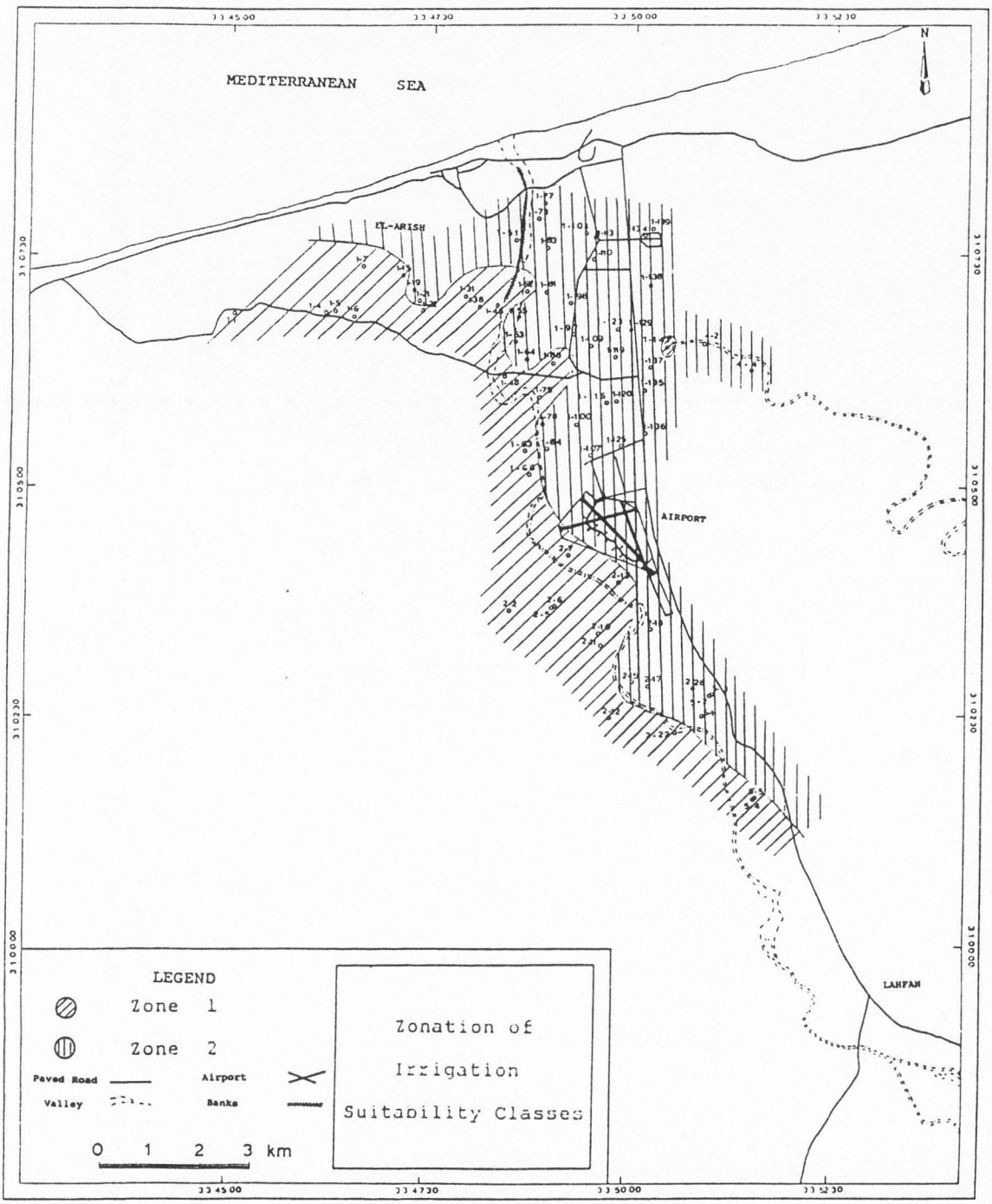

Fig. 45. Zonation of irrigation suitability classes.

EC = 2300 - 8100 μmhos/cm

SAR = 7.24 - 15.79

These groundwater characteristics are included in classes C_4 S_3, C_4 S_4, C_5 S_3, and C_5 S_4. These areas are suitable only for very high salt tolerant crops, and they also need excessive leaching and drainage.

The groundwater in the delta Wadi El-Arish area can be classified into three water groups for irrigation suitability purposes based upon the percent sodium (Todd, 1980). These three water groups are: 1) good, 2) permissible, and 3) doubtful, as shown in Table 7. Sodium is generally expressed as a percentage of the total cations as defined by the following relationship:

$$\% \, Na^{+} = \frac{(Na^{+} + K^{+}) \, 100}{Ca^{++} + Mg^{++} + Na^{+} + K^{+}} \qquad (14)$$

where all the ionic concentrations are expressed in milliequivalents per liter.

The areal distribution of the three irrigation suitability groups is shown in Figure 46. The good group is concentrated in the western part of the study area west of the Wadi El-Arish channel, while the permissible group is concentrated to the east of the Wadi El-Arish channel and also in the northwestern part of the area north of the El-Arish El-Massaeid middle road. The doubtful group is

Table 7. Suitability of Water for Irrigation in October 1989

Well Group	Well Number	Percent Sodium	Irrigation Suitability
1	1-22, 1-48 2-7, 2-22	20-40	Good
2	1-7, 1-15 1-31, 1-38 1-45, 1-62 1-63, 1-66 1-75, 1-77 1-84, 1-88 1-98, 1-123 1-129, 1-135 1-136, 1-141 2-2, 2-12 2-13, 4-2 5-1, 5-4	40-60	Permissible
3	1-19, 1-64 1-81, 1-83 1-97, 1-100 1-104, 1-109 1-119, 1-125 1-138, 1-139 2-11, 2-15 2-18, 4-4 5-2	60-80	Doubtful

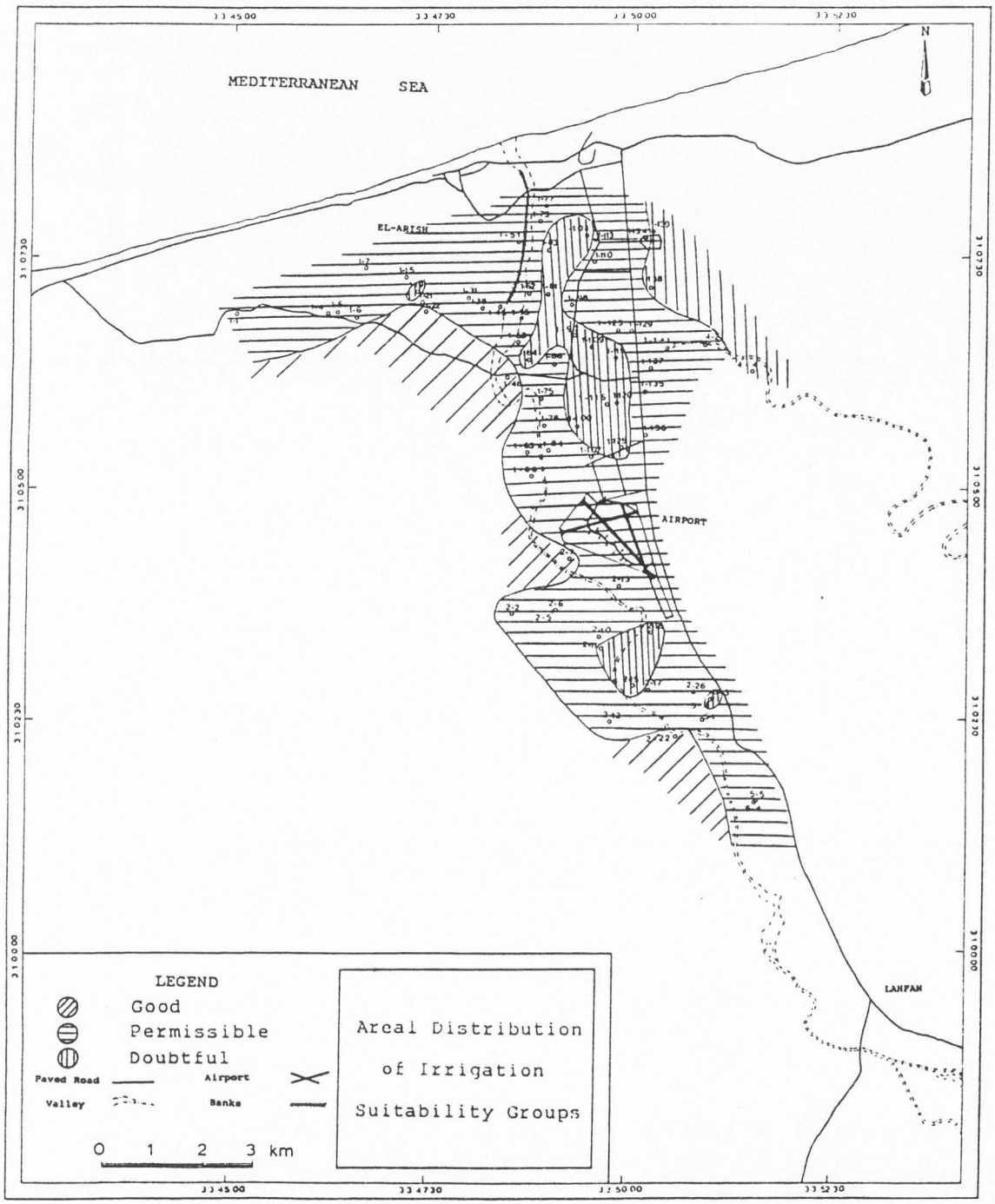

Fig. 46. Areal distribution of irrigation suitability groups.

concentrated in three areas. The first area is located in the central part of the study area north of the El-Arish airport, east of Wadi El-Arish channel and west of El-Arish--Lahfan road. The second is located in the northeastern part of the study area, and the third is located in the southern part of the area south of the El-Arish airport at the bend of Wadi El-Arish channel. There is a remarkable correlation between irrigation suitability and groundwater type (Figures 41 and 46), where the Na Cl, Na (Ca-Mg) Cl, and (Ca-Mg) Cl types match the doubtful, permissible, and good suitability groups, respectively.

CHAPTER V

SUMMARY, CONCLUSIONS, AND RECOMMENDATIONS

Summary

The delta Wadi El-Arish area is between latitude 31° 00′ and the Mediterranean Sea to the north, and between longitude 33° 45′ and 33° 52′ east. Wadi El-Arish occupies an area of about 19.5 km^2, which corresponds to one-third of the Sinai Peninsula. Wadi El-Arish is the main and the most important drainage in the Sinai Peninsula.

The stratigraphic succession in the delta Wadi El-Arish area is composed of sedimentary rocks of Tertiary and Quaternary ages. The Tertiary formations are Eocene, Miocene, and Pliocene in age, and Quaternary formations consist of Pleistocene and Holocene deposits. The Quaternary deposits cover most of the delta Wadi El-Arish area except for a small area where the Tertiary and Cretaceous rocks are exposed.

Groundwater in the delta Wadi El-Arish exists primarily in two units within the Quaternary deposits, namely the upper Pleistocene gravel unit and the lower Pleistocene calcareous sandstone (kurkar) unit. The potentiometric surface maps reflect seasonal changes in the elevation of the potentiometric surface; the elevation of the potentiometric surface is high in winter and is low in summer. The low potentiometric surface in the summer is attributable to the increase in the extraction rate at that

time. In addition, the lateral facies change of the alluvium from a gravelly layer to a sandy clay layer caused a decrease in the transmissivity of the aquifer, resulting in deeper cones of depression. The potentiometric surface maps indicate that groundwater flows generally from south to north.

The extraction rate was 5,600 m^3/day in 1954. However, the groundwater extraction rate had increased to 51,700 m^3/day in 1988 from 145 wells drilled in the Quaternary aquifer; 25,000 m^3/day were used for domestic purposes while 26,700 m^3/day were used for irrigation purposes.

The behavior of the water levels during the pumping tests shows that they were influenced either by a recharge boundary or by leakage from the overlying Holocene sand deposits through the intervening sandy clay aquitard. Consequently, the hydraulic properties of the Quaternary aquifer in the delta Wadi El-Arish area, based on an analysis of constant discharge test data, have been estimated using both the Stallman (1963) method and the Hantush and Jacob (1955) method. The results of this analysis suggest that the Quaternary aquifer in the delta Wadi El-Arish area behaves as a leaky aquifer without storage in the aquitard. Using the Hantush and Jacob method, the transmissivity ranges from 7 m^2/day in the thinnest alluvial deposits of the Quaternary aquifer to 1100 m^2/day in the calcareous sandstone (kurkar) unit. The

storativity of the aquifer ranges from 0.007 to 0.0008. The storativity values indicate that the Quaternary aquifer behaves as a semi-confined aquifer. The hydraulic conductivity of the confining layer ranges from 10^{-7} m/sec to 10^{-5} m/sec.

Step-drawdown test data have been used to calculate the specific capacities and the well efficiencies. The well efficiency values show that the efficiency of most wells decreases with increasing discharge. The specific capacity values range from 26 to 838 m^2/day. The distribution of specific capacity values shows that wells with high values are completed into either the kurkar or both the kurkar and the alluvial deposits, while wells with low values are only completed into the alluvial deposits. The higher specific capacities of the kurkar result from the higher transmissivity of the kurkar unit relative to the alluvium.

Five sets of water samples were collected and the concentrations of the major inorganic ions were determined to define the hydrochemical characteristics of the groundwater. The TDS contour maps prepared from the five sets of water samples show that the TDS increases from west to east as well as from the southern to the northern parts of the study area. The TDS of the water ranges from 1,500 ppm in the west to 4,500 ppm in the east, and from 1,500 ppm in the south to 8,000 ppm in the north. The higher TDS values measured in the northern part of the study area are

due to sea water intrusion from the Mediterranean Sea. The higher TDS values measured in the eastern part of the area are due to the fact that the wells in this area are completed into the kurkar. The TDS of the kurkar is higher than that of the alluvium because the kurkar is marine in origin, and also because it does not receive recharge directly from Wadi El-Arish. Deep percolation of return flow through irrigated lands with high salt contents may also contribute to the high TDS of the kurkar.

The seasonal variation in TDS reflects a general increase in TDS in summer due to an increase in the extraction rate. In addition, a deterioration of water quality with time is evidenced by an increase in TDS in the eastern and northern parts of the study area. TDS profiles show that the increase in TDS from 1962 to 1990 is due to the increase in groundwater extraction.

The distribution of the major inorganic ions $Na^{+} + K^{+}$, Mg^{++}, Ca^{++}, Cl^{-}, SO_4^{--}, and HCO_3^{-}, as shown in the ion contour maps, coincides to some degree with the distribution of TDS. The ion concentration maps show an increase in concentrations toward the eastern and northern parts of the area. The distributions of the major inorganic ions show that the highest concentrations are found in the northern and eastern parts of the study area. Once again, this is due to sea water intrusion from the Mediterranean Sea in the northern part of the area, and the fact that the wells in

the eastern part are completed into the kurkar.

Three main water types can be identified using a Piper (trilinear) diagram. The first water type is a sodium-chloride type, which is present primarily in the north-central part of the area. This is evidence of sea water intrusion in this area due to high groundwater extraction rates. Chloride and sodium are still the dominant anion and cation, respectively, for the second water type, but some calcium or magnesium is present in significant concentrations in addition to sodium. This water type is found in most of the water wells, particularly the wells located in the northwestern and eastern parts of the area and along the Wadi El-Arish channel, suggesting that this water comes primarily from the kurkar but that it is diluted by meteoric water from the Wadi El-Arish channel. The third water type is still dominated by chloride, but calcium and/or magnesium, rather than sodium, are the dominant cations. This is evidence of mixing of meteoric water with the kurkar. The marine origin of the kurkar, the proximity of the sea, the lack of direct recharge from Wadi El-Arish, and the deep percolation of return flow from irrigated lands with high salt contents are the main reasons for the predominance of sodium and chloride in these waters.

Most of the ratios of $\frac{Na}{Cl}$ in the water samples are less than the standard sea water value. The extremely low $\frac{Na}{Cl}$

ratios are due to the adsorption of sodium from sea water onto fine-grained sediments. The $\frac{Na}{Cl}$ ratios that are higher than the standard value for sea water are due to mixing of saline water from the Mediterranean Sea or the kurkar with water of meteoric origin.

The classification of groundwater based on Sulin's (1948) graph indicates that most of the groundwater in the study area has a marine origin, where a $Mg\ Cl_2$ water represents an old marine (connate water) origin and a $Ca\ Cl_2$ water represents a recent marine origin. These two types of water are found throughout most of the delta Wadi El-Arish area, except in the southern part of the area south of the El-Arish airport where a $Na_2\ SO_4$ water indicative of deep meteoric origin is present. The spatial distribution of these three types of water shows that the recent marine water is concentrated in the northern part of the study area due to sea water intrusion from the Mediterranean Sea, and the old marine water is concentrated in the central part of the area where most of the wells are completed in the marine calcareous sandstone (kurkar) unit.

The classification of groundwater for irrigation purposes indicates that eight classes of irrigation water, based on the classification scheme developed by the U.S. Salinity Laboratory (1954), are present within the delta Wadi El-Arish area. These classes are $C_3\ S_1$, $C_4\ S_1$, $C_3\ S_2$, $C_4\ S_2$, $C_4\ S_3$, $C_5\ S_3$, $C_4\ S_4$, and $C_5\ S_4$; but the dominant types are

C_4 S_3 and C_4 S_4, which have very high salinities and medium to very high sodium adsorption ratios. The suitability of the groundwater for irrigation can be divided into three categories based on the percent sodium. These three categories are good, permissible, and doubtful. Most of the water in the delta Wadi El-Arish area falls into the permissible and doubtful categories. The only water falling into the good category is located in the western part of the study area west of the Wadi El-Arish channel.

Conclusions and Recommendations

Groundwater in the delta Wadi El-Arish area is the most important water resource for both domestic and agricultural purposes. Unfortunately, as a result of increasing groundwater extraction from the Quaternary aquifer, a continuous deterioration of the water quality and a general decline of the potentiometric surface elevations have occurred during the last decade. The important conclusions can be stated as follows:

1. TDS concentrations have been increased by an average of about 1,500 ppm.

2. An increase in sea water intrusion in the northern part of the study area has occurred.

3. Potentiometric surface elevations vary inversely with groundwater extraction rates.

4. Potentiometric surface elevations have declined by an average of about 0.5 m.

5. The transmissivity of the kurkar unit is higher than the transmissivity of the alluvium.

6. Groundwater in the Pleistocene aquifer is augmented with groundwater leaking through the sandy clay aquitard from the overlying Holocene sand deposits.

7. Groundwater in the kurkar is of lower quality than groundwater in the alluvium.

Management of the groundwater resources in the delta Wadi El-Arish area should include the following recommendations:

1. No new pumping wells should be drilled in the area.

2. Accurate estimates for the quantity of total recharge should be determined by installing some meteorological stations around the area. In addition, a more detailed water budget for the area should be prepared. In order to prepare a more detailed water budget, additional data on evapotranspiration, surface water and groundwater inflow and outflow, the amount of water imported from the Nile River, and changes in groundwater storage will have to be collected.

3. There should be a change from flood irrigation systems to drip or sprinkler systems, and better management of the irrigation schedule in order to reduce the water loss.

4. Automatic well control systems should be used in order to manage the hours of operation and the pumping rates.

REFERENCES

Al-Ruwaih, F. 1984. Groundwater chemistry of Dibdiba formation, North Kuwait. Ground Water. v. 22, no. 4, pp. 412-417.

Dames and Moore. 1984. Sinai Development Study--Phase I. Water Resources, Vols. II-A and II-B. Submitted to the Advisory Committee for Reconstruction, Ministry of Development, Cairo, Egypt.

El-Kiki, F.E. 1981. Hydrogeochemical compositions and variations of the shallow sandstone aquifer in Kharga Oasis. Bull. Fac. Sci., Cairo University, Cairo, Egypt. no. 47, pp. 323-333.

El-Shazly, E.M., M.A. Abdel Hady, M.A. El Ghawaby, A.B. Salman, M.L. El-Rakaiby and I.I.E. El Aassy. 1980. Sinai Peninsula, Landsat Imagery Interpretation Maps. Remote Sensing Center, Academy of Scientific Research and Technology, Cairo, Egypt. 1:250,000.

Farag, I.A.M. 1947. Preliminary note on the geology of Risan Eniza. Bull. Fac. Sci., Cairo University, Cairo, Egypt. no. 26, pp. 1-38.

Fetter, C.W. 1988. Applied Hydrogeology. Merrill Pub. Co., Columbus, OH. 592 pp.

Freeze, R.A. and J.A. Cherry. 1979. Groundwater. Prentice-Hall, Englewood Cliffs, NJ. 604 pp.

GARPAD. 1984. Regional Plan Study of El-Arish, El-Sheikh Zuwayid-Rafaa Coastal Zone, Groundwater Conditions. Submitted to CICAS Consulting Group, Cairo, Egypt.

Geofizika. 1963. Final Report on Investigation of Water and Soil Resources in North and Central Parts of Sinai Peninsula. Submitted to the General Desert Development Organization, Cairo, Egypt.

Hantush, M.S. and C.E. Jacob. 1955. Nonsteady radial flow in an infinite leaky aquifer. Am. Geophys. Union Trans. v. 36, no. 1, pp. 95-100.

Hume, W.F. 1929. The surface dislocation in Egypt and Sinai. Their nature and significance. Bull. Sci. Geograph. v. 17, pp. 1-11.

Jacob, C.E. 1947. Drawdown test to determine effective radius of artesian well. Am. Soc. Civil Engineers Trans. v. 112, pp. 1047-1070.

Moon, F.W. and H. Sadek. 1921. Topography and geology of North Sinai. Petrol. Research Bull., Government Press, Cairo, Egypt. v. 10, 154 p.

Paver, G.L. and J.N. Jordan. 1956. Report of the Ministry of Public Works on the Reconnaissance Hydrogeological and Geophysical Observation in North Sinai Coastal Area of Egypt. Publ. Desert Institute, Cairo, Egypt. no. 7, pp. 7-9.

Pavlov, M. and M. Ayuty. 1961. Groundwaters of Sinai Peninsula. Report to the director of the General Desert Development Organization, Cairo, Egypt. pp. 31-37.

Piper, A.M. 1944. A graphic procedure in the geochemical interpretation of water analyses. Trans. Amer. Geophys. Union. v. 25, pp. 914-923.

REGWA Co. 1982. Hydrogeologic Basic Data Report of the El-Arish, El-Sheikh Zuwayid-Rafaa Coastal Area. Submitted to the General Authority for Rehabilitation Projects and Agricultural Development, Cairo, Egypt. (in Arabic)

RIWR. 1989. Groundwater Management Study in El-Arish-Rafaa Plain Area. Unpublished report, Cairo, Egypt.

Saad, K.F. 1962. Hydrology of Groundwater in Wadi-El-Arish, North Sinai. Unpublished report, Desert Institute, Cairo, Egypt. (in Arabic)

Said, R. 1962. The Geology of Egypt. Elsevier Publishing Company, Amsterdam, NY. 377 pp.

Said, R. and M.G. Barakat. 1958. Jurassic microfossils from Gebel Maghara, Sinai, Egypt. Micropaleontology. no. 4, pp. 231-272.

Salem, M.R. 1963. Geology of groundwater in the area between El-Arish and Gaza. Unpublished M.S. thesis, Cairo University, Cairo, Egypt.

Shata, A. 1955. The General Geology of the Sinai Peninsula and Its Relationship to Petroleum Occurrences. Submitted to the Symposium on the Applied Geology in the Middle East Countries, Ankara, Turkey.

Shata, A. 1959. Groundwater and geomorphology of the northern sector of wadi El-Arish Basin. Bull. Soc. Geogr. no. 32, pp. 247-262.

Shata, A. 1960. The geology and geomorphology of El-Qusaima area. Bull. Soc. Geogr. no. 33, pp. 95-146.

Stallman, R.V. 1963. Type curves for the solution of single boundary problems. In: Bentall, R. (compiler) Shortcuts and special problems in aquifer tests. U.S. Geol. Survey Water-Supply Paper 1545-C, pp. C45-C47.

Sulin, V.A. 1948. Condition of formation, principles of classification and constituents of natural waters. Particularly water petroleum accumulation. Leningrad Acad. of Sci., Moscow, U.S.S.R. (in Russian).

Taha, A.A. 1968. Geology of groundwater supplies of El Arish-Rafaa area, Northeastern Sinai, U.A.R. Unpublished M.S. thesis, Cairo University, Cairo, Egypt.

Todd, D.K. 1980. Groundwater Hydrology. John Wiley and Sons, New York, NY. pp. 133-302.

U.S. Salinity Lab. 1954. Diagnosis and Improvement of Saline and Alkali Soils. U.S. Dept. Agr. Handbook 60.

APPENDIXES

Appendix A

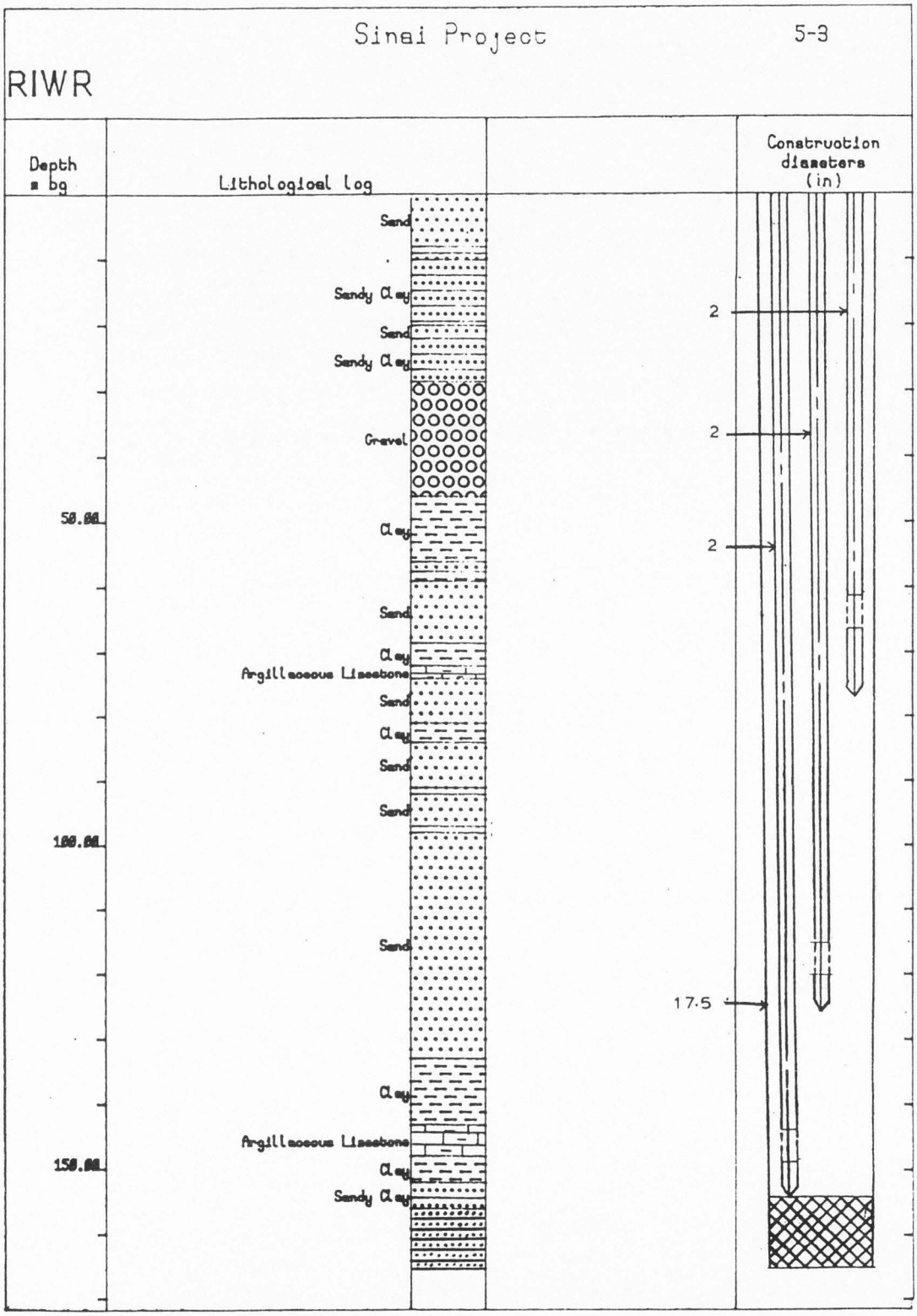

Fig. 47. Lithologic logs.

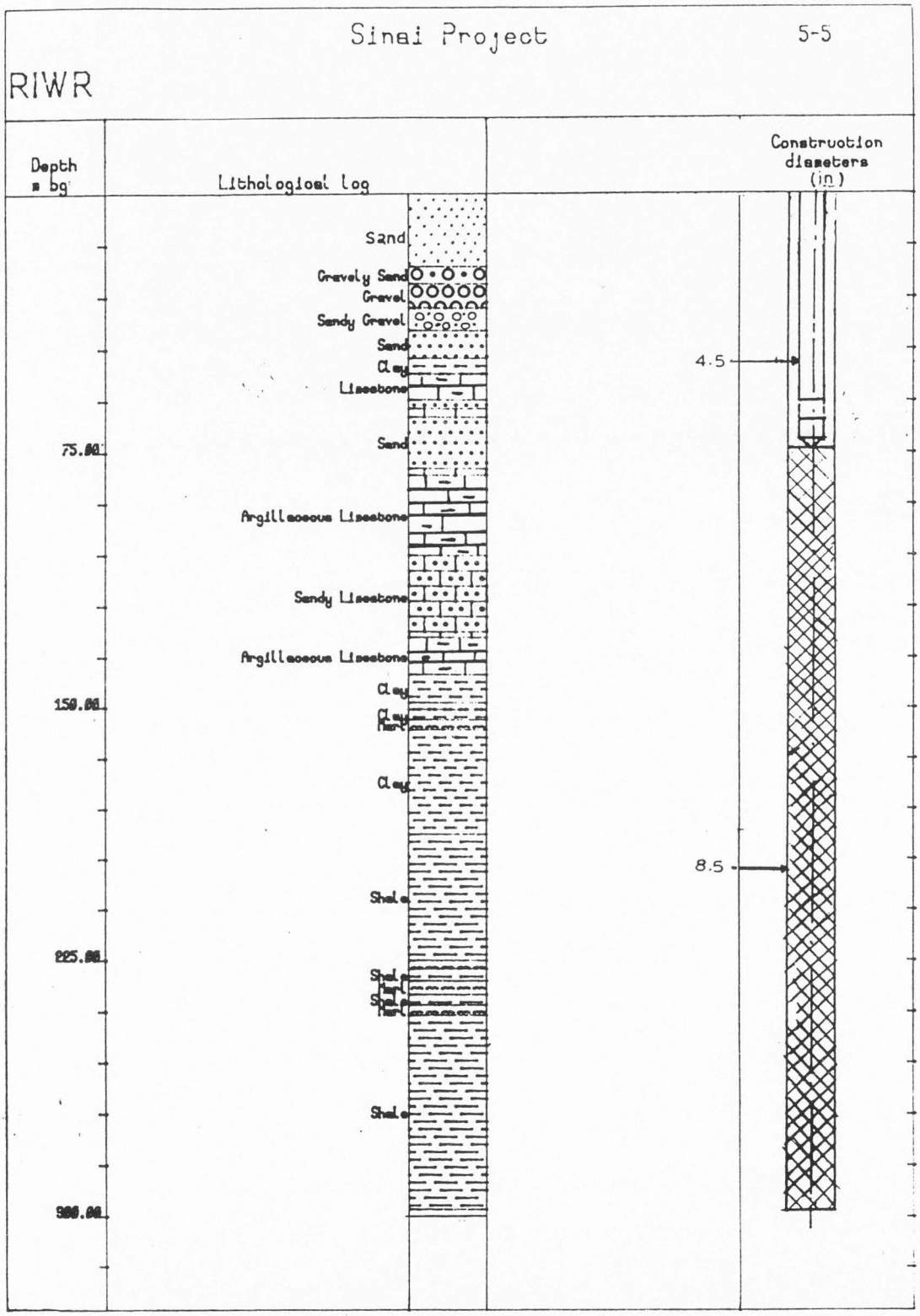

Fig. 47. Lithologic logs (continued).

Appendix B

Table 8. Constant Discharge Pumping Test Data for Well 2-5 in the Delta Wadi El-Arish Area

Static Water Level	Duration of Pumping	Pumping Rate	Distance from pumping well
33.2 m	1440 min	1357.7 m^3/d	10.2 m

Time (min)	Drawdown (m)	Time (min)	Drawdown (m)	Time (min)	Drawdown (m)	Time (min)	Drawdown (m)
0.5	0.05	16	0.302	100	0.365	530	0.368
1	0.09	18	0.305	110	0.365	590	0.365
1.5	0.14	20	0.31	120	0.363	650	0.369
2	0.16	22	0.315	135	0.36	710	0.37
2.5	0.18	24	0.32	150	0.363	770	0.372
3	0.2	26	0.325	165	0.363	830	0.37
3.5	0.21	28	0.33	180	0.369	890	0.373
4	0.22	30	0.33	200	0.37	950	0.375
4.5	0.23	35	0.34	220	0.37	1010	0.38
5	0.235	40	0.343	240	0.361	1070	0.385
6	0.25	45	0.345	260	0.359	1130	0.393
7	0.26	50	0.35	290	0.362	1190	0.39
8	0.265	55	0.355	320	0.365	1250	0.388
9	0.27	60	0.365	350	0.368	1310	0.383
10	0.28	70	0.365	380	0.369	1370	0.382
12	0.285	80	0.365	410	0.37	1430	0.385
14	0.3	90	0.365	470	0.375	1440	0.385

Table 9. Constant Discharge Pumping Test Data for Well 5-2 in the Delta Wadi El-Arish Area

Static Water Level	Duration of Pumping	Pumping Rate	Distance from pumping well
40.65 m	1440 min	216.0 m^3/d	10.0 m

Time (min)	Drawdown (m)	Time (min)	Drawdown (m)	Time (min)	Drawdown (m)	Time (min)	Drawdown (m)
0.5	0.02	16	2.2	100	5.41	630	5.952
1	0.07	18	2.44	110	5.49	690	5.965
1.5	0.13	20	2.66	120	5.56	750	5.965
2	0.2	22	2.87	135	5.66	810	5.955
2.5	0.27	24	3.06	150	5.73	870	5.97
3	0.35	26	3.24	165	5.76	930	6.005
3.5	0.43	28	3.42	180	5.78	990	5.971
4	0.49	30	3.56	200	5.83	1050	5.983
4.5	0.58	35	3.93	220	5.86	1110	5.945
5	0.66	40	4.11	240	5.88	1170	5.96
6	0.81	45	4.36	270	5.885	1230	5.955
7	0.96	50	4.5	300	5.895	1290	5.98
8	1.13	55	4.65	330	5.905	1350	5.98
9	1.27	60	4.88	390	5.915	1440	5.94
10	1.43	70	5.01	450	5.91		
12	1.71	80	5.18	510	5.93		
14	1.74	90	5.33	570	5.935		

Table 10. Constant Discharge Pumping Test Data for Well 5-4 in the Delta Wadi El-Arish Area

Static Water Level	Duration of Pumping	Pumping Rate	Distance from pumping well
43.915 m	720.0 min	180.0 m^3/d	10.0 m

Time (min)	Drawdown (m)	Time (min)	Drawdown (m)	Time (min)	Drawdown (m)	Time (min)	Drawdown (m)
0.5	0.045	6	0.18	30	0.215	180	0.243
1	0.075	7	0.185	35	0.213	210	0.245
1.5	0.095	8	0.195	40	0.217	240	0.245
2	0.105	9	0.2	50	0.227	300	0.247
2.5	0.125	10	0.2	60	0.23	360	0.247
3	0.14	12	0.205	75	0.233	420	0.247
3.5	0.15	14	0.207	90	0.233	480	0.24
4	0.16	16	0.213	105	0.235	540	0.245
4.5	0.165	20	0.213	120	0.24	660	0.245
5	0.17	25	0.215	150	0.245	720	0.245

Appendix C

Table 11. Chemical Analyses of Groundwater from Delta Wadi El-Arish Area (Oct. 1987)

Well No.	E.C µmhos/cm at 25°C	TDS mg/l	Unit	Ca	Mg	Na	K	HCO_3	Cl	SO_4	pH
1-19	4500	3029	PPM	230.00	174.00	607.00	15.00	134.00	1562.00	307.00	7.5
			meq/l	11.50	14.30	26.40	0.39	2.20	44.00	6.39	
			%	21.87	27.19	50.20	0.74	4.18	83.67	12.15	
1-22	1500	1059	PPM	103.00	74.00	143.00	9.00	134.00	408.00	188.00	7.6
			meq/l	5.15	6.05	6.20	0.22	2.20	11.50	3.92	
			%	29.23	34.34	35.19	1.25	12.49	65.27	22.25	
1-31	3500	2547	PPM	297.00	136.00	304.00	60.00	232.00	728.00	790.00	7.3
			meq/l	14.85	11.15	13.20	1.55	3.80	20.50	16.45	
			%	36.44	27.36	32.39	3.80	9.33	50.31	40.37	
1-38	2500	1699	PPM	210.00	84.00	221.00	15.00	195.00	533.00	441.00	7.4
			meq/l	10.50	6.90	9.60	0.39	3.20	15.00	9.19	
			%	38.34	25.19	35.05	1.42	11.68	54.76	33.55	
1-45	2900	2205	PPM	303.00	95.00	273.00	16.00	201.00	746.00	526.00	7.9
			meq/l	15.15	7.85	11.85	0.40	3.30	21.00	10.95	
			%	42.98	22.27	33.62	1.13	9.36	59.57	31.06	
1-51	3700	2533	PPM	307.00	138.00	345.00	19.00	207.00	994.00	504.00	7.2
			meq/l	15.35	11.35	15.00	0.49	3.70	28.00	10.49	
			%	36.38	26.90	35.55	1.16	8.77	66.37	24.86	
1-53	2400	1721	PPM	162.00	112.00	248.00	11.00	238.00	639.00	311.00	7.6
			meq/l	8.08	9.22	10.80	0.27	3.90	18.00	6.47	
			%	28.48	32.50	38.07	0.95	13.75	63.45	22.81	
1-55	3400	2144	PPM	234.00	171.00	253.00	11.00	238.00	1012.00	225.00	7.8
			meq/l	11.72	14.08	11.00	0.29	3.90	28.50	4.69	
			%	31.60	37.96	29.66	0.78	10.51	76.84	12.64	
1-62	5100	3170	PPM	424.00	191.00	414.00	17.00	256.00	1669.00	199.00	7.2
			meq/l	21.21	15.69	18.00	0.44	4.20	47.00	4.14	
			%	38.33	28.35	32.53	0.80	7.59	84.93	7.48	
1-64	3000	2537	PPM	224.00	141.00	455.00	10.00	232.00	1136.00	339.00	7.1
			meq/l	11.21	11.59	19.80	0.26	3.80	32.00	7.06	
			%	26.15	27.04	46.20	0.61	8.87	74.66	16.47	
1-73	7000	4699	PPM	553.00	272.00	759.00	24.00	153.00	2716.00	222.00	7.3
			meq/l	27.67	22.33	33.00	0.62	2.50	76.50	4.62	
			%	33.09	26.70	39.46	0.74	2.99	91.49	5.52	
1-77	7800	5802	PPM	602.00	388.00	920.00	25.00	159.00	3106.00	602.00	7.3
			meq/l	30.09	31.91	40.00	0.64	2.60	87.50	12.54	
			%	29.32	31.09	38.97	0.62	2.53	85.25	12.22	
1-81	4500	2580	PPM	339.00	159.00	280.00	13.00	195.00	1420.00	174.00	7.5
			meq/l	16.97	13.03	16.50	0.33	3.20	40.00	3.63	
			%	36.24	27.82	35.23	0.70	6.83	85.42	7.75	
1-83	4200	3506	PPM	222.00	208.00	713.00	5.00	165.00	1491.00	702.00	7.2
			meq/l	11.11	17.09	31.00	0.13	2.70	42.00	14.63	
			%	18.73	28.80	52.25	0.22	4.55	70.79	24.66	

1-84	3200	2747	PPM	264.00	131.00	476.00	7.00	244.00	959.00	666.00	7.3
			meq/l	13.21	10.79	20.70	0.19	4.00	27.00	13.89	
			%	29.43	24.04	46.11	0.42	8.91	60.15	30.94	
1-88	3200	2443	PPM	248.00	153.00	398.00	9.00	207.00	1278.00	150.00	7.2
			meq/l	12.41	12.59	17.30	0.23	3.40	36.00	3.13	
			%	29.18	29.60	40.68	0.54	7.99	84.65	7.36	
1-97	4000	2472	PPM	273.00	169.00	363.00	11.00	177.00	1349.00	130.00	7.9
			meq/l	13.64	13.87	15.80	0.29	2.90	38.00	2.70	
			%	31.28	31.81	36.24	0.67	6.65	87.16	6.19	
1-98	4200	2723	PPM	273.00	132.00	494.00	12.00	177.00	1296.00	336.00	7.5
			meq/l	13.64	10.86	21.60	0.30	2.90	36.50	7.00	
			%	29.40	23.41	46.55	0.65	6.25	78.66	15.09	
1-100	3100	2454	PPM	186.00	118.00	488.00	8.00	244.00	959.00	451.00	7.2
			meq/l	9.29	9.71	21.20	0.20	4.00	27.00	9.40	
			%	23.00	24.03	52.48	0.50	9.90	66.83	23.27	
1-104	4200	3437	PPM	178.00	249.00	667.00	11.00	183.00	1491.00	658.00	7.3
			meq/l	8.89	20.51	29.00	0.30	3.00	42.00	13.70	
			%	15.14	34.94	49.40	0.51	5.11	71.55	23.34	
1-107	4000	2789	PPM	174.00	127.00	649.00	8.00	177.00	1385.00	269.00	7.2
			meq/l	8.69	10.41	28.20	0.20	2.90	39.00	5.60	
			%	18.29	21.92	59.37	0.42	6.11	82.11	11.79	
1-109	4800	4063	PPM	393.00	264.00	690.00	5.00	165.00	1669.00	927.00	7.2
			meq/l	17.17	21.72	30.00	0.12	2.70	47.00	19.31	
			%	24.88	31.47	43.47	0.17	3.91	68.11	27.98	
1-113	4000	2960	PPM	178.00	172.00	630.00	9.00	195.00	1420.00	356.00	8.0
			meq/l	8.88	14.11	27.40	0.22	3.20	40.00	7.41	
			%	17.55	27.88	54.14	0.43	6.32	79.04	14.64	
1-116	4600	2846	PPM	232.00	153.00	564.00	11.00	159.00	1420.00	307.00	8.1
			meq/l	11.62	12.59	24.50	0.28	2.60	40.00	6.39	
			%	23.72	25.70	50.01	0.57	5.31	81.65	13.04	
1-119	4900	3929	PPM	311.00	269.00	690.00	5.00	183.00	1669.00	802.00	7.2
			meq/l	15.55	22.15	30.00	0.10	3.00	47.00	16.70	
			%	22.94	32.67	44.25	0.15	4.42	69.32	24.63	
1-120	5000	3139	PPM	303.00	192.00	552.00	13.00	214.00	1757.00	108.00	7.9
			meq/l	15.15	15.75	24.00	0.34	3.50	49.50	2.24	
			%	27.43	28.51	43.45	0.62	6.34	89.61	4.06	
1-123	3800	3297	PPM	291.00	143.00	644.00	5.00	183.00	1243.00	788.00	7.2
			meq/l	14.54	11.76	28.00	0.12	3.00	35.00	16.42	
			%	26.72	21.61	51.45	0.22	5.51	64.31	30.17	
1-125	3400	2717	PPM	248.00	102.00	552.00	8.00	220.00	1136.00	451.00	7.2
			meq/l	12.41	8.39	24.00	0.20	3.60	32.00	9.40	
			%	27.53	18.61	53.24	0.44	7.99	70.98	20.85	
1-129	4500	2760	PPM	206.00	209.00	495.00	9.00	189.00	1598.00	54.00	7.7
			meq/l	10.30	17.20	21.50	0.22	3.10	45.00	1.12	
			%	20.93	34.95	43.68	0.45	6.30	91.43	2.28	
1-134	4500	3062	PPM	180.00	180.00	667.00	7.00	201.00	1598.00	229.00	7.9
			meq/l	8.99	14.81	29.00	0.18	3.30	45.00	4.78	
			%	16.97	27.95	54.74	0.34	6.23	84.94	9.02	
1-135	3700	2738	PPM	154.00	122.00	644.00	10.00	183.00	1243.00	382.00	7.5
			meq/l	7.68	10.02	28.00	0.25	3.00	35.00	7.95	
			%	16.71	21.81	60.94	0.54	6.53	76.17	17.30	

1-136	6200	4540	PPM	388.00	176.00	1012.00	8.00	207.00	2379.00	370.00	7.1
			meq/l	19.39	14.51	44.00	0.21	3.40	67.00	7.71	
			%	24.82	18.58	56.33	0.27	4.35	85.78	9.87	
1-137	3900	2727	PPM	174.00	153.00	564.00	5.00	183.00	1172.00	476.00	7.1
			meq/l	8.69	12.61	24.50	0.12	3.00	33.00	9.92	
			%	18.92	27.46	53.35	0.26	6.53	71.86	21.60	
1-138	4700	3232	PPM	250.00	169.00	667.00	9.00	201.00	1633.00	303.00	7.9
			meq/l	12.52	13.88	29.00	0.22	3.30	46.00	6.32	
			%	22.51	24.96	52.14	0.40	5.93	82.70	11.36	
1-139	4100	2659	PPM	182.00	145.00	570.00	9.00	177.00	1402.00	174.00	7.5
			meq/l	9.09	11.91	24.80	0.22	2.90	39.50	3.62	
			%	19.75	25.88	53.89	0.48	6.30	85.83	7.87	
1-141	3500	2620	PPM	133.00	174.00	552.00	5.00	214.00	1296.00	246.00	7.1
			meq/l	6.66	14.33	24.00	0.12	3.50	36.50	5.12	
			%	14.76	31.77	53.20	0.27	7.76	80.91	11.35	
2-26	1900	1414	PPM	101.00	120.00	182.00	10.00	268.00	462.00	271.00	7.8
			meq/l	5.05	9.85	7.90	0.25	4.40	13.00	5.65	
			%	21.91	42.73	34.27	1.08	19.09	56.40	24.51	

Table 12. Chemical Analyses of Groundwater from Delta Wadi El-Arish Area (Apr. 1988)

Well No.	E.C µmhos/cm at 25°C	TDS mg/l	Unit	Ca	Mg	Na	K	HCO_3	Cl	SO_4	pH
1-31	4300	2836	PPM	286.00	132.00	460.00	31.00	214.00	921.00	792.00	7.8
			meq/l	14.30	10.86	20.00	0.80	3.50	25.95	16.51	
			%	31.11	23.63	43.52	1.74	7.62	56.46	35.92	
1-38	3000	2074	PPM	144.00	136.00	345.00	15.00	153.00	628.00	653.00	7.6
			meq/l	7.19	11.21	15.00	0.38	2.50	17.68	13.60	
			%	21.28	33.19	44.40	1.12	7.40	52.34	40.26	
1-45	3400	2312	PPM	133.00	174.00	382.00	18.00	183.00	742.00	680.00	8.0
			meq/l	6.66	14.34	16.60	0.46	3.00	20.90	14.16	
			%	17.50	37.68	43.62	1.21	7.88	54.91	37.20	
1-51	4300	3252	PPM	285.00	212.00	478.00	22.00	159.00	928.00	1168.00	7.1
			meq/l	14.25	17.45	20.80	0.56	2.60	26.13	24.33	
			%	26.86	32.89	39.20	1.06	4.90	49.25	45.85	
1-53	2800	1906	PPM	176.00	102.00	294.00	11.00	275.00	540.00	508.00	8.2
			meq/l	8.79	8.41	12.80	0.29	4.50	15.20	10.59	
			%	29.02	27.76	42.26	0.96	14.86	50.18	34.96	
1-55	4100	2509	PPM	263.00	166.00	345.00	14.00	195.00	976.00	550.00	8.1
			meq/l	13.13	13.67	15.00	0.35	3.20	27.50	11.45	
			%	31.15	32.43	35.59	0.83	7.59	65.24	27.16	
1-64	3700	2554	PPM	244.00	158.00	382.00	12.00	262.00	905.00	591.00	7.6
			meq/l	12.20	13.00	16.60	0.31	4.30	25.50	12.31	
			%	28.97	30.87	39.42	0.74	10.21	60.56	29.23	
1-73	8600	5375	PPM	527.00	357.00	863.00	23.00	104.00	2614.00	887.00	8.0
			meq/l	26.36	29.34	37.50	0.60	1.70	73.63	18.47	
			%	28.10	31.28	39.98	0.64	1.81	78.50	19.69	
1-77	9400	6482	PPM	566.00	361.00	1242.00	10.00	122.00	3153.00	1028.00	7.7
			meq/l	28.28	29.72	54.00	0.25	2.00	88.83	21.42	
			%	25.19	26.48	48.11	0.22	1.78	79.14	19.08	
1-78	3500	2238	PPM	166.00	82.00	474.00	11.00	323.00	809.00	373.00	7.4
			meq/l	8.28	6.72	20.60	0.28	5.30	22.80	7.78	
			%	23.08	18.73	57.41	0.78	14.77	63.55	21.68	
1-83	5300	3460	PPM	263.00	175.00	681.00	11.00	183.00	1315.00	832.00	7.6
			meq/l	13.13	14.37	29.60	0.28	3.00	37.05	17.33	
			%	22.88	25.04	51.59	0.49	5.23	64.57	30.20	
1-84	3800	2687	PPM	246.00	109.00	520.00	12.00	104.00	978.00	718.00	7.9
			meq/l	12.32	8.98	22.60	0.31	1.70	27.55	14.96	
			%	27.87	20.31	51.12	0.70	3.85	62.32	33.84	
1-88	4000	2579	PPM	121.00	206.00	432.00	29.00	275.00	877.00	639.00	8.1
			meq/l	6.06	16.94	18.80	0.75	4.50	24.70	13.32	
			%	14.24	39.81	44.18	1.76	10.58	58.05	31.30	
1-97	4900	3211	PPM	289.00	167.00	575.00	11.00	195.00	1250.00	724.00	8.1
			meq/l	14.44	13.76	25.00	0.28	3.20	35.20	15.08	
			%	27.00	25.73	46.75	0.52	5.98	65.82	28.20	
1-98	5000	3474	PPM	293.00	172.00	650.00	11.00	220.00	1349.00	779.00	7.3
			meq/l	14.65	14.65	28.25	0.28	3.60	38.00	16.23	
			%	25.33	25.33	48.85	0.48	6.23	65.71	28.07	

1-100	3800	2442	PPM	158.00	129.00	497.00	11.00	195.00	944.00	508.00	7.9
			meq/l	7.88	10.62	21.60	0.28	3.20	26.60	10.58	
			%	19.51	26.30	53.49	0.69	7.92	65.87	26.20	
1-104	4800	3172	PPM	230.00	196.00	566.00	11.00	171.00	1099.00	899.00	7.9
			meq/l	11.48	16.12	24.60	0.27	2.80	30.95	18.72	
			%	21.88	30.72	46.88	0.51	5.34	58.99	35.68	
1-107	4900	3107	PPM	250.00	169.00	598.00	12.00	256.00	1438.00	384.00	7.6
			meq/l	12.52	13.88	26.00	0.30	4.20	40.50	8.00	
			%	23.76	26.34	49.34	0.57	7.97	76.85	15.18	
1-109	5500	3977	PPM	299.00	209.00	794.00	12.00	22.00	1619.00	952.00	7.8
			meq/l	14.93	17.17	34.52	0.31	1.50	45.60	19.83	
			%	22.31	25.65	51.58	0.46	2.24	68.13	29.63	
1-110	5500	3707	PPM	265.00	135.00	865.00	11.00	122.00	1645.00	664.00	7.9
			meq/l	13.23	11.07	37.60	0.27	2.00	46.33	13.84	
			%	21.28	17.81	60.48	0.43	3.22	74.52	22.26	
1-116	5300	3519	PPM	269.00	125.00	788.00	10.00	183.00	1438.00	706.00	7.4
			meq/l	13.43	10.27	34.25	0.26	3.00	40.50	14.71	
			%	23.07	17.64	58.84	0.45	5.15	69.58	25.27	
1-120	6100	3803	PPM	313.00	187.00	759.00	14.00	305.00	1775.00	450.00	7.6
			meq/l	15.66	15.34	33.00	0.37	5.00	50.00	9.37	
			%	24.33	23.83	51.27	0.57	7.77	77.68	14.56	
1-123	4700	2887	PPM	226.00	148.00	598.00	10.00	195.00	1491.00	219.00	7.9
			meq/l	11.31	12.19	26.00	0.26	3.20	42.00	4.56	
			%	22.73	24.50	52.25	0.52	6.43	84.41	9.16	
1-125	4400	2656	PPM	184.00	141.00	552.00	11.00	140.00	1207.00	421.00	8.1
			meq/l	9.19	11.61	24.00	0.27	2.30	34.00	8.77	
			%	9.69	12.24	25.31	0.28	2.43	35.85	9.25	
1-129	5900	3809	PPM	279.00	176.00	851.00	10.00	139.00	1828.00	526.00	8.2
			meq/l	13.94	14.46	37.00	0.25	3.20	51.50	10.95	
			%	21.23	22.03	56.36	0.38	4.87	78.45	16.68	
1-134	5700	3654	PPM	232.00	153.00	863.00	9.00	176.00	1633.00	588.00	8.3
			meq/l	11.62	12.58	37.50	0.24	3.70	46.00	12.24	
			%	18.76	20.31	60.54	0.39	5.97	74.27	19.76	
1-135	4600	2936	PPM	208.00	133.00	649.00	9.00	182.00	1278.00	477.00	8.3
			meq/l	10.40	10.90	28.20	0.23	3.80	36.00	9.93	
			%	20.91	21.92	56.71	0.46	7.64	72.39	19.97	
1-136	7000	5091	PPM	345.00	209.00	1150.00	13.00	226.00	2108.00	1040.00	7.5
			meq/l	17.23	17.17	50.00	0.34	3.70	59.38	21.66	
			%	20.33	20.26	59.00	0.40	4.37	70.07	25.56	
1-137	4400	2773	PPM	149.00	161.00	575.00	8.00	232.00	1047.00	601.00	8.2
			meq/l	7.47	13.23	25.00	0.21	3.80	29.50	12.52	
			%	16.27	28.82	54.45	0.46	8.28	64.26	27.27	
1-139	5200	3223	PPM	175.00	210.00	649.00	9.00	228.00	1370.00	582.00	8.1
			meq/l	8.75	17.25	28.20	0.22	3.70	38.60	12.12	
			%	16.08	31.70	51.82	0.40	6.80	70.93	22.27	
1-141	4300	2860	PPM	188.00	157.00	552.00	9.00	226.00	1012.00	716.00	8.1
			meq/l	9.39	12.91	24.00	0.22	3.70	28.50	14.92	
			%	20.18	27.75	51.59	0.47	7.95	61.26	32.07	
5-1	2100	1580	PPM	151.00	66.00	248.00	10.00	238.00	422.00	445.00	8.1
			meq/l	7.55	5.45	10.80	0.26	2.90	11.88	9.28	
			%	31.38	22.65	44.89	1.08	12.05	49.38	38.57	

Table 13. Chemical Analyses of Groundwater from Delta Wadi El-Arish Area (Jul. 1989)

Well No.	E.C µmhos/cm at 25°C	TDS mg/l	Unit	Ca	Mg	Na	K	HCO_3	Cl	SO_4	pH
1-6	3300	1992	PPM	99.00	93.00	479.00	5.00	191.00	968.00	157.00	7.8
			meq/l	4.94	7.62	20.80	0.13	3.13	27.26	3.26	
			%	14.75	22.75	62.11	0.39	9.30	81.01	9.69	
1-7	2600	1559	PPM	63.00	41.00	460.00	10.00	104.00	834.00	47.00	8.2
			meq/l	3.14	3.36	20.00	0.25	2.27	23.50	0.98	
			%	11.74	12.56	74.77	0.93	8.49	87.85	3.66	
1-15	2300	1487	PPM	87.00	130.00	214.00	5.00	208.00	373.00	470.00	8.2
			meq/l	4.32	10.64	9.30	0.13	4.02	10.50	9.79	
			%	17.71	43.62	38.13	0.53	16.54	43.19	40.27	
1-21	1400	1126	PPM	90.00	45.00	230.00	7.00	159.00	359.00	236.00	8.4
			meq/l	4.48	3.66	10.00	0.19	3.32	10.10	4.91	
			%	24.44	19.97	54.56	1.04	18.11	55.10	26.79	
1-31	3900	2469	PPM	261.00	70.00	477.00	8.00	159.00	820.00	674.00	7.7
			meq/l	13.04	5.74	20.75	0.21	2.60	23.10	14.04	
			%	32.81	14.44	52.21	0.53	6.54	58.13	35.33	
1-38	2500	1728	PPM	162.00	13.00	414.00	2.00	293.00	664.00	180.00	7.7
			meq/l	8.08	1.10	18.00	0.06	4.80	18.70	3.74	
			%	29.66	4.04	66.08	0.22	17.62	68.65	13.73	
1-45	2800	2032	PPM	198.00	28.00	477.00	2.00	198.00	852.00	277.00	7.2
			meq/l	9.90	2.30	20.75	0.05	3.24	24.00	5.76	
			%	30.00	6.97	62.88	0.15	9.82	72.73	17.45	
1-48	2200	1583	PPM	109.00	85.00	305.00	4.00	151.00	525.00	404.00	8.2
			meq/l	5.44	7.02	13.25	0.10	2.59	14.80	8.42	
			%	21.08	27.20	51.34	0.39	10.03	57.34	32.62	
1-51	3400	3030	PPM	262.00	71.00	690.00	2.00	147.00	1069.00	789.00	8.1
			meq/l	13.06	5.82	30.00	0.06	2.41	30.10	16.43	
			%	26.69	11.89	61.30	0.12	4.92	61.50	33.57	
1-53	2700	2065	PPM	144.00	69.00	460.00	2.00	190.00	653.00	547.00	7.8
			meq/l	7.20	5.66	20.00	0.04	3.11	18.40	11.39	
			%	21.88	17.20	60.79	0.12	9.45	55.93	34.62	
1-55	4100	2608	PPM	218.00	57.00	607.00	5.00	204.00	969.00	548.00	7.5
			meq/l	10.88	4.66	26.40	0.12	3.34	27.30	11.42	
			%	25.87	11.08	62.77	0.29	7.94	64.91	27.15	
1-62	5000	3448	PPM	257.00	40.00	915.00	2.00	253.00	1445.00	536.00	7.3
			meq/l	12.86	3.30	39.80	0.05	4.14	40.70	11.17	
			%	22.96	5.89	71.06	0.09	7.39	72.67	19.94	
1-63	1700	1134	PPM	81.00	31.00	281.00	4.00	137.00	444.00	156.00	8.2
			meq/l	4.06	2.52	12.20	0.10	3.25	12.50	3.13	
			%	21.50	13.35	64.62	0.53	17.21	66.21	16.58	
1-64	2800	1906	PPM	198.00	30.00	442.00	2.00	151.00	834.00	249.00	8.2
			meq/l	9.88	2.46	19.20	0.05	2.91	23.50	5.18	
			%	31.28	7.79	60.78	0.16	9.21	74.39	16.40	
1-66	5100	3286	PPM	196.00	83.00	865.00	4.00	120.00	1285.00	733.00	8.3
			meq/l	9.80	6.84	37.60	0.10	2.86	36.20	15.28	
			%	18.03	12.59	69.19	0.18	5.26	66.62	28.12	

1-73	6900	4433	PPM	457.00	53.00	1118.00	14.00	117.00	2421.00	253.00	8.2
			meq/l	22.84	4.34	48.60	0.35	2.66	68.20	5.27	
			%	30.00	5.70	63.84	0.46	3.49	89.58	6.92	
1-75	3600	2719	PPM	256.00	15.00	713.00	5.00	132.00	1225.00	373.00	8.2
			meq/l	12.80	1.20	31.00	0.13	2.87	34.50	7.76	
			%	28.36	2.66	68.69	0.29	6.36	76.45	17.19	
1-77	14740	8896	PPM	727.00	77.00	2510.00	7.00	228.00	5027.00	320.00	7.7
			meq/l	36.34	6.34	109.14	0.18	3.37	141.60	6.67	
			%	23.91	4.17	71.80	0.12	2.22	93.38	4.40	
1-78	3400	2219	PPM	162.00	41.00	575.00	4.00	207.00	987.00	243.00	8.3
			meq/l	8.12	3.40	25.00	0.09	3.75	27.80	5.06	
			%	22.18	9.29	68.29	0.25	10.24	75.94	13.82	
1-81	5000	3586	PPM	292.00	107.00	823.00	8.00	164.00	1544.00	648.00	8.0
			meq/l	14.60	8.80	35.80	0.20	2.69	43.50	13.21	
			%	24.58	14.81	60.27	0.34	4.53	73.23	22.24	
1-83	4800	3606	PPM	299.00	96.00	846.00	9.00	138.00	1512.00	707.00	8.1
			meq/l	14.94	7.86	36.80	0.23	2.51	42.60	14.72	
			%	24.97	13.14	61.51	0.38	4.20	71.20	24.60	
1-88	4100	2623	PPM	141.00	19.00	796.00	13.00	170.00	1306.00	178.00	8.3
			meq/l	7.06	1.52	34.60	0.32	3.00	36.80	3.70	
			%	16.23	3.49	79.54	0.74	6.90	84.60	8.51	
1-97	4800	3073	PPM	264.00	172.00	570.00	14.00	148.00	1409.00	496.00	7.8
			meq/l	13.18	14.13	24.80	0.35	2.43	39.70	10.33	
			%	25.12	26.93	47.27	0.67	4.63	75.68	19.69	
1-98	4800	2948	PPM	289.00	144.00	534.00	14.00	170.00	1308.00	489.00	7.6
			meq/l	14.44	11.82	23.20	0.35	2.78	36.85	10.18	
			%	28.99	23.73	46.58	0.70	5.58	73.98	20.44	
1-104	4900	3320	PPM	221.00	135.00	759.00	8.00	167.00	1377.00	653.00	8.2
			meq/l	11.03	11.12	33.00	0.20	2.95	38.80	13.60	
			%	19.93	20.09	59.62	0.36	5.33	70.10	24.57	
1-107	4600	3032	PPM	224.00	204.00	552.00	12.00	104.00	1397.00	539.00	8.0
			meq/l	11.18	16.81	24.00	0.30	1.71	39.35	11.23	
			%	21.38	32.15	45.90	0.57	3.27	75.25	21.48	
1-116	5300	3794	PPM	264.00	138.00	863.00	15.00	162.00	1477.00	875.00	8.1
			meq/l	13.22	11.38	37.50	0.38	2.65	41.60	18.23	
			%	21.16	18.21	60.02	0.61	4.24	66.58	29.18	
1-119	5600	3957	PPM	280.00	225.00	788.00	15.00	82.00	1679.00	888.00	8.0
			meq/l	13.99	18.51	34.25	0.38	1.34	47.30	18.49	
			%	20.84	27.57	51.02	0.57	2.00	70.46	27.54	
1-125	4400	3013	PPM	191.00	164.00	589.00	10.00	194.00	1447.00	418.00	7.9
			meq/l	9.56	13.45	25.60	0.26	3.18	40.75	8.71	
			%	19.56	27.52	52.38	0.53	6.04	77.41	16.55	
1-136	7000	4651	PPM	176.00	233.00	1196.00	11.00	189.00	2389.00	475.00	8.1
			meq/l	8.81	19.19	52.00	0.30	3.10	67.30	9.90	
			%	10.97	23.90	64.76	0.37	3.86	83.81	12.33	
1-137	4500	3243	PPM	136.00	164.00	788.00	8.00	218.00	1502.00	427.00	7.0
			meq/l	6.82	13.50	34.25	0.20	3.58	42.30	8.89	
			%	12.45	24.65	62.53	0.37	6.54	77.23	16.23	
1-139	4800	3247	PPM	83.00	130.00	929.00	8.00	139.00	1656.00	302.00	8.1
			meq/l	4.14	10.69	40.40	0.20	2.28	46.65	6.29	
			%	7.47	19.29	72.88	0.36	4.13	84.48	11.39	

1-141	4300	2710	PPM	116.00	127.00	681.00	8.00	232.00	1372.00	174.00	7.6
			meq/l	5.80	10.47	29.60	0.20	3.80	38.65	3.62	
			%	12.59	22.73	64.25	0.43	8.25	83.89	7.86	
2-2	3800	2232	PPM	132.00	216.00	317.00	12.00	0.00	829.00	726.00	7.8
			meq/l	6.61	17.76	13.80	0.30	0.00	23.35	15.13	
			%	17.18	46.17	35.87	0.78	0.00	60.68	39.32	
2-5	3300	1761	PPM	113.00	226.00	317.00	10.00	77.00	738.00	280.00	7.4
			meq/l	5.66	18.58	13.80	0.26	1.26	20.80	16.24	
			%	14.78	48.51	36.03	0.68	3.29	54.31	42.40	
2-7	3500	2249	PPM	122.00	181.00	396.00	10.00	203.00	982.00	355.00	7.9
			meq/l	6.08	14.84	17.20	0.25	3.33	27.65	7.39	
			%	15.85	38.68	44.83	0.65	8.68	72.06	19.26	
2-12	1600	1112	PPM	97.00	69.00	159.00	10.00	129.00	325.00	323.00	8.1
			meq/l	4.86	5.69	6.90	0.26	2.12	9.15	6.72	
			%	27.44	32.13	38.96	1.47	11.78	50.86	37.35	
2-15	1100	1057	PPM	65.00	95.00	115.00	5.00	200.00	257.00	320.00	8.1
			meq/l	3.23	7.78	5.00	0.12	3.27	7.25	6.66	
			%	20.02	48.23	31.00	0.74	19.03	42.20	38.77	
2-17	2600	1894	PPM	71.00	135.00	354.00	10.00	279.00	540.00	505.00	8.0
			meq/l	3.57	11.06	15.40	0.26	4.58	15.20	10.51	
			%	11.79	36.51	50.84	0.86	15.12	50.18	34.70	
2-22	2200	1823	PPM	146.00	113.00	239.00	9.00	326.00	367.00	553.00	7.6
			meq/l	7.30	9.29	10.40	0.24	5.35	10.35	11.53	
			%	26.81	34.12	38.19	0.88	19.65	38.01	42.34	
4-2	3600	2524	PPM	140.00	124.00	570.00	16.00	61.00	1063.00	550.00	7.7
			meq/l	7.00	10.21	24.80	0.40	1.00	29.95	11.46	
			%	16.51	24.07	58.48	0.94	2.36	70.62	27.02	
4-4	7300	4945	PPM	336.00	255.00	1104.00	2.00	158.00	2607.00	477.00	7.5
			meq/l	16.80	20.96	48.00	0.21	2.59	73.45	9.93	
			%	19.54	24.38	55.83	0.24	3.01	85.44	11.55	
5-1	2100	1546	PPM	88.00	108.00	260.00	8.00	160.00	401.00	521.00	8.0
			meq/l	4.38	8.91	11.30	0.20	2.63	11.30	10.88	
			%	17.67	35.94	45.58	0.81	10.60	45.55	43.85	

Table 14. Chemical Analyses of Groundwater From Delta Wadi El-Arish Area (Oct. 1989)

Well NO.	E.C µmhos/cm at 25°C	TDS mg/l	Unit	Ca	Mg	Na	K	HCO_3	Cl	SO_4	pH
1-7	2800	1682	PPM	111.00	109.00	324.00	11.00	152.00	760.00	215.00	8.2
			meq/l	5.53	8.97	14.10	0.27	3.00	21.40	4.47	
			%	19.15	31.07	48.84	0.94	10.39	74.13	15.48	
1-15	2100	1308	PPM	111.00	66.00	248.00	9.00	134.00	559.00	181.00	8.2
			meq/l	5.55	5.45	10.80	0.22	2.50	15.75	3.77	
			%	25.20	24.75	49.05	1.00	11.35	71.53	17.12	
1-19	3900	2241	PPM	111.00	121.00	534.00	12.00	116.00	1203.00	144.00	8.0
			meq/l	5.55	9.95	23.20	0.31	2.10	33.90	3.01	
			%	14.23	25.51	59.47	0.79	5.38	86.90	7.72	
1-22	1600	1163	PPM	121.00	90.00	138.00	7.00	49.00	394.00	364.00	8.5
			meq/l	6.06	7.44	6.00	0.18	1.00	11.10	7.58	
			%	30.79	37.80	30.49	0.91	5.08	56.40	38.52	
1-31	4200	2910	PPM	283.00	160.00	428.00	80.00	207.00	1056.00	696.00	8.2
			meq/l	14.14	13.16	18.60	2.05	3.70	29.75	14.50	
			%	29.49	27.45	38.79	4.28	7.72	62.04	30.24	
1-38	3000	2137	PPM	121.00	170.00	354.00	16.00	195.00	808.00	473.00	7.3
			meq/l	6.06	13.94	15.40	0.40	3.20	22.75	9.85	
			%	16.93	38.94	43.02	1.12	8.94	63.55	27.51	
1-45	3800	2273	PPM	268.00	22.00	455.00	14.00	212.00	873.00	429.00	7.5
			meq/l	13.40	1.80	19.80	0.35	3.80	24.60	8.95	
			%	37.91	5.09	56.01	0.99	10.17	65.86	23.96	
1-48	2500	1861	PPM	242.00	86.00	239.00	11.00	213.00	557.00	513.00	7.1
			meq/l	12.12	7.08	10.40	0.29	3.50	15.70	10.69	
			%	40.55	23.69	34.79	0.97	11.71	52.53	35.76	
1-62	4500	2768	PPM	356.00	65.00	520.00	18.00	220.00	1303.00	286.00	7.4
			meq/l	17.80	5.40	22.60	0.45	3.60	36.70	5.95	
			%	38.49	11.68	48.86	0.97	7.78	79.35	12.86	
1-63	3500	2167	PPM	202.00	60.00	469.00	10.00	183.00	921.00	322.00	7.5
			meq/l	10.10	4.90	20.40	0.26	3.00	25.95	6.71	
			%	28.32	13.74	57.21	0.73	8.41	72.77	18.82	
1-64	3200	2124	PPM	48.00	62.00	602.00	14.00	366.00	905.00	127.00	7.5
			meq/l	2.40	5.20	26.20	0.35	6.00	25.50	2.65	
			%	7.03	15.23	76.72	1.02	17.57	74.67	7.76	
1-66	2600	1693	PPM	145.00	82.00	294.00	11.00	281.00	568.00	312.00	7.4
			meq/l	7.27	6.73	12.80	0.29	4.60	16.00	6.49	
			%	26.84	24.84	47.25	1.07	16.98	59.06	23.96	
1-75	3500	2292	PPM	202.00	72.00	497.00	14.00	214.00	1024.00	269.00	7.7
			meq/l	10.10	5.90	21.60	0.35	3.50	28.85	5.60	
			%	26.61	15.55	56.92	0.92	9.22	76.02	14.76	
1-77	8100	5394	PPM	505.00	252.00	1093.00	23.00	140.00	2907.00	474.00	7.5
			meq/l	25.25	20.75	47.50	0.58	2.30	81.90	9.88	
			%	26.84	22.06	50.49	0.62	2.44	87.05	10.50	
1-81	5000	3206	PPM	240.00	50.00	828.00	24.00	201.00	1455.00	408.00	7.7
			meq/l	12.00	4.20	36.00	0.62	3.30	41.00	8.50	
			%	22.72	7.95	68.16	1.17	6.25	77.65	16.10	

1-83	3500	2318	PPM	160.00	19.00	639.00	16.00	153.00	1033.00	298.00	7.8
			meq/l	8.00	1.60	27.80	0.40	2.50	29.10	6.20	
			%	21.16	4.23	73.54	1.06	6.61	76.98	16.40	
1-84	4000	2545	PPM	192.00	114.00	524.00	12.00	244.00	1049.00	410.00	7.7
			meq/l	9.60	9.40	22.80	0.30	4.00	29.55	8.55	
			%	22.80	22.33	54.16	0.71	9.50	70.19	20.31	
1-88	3600	2311	PPM	184.00	82.00	497.00	17.00	195.00	955.00	381.00	7.8
			meq/l	9.20	6.80	21.60	0.44	3.20	26.90	7.94	
			%	24.19	17.88	56.78	1.16	8.41	70.72	20.87	
1-97	4600	2886	PPM	228.00	36.00	819.00	20.00	213.00	1434.00	136.00	7.3
			meq/l	11.40	3.00	35.60	0.52	3.50	40.40	2.83	
			%	22.57	5.94	70.47	1.03	7.49	86.45	6.06	
1-98	4500	2940	PPM	289.00	111.00	589.00	11.00	158.00	1305.00	477.00	8.8
			meq/l	14.44	9.16	25.60	0.28	2.80	36.75	9.93	
			%	29.18	18.51	51.74	0.57	5.66	74.27	20.07	
1-100	3500	2407	PPM	172.00	14.00	658.00	12.00	281.00	1040.00	230.00	7.9
			meq/l	8.60	1.20	28.60	0.30	4.60	29.30	4.80	
			%	22.22	3.10	73.90	0.78	11.89	75.71	12.40	
1-104	4500	2742	PPM	288.00	5.00	704.00	12.00	238.00	1399.00	96.00	7.3
			meq/l	14.40	0.40	30.60	0.30	3.90	39.40	2.00	
			%	31.51	0.88	66.96	0.66	8.61	86.98	4.42	
1-109	4500	2824	PPM	204.00	2.00	828.00	12.00	189.00	1431.00	158.00	7.8
			meq/l	10.20	0.20	36.00	0.30	3.10	40.30	3.30	
			%	21.84	0.43	77.09	0.64	6.64	86.30	7.07	
1-119	5000	3028	PPM	236.00	43.00	819.00	12.00	195.00	1661.00	62.00	7.6
			meq/l	11.80	3.60	35.60	0.30	3.20	46.80	1.30	
			%	23.00	7.02	69.40	0.58	6.24	91.23	2.53	
1-123	4500	2910	PPM	113.00	235.00	589.00	9.00	146.00	1440.00	378.00	7.8
			meq/l	5.66	19.34	25.60	0.23	2.40	40.55	7.88	
			%	11.14	38.05	50.36	0.45	4.72	79.78	15.50	
1-125	4000	2471	PPM	144.00	46.00	672.00	12.00	195.00	1104.00	298.00	7.9
			meq/l	7.20	3.80	29.20	0.30	3.20	31.10	6.20	
			%	17.78	9.38	72.10	0.74	7.90	76.79	15.31	
1-129	5800	3884	PPM	271.00	188.00	863.00	9.00	153.00	1928.00	472.00	7.5
			meq/l	13.53	15.47	37.50	0.24	2.50	54.30	9.84	
			%	20.27	23.18	56.19	0.36	3.75	81.48	14.77	
1-135	4100	2449	PPM	182.00	121.00	534.00	9.00	134.00	1283.00	186.00	8.2
			meq/l	9.09	9.91	23.20	0.22	2.40	36.15	3.87	
			%	21.43	23.36	54.69	0.52	5.66	85.22	9.12	
1-136	7000	4775	PPM	323.00	227.00	1081.00	12.00	183.00	2394.00	555.00	7.3
			meq/l	16.16	18.64	47.00	0.31	3.00	67.45	11.56	
			%	19.68	22.70	57.24	0.38	3.66	82.25	14.10	
1-138	5500	3644	PPM	327.00	87.00	851.00	9.00	171.00	1653.00	546.00	7.5
			meq/l	16.36	7.19	37.00	0.23	2.80	46.55	11.38	
			%	26.92	11.83	60.88	0.38	4.61	76.65	18.74	
1-139	4600	2853	PPM	182.00	121.00	676.00	8.00	165.00	1425.00	276.00	7.4
			meq/l	9.09	9.91	29.40	0.21	2.70	40.15	5.76	
			%	18.70	20.39	60.48	0.43	5.55	82.60	11.85	
1-141	3800	2445	PPM	168.00	118.00	520.00	10.00	238.00	1115.00	276.00	7.9
			meq/l	8.40	9.80	22.60	0.26	3.90	31.40	5.76	
			%	20.46	23.87	55.04	0.63	9.50	76.47	14.03	

2-2	3100	2142	PPM	137.00	152.00	368.00	11.00	250.00	831.00	393.00	7.8
			meq/l	6.87	12.53	16.00	0.28	4.10	23.40	8.18	
			%	19.25	35.12	44.84	0.78	11.49	65.58	22.93	
2-7	3400	2112	PPM	212.00	145.00	290.00	10.00	244.00	836.00	375.00	7.7
			meq/l	10.61	11.89	12.60	0.26	4.00	23.55	7.81	
			%	30.01	33.63	35.63	0.74	11.31	66.60	22.09	
2-11	2000	1339	PPM	48.00	70.00	289.00	10.00	250.00	405.00	267.00	7.8
			meq/l	2.40	5.80	12.60	0.26	4.10	11.40	5.56	
			%	11.40	27.54	59.83	1.23	19.47	54.13	26.40	
2-12	4200	2773	PPM	202.00	171.00	534.00	12.00	146.00	1326.00	382.00	7.7
			meq/l	10.10	14.10	23.20	0.30	2.40	37.35	7.95	
			%	21.17	29.56	48.64	0.63	5.03	78.30	16.67	
2-13	2300	1596	PPM	152.00	62.00	276.00	12.00	299.00	493.00	302.00	7.5
			meq/l	7.60	5.20	12.00	0.30	4.90	13.90	6.30	
			%	30.28	20.72	47.81	1.20	19.52	55.38	25.10	
2-15	2300	1577	PPM	124.00	12.00	391.00	12.00	335.00	593.00	110.00	7.3
			meq/l	6.20	1.00	17.00	0.30	5.50	16.70	2.30	
			%	25.31	4.08	69.39	1.22	22.45	68.16	9.39	
2-18	3600	2327	PPM	196.00	55.00	511.00	8.00	195.00	1122.00	240.00	7.7
			meq/l	9.80	4.60	22.20	0.20	3.20	31.60	5.00	
			%	26.63	12.50	60.33	0.54	8.04	79.40	12.56	
2-22	2100	1717	PPM	237.00	69.00	198.00	9.00	366.00	394.00	444.00	7.6
			meq/l	11.84	5.66	8.60	0.24	6.00	11.10	9.24	
			%	44.95	21.49	32.65	0.91	22.78	42.14	35.08	
4-2	3500	2268	PPM	164.00	82.00	520.00	31.00	189.00	1172.00	110.00	7.6
			meq/l	9.20	6.80	22.60	0.80	3.10	33.00	2.30	
			%	23.35	17.26	57.36	2.03	8.07	85.94	5.99	
4-4	4500	3567	PPM	268.00	29.00	1003.00	14.00	92.00	1983.00	578.00	8.1
			meq/l	13.40	2.40	43.60	0.35	1.50	44.60	12.05	
			%	22.43	4.02	72.97	0.59	2.58	76.70	20.72	
5-1	2600	1804	PPM	152.00	69.00	322.00	10.00	384.00	447.00	420.00	7.7
			meq/l	7.60	5.80	14.00	0.26	6.30	12.60	8.76	
			%	27.48	20.97	50.61	0.94	22.78	45.55	31.67	
5-2	3000	1990	PPM	144.00	29.00	492.00	12.00	299.00	721.00	293.00	7.6
			meq/l	7.20	2.40	21.40	0.30	4.90	20.30	6.10	
			%	23.00	7.67	68.37	0.96	15.65	64.86	19.49	
5-4	2400	1610	PPM	91.00	109.00	283.00	9.00	281.00	547.00	280.00	7.8
			meq/l	4.55	8.95	12.30	0.24	4.60	15.40	6.04	
			%	17.47	34.37	47.24	0.92	17.67	59.14	23.20	

Table 15. Chemican Analyses of Groundwater From Delta Wadi El-Arish Area (Jan. 1990)

Well No.	E.C µmhos/cm at 25°C	TDS mg/l	Unit	Ca	Mg	Na	K	HCO_3	Cl	SO_4	pH
1-7	2400	1517	PPM	34	57	421	11	78	602	314	7.9
			meq/l	1.68	4.77	18.3	0.28	1.28	17.2	6.55	
			%	6.71	19.06	73.11	1.12	5.11	68.72	26.17	
1-22	2000	1347	PPM	32	67	329	8	195	465	251	7.9
			meq/l	1.6	5.6	14.3	0.21	3.2	13.28	5.23	
			%	7.37	25.79	65.87	0.97	14.74	61.17	24.09	
1-45	3600	2305	PPM	35	130	552	20	293	736	539	8.0
			meq/l	1.77	10.8	24	0.5	4.8	21.04	11.23	
			%	4.77	29.13	64.74	1.35	12.95	56.76	30.29	
1-48	2400	1696	PPM	37	121	322	11	381	359	466	7.7
			meq/l	1.85	10.07	14	0.28	6.24	10.25	9.71	
			%	7.06	38.44	53.44	1.07	23.82	39.12	37.06	
1-53	2300	1531	PPM	37	79	352	11	342	470	240	8.1
			meq/l	1.85	6.6	15.3	0.28	5.6	13.44	4.99	
			%	7.70	27.47	63.67	1.17	23.30	55.93	20.77	
1-62	5200	3364	PPM	34	224	782	22	337	1096	869	7.8
			meq/l	1.68	18.7	34	0.57	5.52	31.32	18.11	
			%	3.06	34.03	61.87	1.04	10.05	57.00	32.96	
1-63	3600	2378	PPM	34	81	656	11	342	700	556	7.9
			meq/l	1.68	6.72	28.5	0.28	5.6	20	11.58	
			%	4.52	18.07	76.65	0.75	15.06	53.79	31.15	
1-64	3300	2130	PPM	37	101	543	14	342	739	355	7.8
			meq/l	1.85	8.4	23.6	0.35	5.6	21.12	7.4	
			%	5.42	24.59	69.09	1.02	16.39	61.83	21.66	
1-66	2600	1809	PPM	24	130	380	11	425	556	285	7.9
			meq/l	1.19	10.8	16.5	0.28	6.96	15.88	5.93	
			%	4.14	37.54	57.35	0.97	24.19	55.20	20.61	
1-75	3800	2540	PPM	37	154	598	11	376	826	539	7.8
			meq/l	1.85	12.85	26	0.28	6.16	23.6	11.22	
			%	4.51	31.36	63.45	0.68	15.03	57.59	27.38	
1-77	8300	5169	PPM	77	145	1610	22	181	2351	784	8.1
			meq/l	3.83	12.06	70	0.57	2.96	67.16	16.34	
			%	4.43	13.95	80.96	0.66	3.42	77.68	18.90	
1-78	3400	2183	PPM	24	149	520	11	415	571	643	7.8
			meq/l	1.19	12.43	22.6	0.28	6.8	16.3	13.4	
			%	3.26	34.05	61.92	0.77	18.63	44.66	36.71	
1-83	4500	3092	PPM	42	190	736	11	210	919	985	7.4
			meq/l	2.1	15.83	32	0.28	3.44	26.25	20.52	
			%	4.18	31.53	63.73	0.56	6.85	52.28	40.87	
1-88	4200	2696	PPM	29	161	667	14	288	959	579	7.8
			meq/l	1.43	13.4	29	0.35	4.72	27.4	12.06	
			%	3.24	30.33	65.64	0.79	10.68	62.02	27.30	

1-97	4700	2981	PPM	27	171	773	14	228	1155	614	7.7
			meq/l	1.36	14.22	33.6	0.35	3.74	33	12.79	
			%	2.75	28.71	67.84	0.71	7.55	66.63	25.82	
1-98	4700	2938	PPM	35	125	837	11	229	1250	450	7.6
			meq/l	1.77	10.4	36.4	0.28	3.76	35.72	9.37	
			%	3.62	21.29	74.51	0.57	7.70	73.12	19.18	
1-100	3700	2521	PPM	134	103	658	11	356	917	342	7.9
			meq/l	1.68	8.6	28.6	0.28	5.84	26.2	7.12	
			%	4.29	21.96	73.03	0.72	14.91	66.91	18.18	
1-104	4700	3081	PPM	39	164	796	11	254	1092	726	7.8
			meq/l	1.94	13.66	34.6	0.28	4.16	31.2	15.12	
			%	3.84	27.06	68.54	0.55	8.24	61.81	29.95	
1-113	4800	3003	PPM	32	121	840	8	283	1022	697	7.7
			meq/l	1.6	10.06	36.5	0.21	4.64	29.2	14.53	
			%	3.31	20.80	75.46	0.43	9.59	60.37	30.04	
1-116	5100	3266	PPM	20	200	805	11	187	954	1089	7.6
			meq/l	1.02	16.69	35	0.28	3.06	27.25	22.68	
			%	1.92	31.50	66.05	0.53	5.77	51.42	42.80	
1-119	5300	3350	PPM	27	224	805	11	234	1129	921	7.7
			meq/l	1.36	18.63	35	0.28	3.84	32.25	19.18	
			%	2.46	33.71	63.33	0.51	6.95	58.35	34.70	
1-120	5500	3630	PPM	24	288	796	14	293	1183	1033	7.2
			meq/l	1.19	23.98	34.6	0.35	4.8	33.8	21.52	
			%	1.98	39.89	57.55	0.58	7.98	56.22	35.80	
1-125	4100	2731	PPM	154	103	621	11	346	875	620	7.2
			meq/l	7.72	8.6	27	0.28	5.68	25	12.92	
			%	17.71	19.72	61.93	0.64	13.03	57.34	29.63	
1-129	6000	3806	PPM	26	190	1070	11	249	1638	623	7.7
			meq/l	1.28	15.8	46.5	0.28	4.08	46.8	12.98	
			%	2.00	24.74	72.82	0.44	6.39	73.29	20.33	
1-134	5000	3163	PPM	26	122	934	8	249	1320	504	8.0
			meq/l	1.28	10.2	40.6	0.21	4.08	37.72	10.49	
			%	2.45	19.51	77.64	0.40	7.80	72.14	20.06	
1-135	4100	2628	PPM	22	191	598	9	249	866	692	7.7
			meq/l	1.1	15.91	26	0.24	4.08	24.75	14.42	
			%	2.54	36.79	60.12	0.55	9.43	57.23	33.34	
1-136	7000	4357	PPM	46	286	1058	14	254	1558	1142	7.5
			meq/l	2.3	23.81	46	0.35	4.16	44.5	23.8	
			%	3.17	32.86	63.48	0.48	5.74	61.41	32.85	
1-137	4000	2730	PPM	34	142	722	8	293	1082	450	7.8
			meq/l	1.68	11.8	31.4	0.21	4.8	30.92	9.37	
			%	3.73	26.17	69.64	0.47	10.65	68.57	20.78	
1-138	5300	3320	PPM	22	193	851	11	239	1143	861	7.7
			meq/l	1.1	16.12	37	0.28	3.92	32.65	17.93	
			%	2.02	29.58	67.89	0.51	7.19	59.91	32.90	
1-139	4800	2942	PPM	26	182	727	8	249	996	755	8.0
			meq/l	1.3	15.15	31.6	0.21	4.08	28.45	15.73	
			%	2.69	31.39	65.48	0.44	8.45	58.95	32.59	
1-141	3200	2120	PPM	57	98	538	8	264	809	346	7.8
			meq/l	2.85	8.17	23.4	0.21	4.32	23.1	7.21	
			%	8.23	23.59	67.57	0.61	12.47	66.71	20.82	

2-2	3100	2172	PPM	134	83	566	12	346	822	208	7.9
			meq/l	1.68	6.9	24.6	0.32	5.68	23.48	4.34	
			%	5.01	20.60	73.43	0.96	16.96	70.09	12.96	
2-5	3200	2155	PPM	32	124	520	11	429	788	251	7.8
			meq/l	1.6	10.3	22.6	0.28	7.04	22.52	5.22	
			%	4.60	29.61	64.98	0.81	20.24	64.75	15.01	
2-7	3400	2139	PPM	32	91	575	11	366	855	208	7.7
			meq/l	1.6	7.6	25	0.28	6	24.44	4.34	
			%	4.62	21.95	72.19	0.81	17.33	70.57	12.53	
2-10	2700	1792	PPM	34	144	329	11	386	438	452	7.9
			meq/l	1.68	11.98	14.3	0.28	6.32	12.5	9.42	
			%	5.95	42.42	50.64	0.99	22.38	44.26	33.36	
2-12	3900	2617	PPM	43	234	430	12	224	275	1399	7.5
			meq/l	2.13	19.52	18.7	0.32	3.68	7.85	29.14	
			%	5.24	48.00	45.98	0.79	9.05	19.30	71.65	
2-18	3300	2032	PPM	30	91	543	8	332	785	242	7.9
			meq/l	1.51	7.6	23.6	0.21	5.44	22.44	5.04	
			%	5.00	25.17	78.15	0.70	18.01	74.30	16.69	
2-22	2200	1582	PPM	32	130	269	11	315	268	558	7.5
			meq/l	1.59	10.86	11.7	0.28	5.16	7.65	11.62	
			%	6.51	44.45	47.89	1.15	21.12	31.31	47.56	
4-2	3600	2194	PPM	32	66	656	31	63	946	399	7.9
			meq/l	1.6	5.5	28.5	0.8	1.04	27.04	8.32	
			%	4.40	15.11	78.30	2.20	2.86	74.29	22.86	
4-4	7800	4815	PPM	89	234	1279	11	229	1827	1146	7.7
			meq/l	4.45	19.5	55.6	0.28	3.76	52.2	23.87	
			%	5.57	24.43	69.65	0.35	4.71	65.39	29.90	
5-1	2100	1405	PPM	61	62	315	11	305	467	184	7.4
			meq/l	3.06	5.14	13.7	0.28	5	13.35	3.83	
			%	13.80	23.17	61.77	1.26	22.54	60.19	17.27	
5-2	2500	1734	PPM	49	33	483	11	293	480	385	7.6
			meq/l	2.47	2.78	21	0.28	4.8	13.7	8.03	
			%	9.31	10.48	79.16	1.06	18.09	51.64	30.27	
5-4	2500	1502	PPM	35	80	345	8	342	476	215	8.2
			meq/l	1.77	6.7	15	0.21	5.6	13.6	4.48	
			%	7.47	28.29	63.34	0.89	23.65	57.43	18.92	